Development of Drug-loaded Nanoparticles for Targeted Chemotherapy

by

Teppei Shirakura

A dissertation submitted in partial fulfillment
of the requirements for the degree of
Doctor of Philosophy
(Biophysics)
in the University of Michigan
2015

Doctoral Committee:

Professor Raoul Kopelman, Chair
Professor Maria G. Castro
Professor Ari Gafni
Assistant Professor Sarah L. Veatch

To My Family

Acknowledgements

I, first of all, thank Professor Raoul Kopelman for giving me an opportunity to work in his group. He made it possible for me to work on the projects that I planned by myself, collect the data by myself, and present by myself. I enjoyed struggling to manage things by myself, and learned a lot of things.

I thank my parents and brother for encouraging me to study abroad, and for supporting me in many ways. I also enjoyed their visit here. I also thank my grandparents for their support and cheering me up. おじいちゃん、おばあちゃん、電話とかお菓子とかうなぎとか、いつもありがとう。元気が出たよ。

I thank Professor Maria Castro and Professor Pedro Lowenstein for their help in our collaborative works. Also, Professor Castro helped me as a member of my thesis committee. I also thank my Biophysics thesis committee members, Professors Ari Gafni, and Sarah Veatch, for all their support and valuable advice about my research. Professor Veatch helped me as member of my candidacy committee as well. I also thank my previous thesis committee member, Professor Mohamed Elsayed, for advice about my research, using his expertise on drug delivery systems. I thank my other candidacy committee members: Professors, Mark Banaszak Holl, Jean Moran, and Ayyalusamy Ramamoorthy, for their valuable advice about my projects. I thank the staffs of the Departments of Biophysics and of Chemistry for their support. With their help, I

could just focus on my research. I thank the Rackham Graduate School, University of Michigan, for financial support of my research.

I also thank Professor Edward Yu, at Iowa State University, for advising me to study in this university. With his advice of "graduate school will be the only time you can focus just on the research," I did my best to focus on the research.

I want to acknowledge our group members. I thank Dr. Yong-Eun Koo Lee for her valuable advice. She gave me numerous comments about my experimental design, possible projects, and data interpretations. Also, she always respected my ideas and what I learned. Following her logic, I have developed skills to organize my research. I thank my colleague, Dr. Ming Qin, for our friendship. He was my best lunch mate, and sports commentator. Also, he gave me a lot of good advice about my research as well. I thank Dr. Aniruddha Ray for our collaborative work. We brainstormed on lots of new projects, and successfully published some of our work. I thank Dr. Shouyan Wang and Dr. Hoe Jin Ha for their support when I joined the Kopelman group. With their help, I could start the research in this group successfully. I also thank Drs. Leshern Karamchand, Hyung Ki Yoon, Remy Elbez, Kristen Hermann, Akiko Kochi, as well as other lab members for their help. I also thank the undergraduate students who worked with me: Ana Patricia Kutschat, Wuliang Zhang, Kyle Lee, Ananya Mukudan, Aulina Chowdhury, Antonina Malyarenko, Yue Hou, Taylor Kelson, Christof Smith, Kevin Refior, Winnie Cheung, Ruba Jiddou, and Christopher Soong-Ho Lee.

I thank my collaborators Hikmat Assi and Robert Doherty in Professors Maria Castro and Pedro Lowenstein's group. They provided me with the antitumor drug, CPA-7, and performed biological assays for our collaboration.

Finally, I want to thank Kanako Sugawara. I enjoyed our daily 10-minute conversation. She gave me lots of gifts. Also, her diligent effort on her work inspired me; otherwise I might have been too lazy to work.

Table of Contents

List of Figures

List of Schemes

List of Tables

Abstract

Cancer is the second highest cause of death in the US, and chemotherapy is one of the common cancer therapies. In order to reduce side effects and avoid cancer's resistance to antitumor drugs, we use nanoparticle (NP)-assisted chemotherapy. This strategy can selectively deliver high concentrations of antitumor drugs to the tumor area, because NPs can encapsulate antitumor drugs, target the tumor area by active and passive targeting mechanisms, and release the drugs inside the cancer cells. This work focuses on three aspects of such NPs: high loading with antitumor drugs, controlled release of antitumor drugs, and high cellular uptake by the NPs. As a model system, polyacrylamide-based NPs were loaded with cisplatin. The effects of functional groups in the NPs, and the effects of matrix densities, were evaluated in terms of the NPs' drug-loading, their release profile, and their cellular uptake. The carboxyl-functionalized NPs achieved 2 times higher loading and faster release of cisplatin than the amine-functionalized NPs. In contrast, the amine-functionalized NPs had 3.5 times better cellular uptake than the carboxyl-functionalized NPs. Tuning the matrix density of those NPs could control the release of cisplatin. Also, cisplatin-loaded, temperature-responsive NPs were synthesized so as to incorporate a trigger for cisplatin release in the cancer cells. The elevated temperature successfully enhanced the release of cisplatin from the synthesized NPs, especially under acidic conditions simulating lysosomes, which were the destination of the NPs inside the cells. Also, the *in vitro* cytotoxicity of the NPs is accelerated at high temperature. Finally, polyethylenimine (PEI) was incorporated into cisplatin-loaded PAA-NPs. Incorporation of PEI enhanced the

cellular uptake of the PAA NPs 7 times, and resulted in significantly higher cytotoxicity. Other properties of these NPs, such as enhanced loading, enhanced release, and endosomal escape may contribute to their higher cytotoxicity. These results confirmed the importance of the following three factors when designing NPs for NP-assisted chemotherapy: (1) high loading with antitumor drugs, (2) controlled release of antitumor drugs, and (3) high cellular uptake of the NPs.

Chapter 1

Introduction

Cancer Statistics.

Thanks to the recent development of early diagnosis and treatment of cancer, the growth in the number of death by cancer has been suppressed, based on the statistics in 2014. [1] However, cancer is still the second highest cause of death in US in recent years, and the first cause of death by disease for people younger than 80, except for males whose age is 20 to 39. [1] Therefore, establishing new methods of treatment of cancer is in high demand.

Cancer Therapies.

Cancer is an uncontrollable and rapid growth of cells in the body. [2] These cells can migrate from an original location to another location through the lymph system and blood stream. [2] The grown tumors can disable normal body functions, and, in the severe case, cause death. [3]

There are various types of proposed cancer treatments: surgery, radiation therapy, chemotherapy, and photodynamic therapy. [4] All these therapies aim for the removal of cancer cells from the body. Surgery is the physical removal of the tumor from the body. Radiation therapy dysfunctions DNA in the cancer cells, and causes apoptosis by radiation, which is most commonly performed utilizing an external radiation source. [5,6] Chemotherapy attacks cancer cells by small molecules, targeted towards rapid growth or biomarkers that are highly expressed in the

tumor area. [7,8] Photodynamic therapy is a relatively new treatment which utilizes reactive oxygen species (ROS), produced by photosensitizers. The ROS oxidize various parts of the cells, and lead to cell death. [4]

Surgery, radiation therapy and chemotherapy are the most common treatment currently. Surgery is the most invasive method, but enables the removal of a large volume of tumor. On the other hand, radiation therapy and chemotherapy are less invasive and indirect treatments. [4] Due to their lesser invasiveness, these therapies are often prescribed prior to surgery, or after the surgery as adjuvant therapies. [8,9]

Problems with Chemotherapy.

Even though chemotherapy is less invasive, it is known to cause severe side effects, due to a nontargeted distribution of drugs. [4] In addition, chemotherapy may not completely eradicate the tumor, and cancer may relapse after chemotherapy. [10]

One of the reasons of the relapse is due to cancer cells' intrinsic resistance against these drugs, the so-called multidrug resistance (MDR). [10] Because of their MDR ability, some cancer cells may survive the chemotherapy. MDR is a combination effect of mechanisms of the tumor cells, to fight antitumor drugs. ATP-binding cassette (ABC) transporters play an important and most widely discussed role among MDR transporters. [11] They actively transport drugs out of the body. For example, ABCC2, ATP7A, and ATP7B are reported to pump out cisplatin, [12,13] and P-gp, MRP1, ABCC2, and ABCG2 are reported to pump out doxorubicin. [12,14,15]

Another MDR mechanism is the so-called quiescent state. Some of the resistant cells are fundamentally arrested in a G0-G1 state. [16] Therefore, chemodrugs that work during the cell

division are not effective.[13] Also, these cells can have an enhanced DNA repairing ability, [17] as well as adapt to a hypoxic environment. [18] Another mechanism of drug resistance is anti-apoptosis. A higher expression of the anti-apoptosis genes (FLIP, BCL-2, BCL-XL, [19] and of the inhibitor of apoptosis protein (IAP) family members[20]) was observed in some of these resistant cells. Also, DNA damages can cause a loss of ability of proceeding to apoptosis. [21] In addition to these cellular functions, the environment in the tumor, such as high interstitial fluid pressure, [22,23] hypoxia[24] and low pH, [25,26] contribute to MDR as well. [12] Due to these MDR abilities, the chemotherapy of cells with MDR is challenging.

Solving the problem of MDR ability of cancer cells is important not simply because we can treat cancer more effectively, but also because cancer stem cells, which play an important role in relapse and metastasis, are known to have such MDR mechanisms. [10] Therefore, in order to completely eradicate the tumor, it is mandatory to overcome the problem of MDR.

Prospective chemotherapy needs to overcome the problems described above: side effects and MDR, so as to improve the quality of life of the patients, as well as increasing the drug efficacy. A simple method to solve the problem of MDR is to increase the amount (dose) of antitumor drugs that are delivered to the tumor areas so that they can override the MDR of tumors. However, simply increasing the dose of drugs causes an increase in the risk of resulting severe side effects. Therefore, instead of increasing the overall dose of antitumor drugs, it is necessary to increase their local dose.

NPs-Assisted Chemotherapy.

1) *Advantages of using NPs-Assisted Chemotherapy.*

Nanoparticle (NP)-assisted selective delivery of antitumor drugs, a so-called drug delivery system, has been proposed as a promising strategy to achieve this goal, because of these systems' intrinsic property to selectively accumulate in the tumor area, due to the size of these NPs. Chemotherapeutic agents are loaded into NPs, and NPs serve as carrier of the agent to the tumor area. Hiroshi Maeda found that cancerous tumors have a bigger than normal size of pores, in their blood vessels, so that macromolecules, like NPs, penetrate through the tumor vasculatures more easily than through the vasculatures of normal tissues ("leaky tumor blood vessels"). [27] Also, cancerous tumors can remove these macromolecules less efficiently than the normal tissues (poor lymphatic drainage). [27] As a result, polyacrylamide-based (PAA)-NPs selectively accumulate in the cancerous tumors, compared to the rest of the body. This phenomenon is called "enhanced permeability and retention" (EPR). [27]

Traditionally, the chemodrug/contrast-agent molecules needed to be chemically modified for improving the *in vivo* efficacy and pharmacokinetic behavior of the drugs. However, these procedures require long times and occasionally these chemical modifications can end up in an unexpected loss of their desirable properties. By encapsulating drugs into NPs, the drug-loaded NPs can gain such improvement, i.e. better *in vivo* efficacy and better pharmacokinetic behavior, without alternating the chemical or physical properties of the drugs itself. One example of NP advantages is the conjugation to the NPs of active targeting moieties. By conjugating targeting moieties such as antibody, small peptide, or aptamer, the cancerous cell-targeting ability of NPs can be enhanced furthermore. [28–30] We have previously shown that the addition of F3, a 34 amino acid peptide originally from the high mobility group protein 2, HMG2N, [31] can enable NPs to stay in the tumor areas for a significantly longer time than non-targeted NPs. [32] Another example is the conjugation of polyethylene glycol (PEG). It is reported that by coating the surface of the

NPs by PEG, the circulation time of NPs in the blood much increases, due to the avoidance of the interaction with blood proteins, and also due to the prevention of NPs from being engulfed by macrophages, and being rapidly cleared from the body. [33,34] The longer circulation also lets more NPs reach the tumor areas.

In addition to enabling drugs to target the tumor, the NPs can protect drugs from degradation. [35,36] A common problem of small molecule drugs is their degradation by enzymes in the blood. [36] The degradation of drugs reduces the number of active drug molecules at the tumor areas. NPs can physically protect these drugs from degradation, by preventing these enzymes from interacting with drugs, by coating the drugs. [36] Therefore, utilizing these properties, more and more drug-encapsulated NPs are being developed for commercialization now.

Doxorubicin-encapsulated liposome, the so-called Doxil, is the first U.S. Food and Drug Administration (FDA) approved nanoparticle-based chemotherapeutic agent. [34] It was approved by the FDA in 1995. [34] It is aiming for the prolonged circulation inside the body, and the protection of doxorubicin from degradation. [34] It is used for metastatic breast cancer, recurrent ovarian cancer, and multiple myeloma, Kaposi's sarcoma. [34] Another example is paclitaxel-bound albumin, called Abraxane. It is developed by Abraxis Bioscience, and approved by the U.S. Food and Drug Administration (FDA) in 2005. It is used for the treatment of pancreatic cancer, non-small cell lung cancer, and breast cancer. [37–39]

2) *Types of NPs-Assisted Chemotherapy.*

Various types of materials and various methods of formation of these nanocarriers have been proposed. Some examples of these nanocarriers are liposomes, [34,40,41] polymeric micelles,

[42–44] dendrimers, [45,46] polysaccharides, [47] and inorganic NPs. [40,48] Liposomes are one of the oldest formulations people have developed as nanocarriers. [41] It is the micelle whose layers are made of lipids. [41] Polymeric micelles use amphiphilic polymer chains, instead of lipids, to form micelles, so as to have additional functionality. [42] Dendrimers are branched polymer networks, which typically have 4-5 generations. [45,46] They are widely used as carriers for genes due to their ability to escape endosomes. [46] Various polysaccharides are used as a carrier of drugs. [47,49] One example is hyaluronic acid; hyaluronic acid is used as a carrier of cisplatin due to the abundance of carboxylic groups in its structure. [47] Typical inorganic NPs used as a drug carrier are iron oxide and gold NPs. [40,48] They typically have a core of inorganic materials and a shell of organic materials, in order to capture drugs and increase the stability of the core material itself. Inorganic NPs themselves do not encapsulate drugs inside their structure, but capture drugs on their surface. These inorganic cores help in controlling the release of drugs. [40,48]

In Dr. Kopelman's group, we utilize the hydrogel polyacrylamide (PAA) as a basic structure of NPs. We have shown that PAA-NPs are biocompatible both *in vitro* and *in vivo*. [30,50] Also, the system has high engineerability as well. By varying the monomers and cross-linkers, along with acrylamide, the charge of the NPs and the hydrophobicity inside NPs' matrix and can be tuned. These properties are important for controlling the retention and release of drugs inside the NPs. Thus, it is ideal for synthesizing highly functional hydrogel NPs for biomedical applications.

PAA-NPs are composed of three different components: acrylamide, secondary monomer, and cross-linker. Acrylamide is the main ingredient of the NPs. Its polymer is chemically inert, has a neutral charge, and is highly biocompatible. The secondary monomer determines the overall charge of the NPs. Some of the secondary monomers we have used are: A primary

amine-containing monomer, 3-(aminopropyl)methacrylamide (APMA), [30] carboxyl-containing monomer, acrylic acid[50] and 2-carboxyethyl acrylate. [35] APMA can be used to load negatively charged drugs such as RNA and DNA, and to conjugate targeting moieties such as F3, via bifunctional PEG, maleimide-PEG-N-hydroxylsuccinimide ester. [51] The amount of the secondary monomer is tuned to minimize the toxicity from a functional group of the secondary monomer, and to also tune the drug retaining and releasing ability of the NPs. [35] The cross-linker links the polymer chains inside the NP to pack the matrix and form a stable spherical shape. By incorporating the ester groups inside the cross-linkers, the NPs gradually degrades inside the body, and can be bio-eliminated from the body. [52,53] Also, by changing the length of the polymer chain, the intermolecular distance of the drug molecules inside the NPs can be tuned. [36]

The PAA-NPs are size tunable. It is reported that PAA-NPs can have a size ranging from 30nm to 10μm. [54] For our purpose, we aimed at a size of PAA-NPs of less than 100 nm, so that these NPs can pass through the blood-brain-barrier, for the treatment of brain tumors. [55] In order to tune the size, PAA-NPs are synthesized using the reverse-micelle polymerization method. [56] This system is composed of three parts; oil, water and surfactants. The oil is the continuous phase in our reverse micelle system. Hexane typically acts as an oil phase in our system. All NP ingredients are dissolved in water, which only has 1/20 to 1/40 of the volume of hexane. An ionic surfactant, dioctyl sulfosuccinate (AOT), and a nonionic surfactant, Brij30, are used as surfactants in our system; [56] the surfactant combination makes the microemulsion temperature independent. [57] By changing the ratio among oil, water, and surfactants, the size of the micelle can be tuned. [56] The polymerization of the NPs ingredients is started by initiators, i.e., ammonium persulfate (APS) and N,N,N',N'-tetramethylethylenediamine (TEMED).

Goals of Dissertation.

In this work, cisplatin-loaded PAA-based NPs were developed for chemotherapy. Cisplatin is a good model drug for my research because it has platinum on its center. [58] The platinum makes the quantification of drugs in the NPs and in the NPs treated-cells easier than other organic chemotherapeutic agents, such as paclitaxel and docetaxel, which need quantification by UV spectroscopy or mass spectroscopy where various molecules in the cells and NPs can interfere. [59–61] Also, it is one of the earliest chemotherapeutic agents, and known to has severe side effects; therefore, delivering cisplatin to the tumor with lower systemic side effects will be a great contribution to current chemotherapy. [62,63]

We previously reported a treatment of ovarian cancer utilizing PAA-based NPs. [30] We aimed to eradicate ovarian cancer in a mouse model. With F3-conjugated NPs, we had success in suppressing the tumor volume, whereas free cisplatin did not show any effect, due to the known cisplatin resistance of the utilized cancer cells. [30] However, the NPs had a low loading of cisplatin, poor results in *in vitro* study, and no analysis on the cisplatin release behavior. [30] Therefore, in my dissertation, I focused on the improvement of the promising NPs formulation.

To improve the efficacy of the NPs, I focused on three critical factors of the NPs-assisted chemotherapy: (1) loading efficiency of cisplatin, (2) release profile of cisplatin, (3) cellular uptake efficiency.

Loading efficiency is a critical factor for NPs-assisted chemotherapy. Even though PAA-NPs are biocompatible, the dose of the NPs is limited. Therefore, in order to deliver an effective amount of drugs to the tumor, the NPs should be able to load a high amount of drugs. In fact, our previous work was successful in the shrinkage of the tumor, but could not completely eradicate

the tumor.[30] This could be because the dose of cisplatin was only one third of the dose of free cisplatin.[30] If the loading of cisplatin had been higher, the efficacy could have been even higher. The loading of cisplatin can be controlled by changing the timing of loading cisplatin, the loading temperature, and the secondary monomer.[44,47] These conditions will be discussed further in chapters 2 and 3.

The controlled release of drugs is also a critical factor for NPs-assisted chemotherapy. In order to maximize the amount of drug delivered to the tumor area, the ideal NPs should release no drugs while the NPs are circulating in the blood, and release all drugs in the tumor area. However, in reality, the drugs are slowly leaching out from NPs even while circulating in the blood. Therefore, it is necessary to tune the release kinetics in a way that it does not rapidly release the entire drug in the blood or that the concentration of the released drug is too high, so as not to cause severe side effects. On the other hand, if the NPs release drugs too slowly, the concentration of the active drugs in the tumor area is insufficient for the treatment. Our PAA-NPs are reported to have a plasma half-life of 35 hours.[33] Therefore, if the NPs can gradually release cisplatin over several days, instead of several hours or several weeks, such NPs can continuously supply effective amounts of drugs to the tumor, while reducing their side effects, due to targeting.

Another method to control the release of drugs is to add a release trigger to the NPs[4]. In this way, the NPs can change the release kinetics drastically when the NPs migrate from the blood vessel to the tumor area. Some examples of triggers are light,[64,65] pH,[66] temperature,[50,66] antigen,[67] glucose,[68] and a reducing environment.[69] By adding such a trigger, the delivery of drugs to the tumor areas will be more effective. An example of a thermally controlled release of drugs from NPs will be discussed in chapter 3.

Cellular uptake efficiency is also a critical factor for these NPs. The closer the drugs are released to the site of action, the more effective the treatment is. For example, cisplatin chelates DNA in nucleus. The closer cisplatin in NPs is released to the nucleus, the better the therapeutic effect is.[70] Therefore, the efficacy will be higher if the drugs are released from the NPs after the NPs are inside the cells than if the drugs are released before entering the cells. Also, it is reported that NPs can avoid MDR pumps.[71,72] The avoidance of MDR is possibly because free drug molecules diffuse through cell membrane, and these pumps work mainly when drug molecules are penetrating through the membrane; however, this remains under discussion.[73] Thus, if we could release drugs after the NPs are taken up by the cells, we could avoid the efflux of drugs, which can further enhance the therapeutic effect.

The surface properties, such as charge, of the NPs are an important factor influencing cellular uptake efficiency. The higher the positive charge, the higher the cellular uptake, because the cell membrane is negatively charged.[74] Also, the lower the negative charge, the better the cellular uptake is.[74] Also, it is reported that pathways NPs take to be uptaken by the cells are different between positively charged NPs and negatively charged NPs, due to the difference in the interaction with blood plasma proteins such as albumin.[75] Positively charged NPs deform the structure of the proteins on the surface of the NPs; therefore, they are uptaken by the scavenger receptor.[75] On the other hand, negatively charged NPs do not deform the structure of the proteins on the surface of the NPs; therefore they are uptaken via protein receptors, such as the albumin receptor.[75] The relationship between the NPs' surface and the cellular uptake is further discussed in chapter 5.

Another approach to increase the cellular uptake is to add some targeting moieties on the surface of the NPs, so as to increase the chance of receptor mediated endocytosis. Some of the

commonly used targeting moieties are anti-VEGF, folic acid, and F3 peptide. We have previously shown that cells that are expressing high amounts of nucleolin on the membrane surface can uptake more F3-conjugated NPs than non-conjugated NPs. [51,76]

In order to analyze these factors, we utilize various analytical methods. The size and surface charge of NPs is measured using dynamic light scattering (DLS) [77] and electrophoretic light scattering, [78] where the instrument can measure the hydrodynamic size, size distribution, and the zeta-potential of the NPs, respectively. Also, transmittance electron microscopy and scanning electron microscopy can be utilized to measure the NPs in the dried state, and evaluate the size uniformity of the NPs. The cisplatin loading content, the amount of cisplatin in the cells, and the cisplatin release from the NPs can all be quantified by using inductively coupled plasma optical emission spectroscopy (ICP-OES). Fluorescence microscopy, especially confocal microscopy, can be utilized to evaluate the location of the NPs in the cells, as well as the amount of NPs uptaken by the cells. Flow cytometry can be utilized as well to measure the amount of NPs uptaken by the cells.

Structure of the Dissertation.

The structure of my dissertation is the following.

Chapter 2.

A nanoparticle (NP)-based antitumor drug carrier has been an emerging strategy for selectively delivering the drugs to the tumor area and, thus, reducing side effects that are associated with a high systemic dose of antitumor drugs. Precise control of the drug release from these NPs is critical so as to maximize the NPs' therapeutic index. Here, we propose a simple

method of synthesizing NPs with tunable drug release while maintaining their loading ability: changing the matrix density of amine-functionalized hydrogel NPs as well as of carboxyl-functionalized hydrogel NPs. The NPs with looser matrix released more cisplatin and at a faster rate. Carboxyl-functionalized NPs loaded more cisplatin and released at faster rate than amine-functionalized NPs. Also, we compared cellular uptake between amine-functionalized NPs and carboxyl-functionalized NPs: The amine-functionalized NPs can deliver 3.5 times more cisplatin into cells than the carboxyl-functionalized NPs. Both the consideration of controlled release and uptake is required for designing potent drug-loaded NPs. Also, we discussed their cytotoxicity.

Shirakura, T., Smith, C. Koo Lee, Y.-E., and Kopelman R. "Hydrogel Nanoparticle Matrix Density and Surface Charge Engineering: Tuning Chemodrug Loading, Release, and Cellular Uptake." **In preparation.**

Chapter 3.

One of the properties that drug-loaded NPs need to have is control of the drug release. Ideally, the drugs are released only at the tumor areas. I incorporated a useful temperature-sensitivity into my NPs. Unlike typical temperature-sensitive NPs, which squeeze out the drugs at the elevated temperature, my NPs swell with temperature, which enhance their drug release at the tumors' elevated temperature. I confirmed the temperature-sensitivity of cisplatin release at the physiological pH of 7.4 and also at pH 4, which is close to the lysosomal pH of 4.5, where these NPs were trapped inside the cells. Also, we observed enhanced cytotoxicity of cisplatin-loaded NPs at elevated temperatures *in vitro*; even though *free* cisplatin is less effective at these elevated temperatures. These finding expanded the choice of possible formulations of the

development of improved drug delivery systems, by demonstrating this new alternative choice of a temperature sensitive material.

Shirakura, T.; Kelson, T.; Ray, A.; Malyarenko, A.; Kopelman, R. "Hydrogel Nanoparticles with Thermally Controlled Drug Release." *ACS Macro Letters* **2014**, *3*, 602606.

Chapter 4.

The efficacy of drug-loaded NPs is directly related to the cellular uptake of NPs. The higher the cellular uptake, the better the efficacy. Therefore, I embedded PEI into our cisplatin-loaded NPs, and compared them with cisplatin-loaded PAA NPs without PEI, in terms of their cellular uptake and cytotoxicity. I found that the cellular uptake was significantly enhanced by PEI, even though there was no enhancement of surface potential (ζ-potential) between the PEI-incorporated NPs and the NPs without PEI. Also, due to their higher cellular uptake, the PEI-embedded NPs had higher cytotoxicity than the NPs without PEI when loaded with cisplatin. Also, PEI-incorporated NPs showed marginal increase of loading, faster release kinetics, and ability of endosomal escape. High cellular uptake and these factors contribute to the higher cytotoxicity of cisplatin-loaded PEI-incorporated PAA NPs than PAA NPs. The finding emphasizes the importance of the cellular uptake of NPs for the efficacy of NPs-based chemotherapy, and suggests a new method for enhancing the cellular uptake.

Shirakura, T. Ray, A. Kopelman R. "Polyethylenimine-Incorporation into Hydrogel Nanoparticles for Enhanced Chemotherapy." **In preparation**.

References

1. Siegel, R.; Ma, J.; Zou, Z.; Jemal, A. Cancer Statistics, 2014. *CA: A Cancer Journal for Clinicians* **2014**, *64*, 9–29.
2. Clark, WH Tumour Progression and the Nature of Cancer. *British journal of cancer* **1991**, *64*, 631.
3. Chambers, A.; Groom, A.; MacDonald, I. Metastasis: Dissemination and Growth of Cancer Cells in Metastatic Sites. *Nature Reviews Cancer* **2002**, *2*, 563–572.
4. Koo Lee, Y.; Kopelman, R. In *Multifunctional Nanoparticles for Drug Delivery Applications*; Svenson, S.; Prud'homme, R. K., Eds.; Nanostructure Science and Technology; Springer US: Boston, MA, 2012; pp. 225–255.
5. Zhang, L.; Chen, H.; Wang, L.; Liu, T.; Yeh, J.; Lu, G.; Yang, L.; Mao, H. Delivery of Therapeutic Radioisotopes Using Nanoparticle Platforms: Potential Benefit in Systemic Radiation Therapy. *Nanotechnology, science and applications* **2009**, *3*, 159–170.
6. Mundt, A. J.; Roeske, J. C. Principles of radiation oncology. In; Springer Berlin Heidelberg, 2003; pp. 9–17.
7. Feldmann, G.; Dhara, S.; Fendrich, V.; Bedja, D.; Beaty, R.; Mullendore, M.; Karikari, C.; Alvarez, H.; Iacobuzio-Donahue, C.; Jimeno, A.; *et al.* Blockade of Hedgehog Signaling Inhibits Pancreatic Cancer Invasion and Metastases: A New Paradigm for Combination Therapy in Solid Cancers. *Cancer research* **2007**, *67*, 2187–96.
8. Chabner, B.; Roberts, T. Chemotherapy and the War on Cancer. *Nature Reviews Cancer* **2005**, *5*, 65–72.
9. Jaffe, N.; Frei, E.; Traggis, D.; Bishop, Y. Adjuvant Methotrexate and Citrovorum-Factor Treatment of Osteogenic Sarcoma. *The New England journal of medicine* **1974**, *291*, 994–7.
10. Dean, M.; Fojo, T.; Bates, S. Tumour Stem Cells and Drug Resistance. *Nat. Rev. Cancer* **2005**, *5*, 275–84.
11. Mimeault, M.; Batra, S. New Promising Drug Targets in Cancer- and Metastasis-Initiating Cells. *Drug discovery today* **2010**, *15*, 354–64.
12. Patel, N.; Pattni, B.; Abouzeid, A.; Torchilin, V. Nanopreparations to Overcome Multidrug Resistance in Cancer. *Advanced Drug Delivery Reviews* **2013**, *65*, 1748–1762.
13. Liu, F.-S. Mechanisms of Chemotherapeutic Drug Resistance in Cancer Therapy—a Quick Review. *Taiwanese Journal of Obstetrics and Gynecology* **2009**, *48*, 239–244.
14. Allen, JD; Brinkhuis, RF; Deemter, L van; Wijnholds, J Extensive Contribution of the Multidrug Transporters P-Glycoprotein and Mrp1 to Basal Drug Resistance. *Cancer Research* **2000**, *60*, 5761–5766.
15. Grant, C. E.; Valdimarsson, Gunnar; Hipfner, D. R.; Almquist, K. C.; Cole, S. P. C.; Deeley, R. G. Overexpression of Multidrug Resistance-Associated Protein (MRP) Increases Resistance to Natural Product Drugs. *Cancer Research* **1994**, *54*, 357–361.
16. Aguirre-Ghiso, J. A. Models, Mechanisms and Clinical Evidence for Cancer Dormancy. *Nat. Rev. Cancer* **2007**, *7*, 834–46.
17. Saini, V.; Shoemaker, R. Potential for Therapeutic Targeting of Tumor Stem Cells. *Cancer science* **2009**, *101*, 16–21.
18. Cortes-Dericks, L.; Carboni, G. L.; Schmid, R. A.; Karoubi, G. Putative Cancer Stem Cells in Malignant Pleural Mesothelioma Show Resistance to Cisplatin and Pemetrexed. *Int. J. Oncol.* **2010**, *37*, 437–44.

19. Liu, G.; Yuan, X.; Zeng, Z.; Tunici, P.; Ng, H.; Abdulkadir, I.; Lu, L.; Irvin, D.; Black, K.; Yu, J. Analysis of Gene Expression and Chemoresistance of CD133+ Cancer Stem Cells in Glioblastoma. *Molecular Cancer* **2006**, *5*, 67.
20. Jin, F.; Zhao, L.; Zhao, H.-Y.; Guo, S.-G.; Feng, J.; Jiang, X.-B.; Zhang, S.-L.; Wei, Y.-J.; Fu, R.; Zhao, J.-S. Comparison between Cells and Cancer Stem-like Cells Isolated from Glioblastoma and Astrocytoma on Expression of Anti-Apoptotic and Multidrug Resistance-Associated Protein Genes. *Neuroscience* **2008**, *154*, 541–50.
21. Jordan, C.; Guzman, M.; Noble, M. Cancer Stem Cells. *The New England journal of medicine* **2006**, *355*, 1253–61.
22. Heldin, C.-H.; Rubin, K.; Pietras, K.; Östman, A. High Interstitial Fluid Pressure — an Obstacle in Cancer Therapy. *Nat Rev Cancer* **2004**, *4*, 806–813.
23. Curti, B. D.; Urba, W. J.; Alvord, G. W.; Janik, J. E.; Smith, J. W.; Madara, K.; Longo, D. L. Interstitial Pressure of Subcutaneous Nodules in Melanoma and Lymphoma Patients: Changes during Treatment. *Cancer research* **1993**, *53*, 2204–2207.
24. Song, X.; Liu, X.; Chi, W.; Liu, Y.; Wei, L.; Wang, X.; Yu, J. Hypoxia-Induced Resistance to Cisplatin and Doxorubicin in Non-Small Cell Lung Cancer Is Inhibited by Silencing of HIF-1α Gene. *Cancer Chemother Pharmacol* **2006**, *58*, 776784.
25. Wojtkowiak, J.; Verduzco, D.; Schramm, K.; Gillies, R. Drug Resistance and Cellular Adaptation to Tumor Acidic pH Microenvironment. *Mol. Pharm.* **2011**, *8*, 2032–2038.
26. Raghunand, N.; Gillies, R. J. pH and Drug Resistance in Tumors. *Drug Resistance Updates* **2000**, *3*, 39–47.
27. Maeda, H. The Enhanced Permeability and Retention (EPR) Effect in Tumor Vasculature: The Key Role of Tumor-Selective Macromolecular Drug Targeting. *Advances in enzyme regulation* **2001**, *41*, 189–207.
28. DeNardo, S. J.; DeNardo, G. L.; Miers, L. A.; Natarajan, A.; Foreman, A. R.; Gruettner, C.; Adamson, G. N.; Ivkov, R. Development of Tumor Targeting Bioprobes ((111)In-Chimeric L6 Monoclonal Antibody Nanoparticles) for Alternating Magnetic Field Cancer Therapy. *Clin. Cancer Res.* **2005**, *11*, 7087s–7092s.
29. Dhar, S.; Gu, F. X.; Langer, R.; Farokhzad, O. C.; Lippard, S. J. Targeted Delivery of Cisplatin to Prostate Cancer Cells by Aptamer Functionalized Pt(IV) Prodrug-PLGA-PEG Nanoparticles. *Proc. Natl. Acad. Sci. U.S.A.* **2008**, *105*, 17356–61.
30. Winer, I.; Wang, S.; Lee, Y.-E.; Lee, Y.-E.; Fan, W.; Gong, Y.; Burgos-Ojeda, D.; Spahlinger, G.; Kopelman, R.; Buckanovich, R. F3-Targeted Cisplatin-Hydrogel Nanoparticles as an Effective Therapeutic That Targets Both Murine and Human Ovarian Tumor Endothelial Cells In Vivo. *Cancer Research* **2010**, *70*, 8674–83.
31. Christian, S.; Pilch, J.; Akerman, M. E.; Porkka, K.; Laakkonen, P.; Ruoslahti, E. Nucleolin Expressed at the Cell Surface Is a Marker of Endothelial Cells in Angiogenic Blood Vessels. *J. Cell Biol.* **2003**, *163*, 871–8.
32. Koo Lee, Y.-E.; Reddy, G.; Bhojani, M.; Schneider, R.; Philbert, M.; Rehemtulla, A.; Ross, B.; Kopelman, R. Brain Cancer Diagnosis and Therapy with Nanoplatforms. *Advanced Drug Delivery Reviews* **2006**, *58*.
33. Wenger, Y.; Schneider, R.; Reddy, G.; Kopelman, R.; Jolliet, O.; Philbert, M. Tissue Distribution and Pharmacokinetics of Stable Polyacrylamide Nanoparticles Following Intravenous Injection in the Rat. *Toxicology and applied pharmacology* **2011**, *251*, 181–90.
34. Barenholz, Y. Doxil®--the First FDA-Approved Nano-Drug: Lessons Learned. *Journal of controlled release : official journal of the Controlled Release Society* **2012**, *160*, 117–34.

35. Qin, M.; Lee, Y.; Ray, A.; Kopelman, R. Overcoming Cancer Multidrug Resistance by Codelivery of Doxorubicin and Verapamil with Hydrogel Nanoparticles. *Macromolecular Bioscience* **2014**, *14*, 1106–1115.
36. Yoon, H.; Lou, X.; Chen, Y.-C.; Lee, Y.-E.; Yoon, E.; Kopelman, R. Nanophotosensitizers Engineered to Generate a Tunable Mix of Reactive Oxygen Species, for Optimizing Photodynamic Therapy, Using a Microfluidic Device. *Chem. Mater.* **2014**, *26*, 1592–1600.
37. US Food and Drug Administration FDA Approves Abraxane for Late-Stage Pancreatic Cancer.
38. Green, M.; Manikhas, G.; Orlov, S.; Afanasyev, B.; Makhson, A.; Bhar, P.; Hawkins, M. Abraxane®, a Novel Cremophor®-Free, Albumin-Bound Particle Form of Paclitaxel for the Treatment of Advanced Non-Small-Cell Lung Cancer. *Annals of Oncology* **2006**, *17*, 1263–1268.
39. Miele, E.; Paolo, G.; Miele, E.; Tomao, F.; Tomao, S. Albumin-Bound Formulation of Paclitaxel (Abraxane® ABI-007) in the Treatment of Breast Cancer. *International journal of nanomedicine 4*, 99.
40. Agarwal, A.; Mackey, M.; El-Sayed, M.; Bellamkonda, R. Remote Triggered Release of Doxorubicin in Tumors by Synergistic Application of Thermosensitive Liposomes and Gold Nanorods. *ACS nano* **2011**, *5*, 4919–26.
41. Woodle, M. Sterically Stabilized Liposome Therapeutics. *Advanced Drug Delivery Reviews* **1995**.
42. Zhu, Z.; Gao, N.; Wang, H.; Sukhishvili, S. Temperature-Triggered on-Demand Drug Release Enabled by Hydrogen-Bonded Multilayers of Block Copolymer Micelles. *Journal of controlled release : official journal of the Controlled Release Society* **2013**, *171*, 73–80.
43. Oberoi, H.; Nukolova, N.; Laquer, F.; Poluektova, L.; Huang, J.; Alnouti, Y.; Yokohira, M.; Arnold, L.; Kabanov, A.; Cohen, S.; *et al.* Cisplatin-Loaded Core Cross-Linked Micelles: Comparative Pharmacokinetics, Antitumor Activity, and Toxicity in Mice. *International journal of nanomedicine* **2011**, *7*, 2557–71.
44. Nishiyama, N.; Yokoyama, M.; Aoyagi, T.; Okano, T.; Sakurai, Y.; Kataoka, K. Preparation and Characterization of Self-Assembled Polymer−Metal Complex Micelle from Cis -Dichlorodiammineplatinum(II) and Poly(ethylene glycol)−Poly(A ,β-Aspartic Acid) Block Copolymer in an Aqueous Medium. *Langmuir* **1999**, *15*.
45. Svenson, S.; Tomalia, D. Dendrimers in Biomedical Applications—reflections on the Field. *Advanced Drug Delivery Reviews* **2012**, *64*, 102115.
46. DUFES, C.; UCHEGBU, I.; SCHATZLEIN, A. Dendrimers in Gene Delivery. *Advanced Drug Delivery Reviews* **2005**, *57*, 2177–2202.
47. Li, S.-D.; Howell, S. CD44-Targeted Microparticles for Delivery of Cisplatin to Peritoneal Metastases. *Molecular pharmaceutics* **2010**, *7*, 280–90.
48. Riedinger, A.; Guardia, P.; Curcio, A.; Garcia, M.; Cingolani, R.; Manna, L.; Pellegrino, T. Subnanometer Local Temperature Probing and Remotely Controlled Drug Release Based on Azo-Functionalized Iron Oxide Nanoparticles. *Nano letters* **2013**, *13*, 2399–406.
49. Li, Y.; Zhu, L.; Liu, Z.; Cheng, R.; Meng, F.; Cui, J.; Ji, S.; Zhong, Z. Reversibly Stabilized Multifunctional Dextran Nanoparticles Efficiently Deliver Doxorubicin into the Nuclei of Cancer Cells. *Angewandte Chemie* **2009**, *121*, 10098–10102.
50. Shirakura, T.; Kelson, T.; Ray, A.; Malyarenko, A.; Kopelman, R. Hydrogel Nanoparticles with Thermally Controlled Drug Release. *ACS macro letters* **2014**, *3*, 602–606.

51. Hah, H. J.; Kim, G.; Lee, Y.-E. K. E.; Orringer, D. A.; Sagher, O.; Philbert, M. A.; Kopelman, R. Methylene Blue-Conjugated Hydrogel Nanoparticles and Tumor-Cell Targeted Photodynamic Therapy. *Macromol Biosci* **2011**, *11*, 90–9.
52. Gao, D.; Xu, H.; Philbert, M.; Kopelman, R. Bioeliminable Nanohydrogels for Drug Delivery. *Nano Lett.* **2008**, *8*, 3320–4.
53. Wang, S.; Kim, G.; Lee, Y.-E. K. E.; Hah, H. J.; Ethirajan, M.; Pandey, R. K.; Kopelman, R. Multifunctional Biodegradable Polyacrylamide Nanocarriers for Cancer Theranostics--a "See and Treat" Strategy. *ACS Nano* **2012**, *6*, 6843–51.
54. Kriwet, B.; Walter, E.; Kissel, T. Synthesis of Bioadhesive Poly(acrylic Acid) Nano- and Microparticles Using an Inverse Emulsion Polymerization Method for the Entrapment of Hydrophilic Drug Candidates. *J Control Release* **1998**, *56*, 149–58.
55. Chen, Y.; Liu, L. Modern Methods for Delivery of Drugs across the Blood-Brain Barrier. *Adv. Drug Deliv. Rev.* **2012**, *64*, 640–65.
56. Poulsen, A.; Arleth, L.; Almdal, K.; Scharff-Poulsen, A. Unusually Large Acrylamide Induced Effect on the Droplet Size in AOT/Brij30 Water-in-Oil Microemulsions. *Journal of colloid and interface science* **2007**, *306*, 143–53.
57. Binks, B. P.; Fletcher, P. D.; Taylor, D. J. Temperature Insensitive Microemulsions. *Langmuir* **1997**, *13*, 7030–7038.
58. Rosenberg, B.; VanCamp, L.; Trosko, J.; Mansour, V. Platinum Compounds: A New Class of Potent Antitumour Agents. *Nature* **1969**, *222*, 385–6.
59. Auzenne, E.; Ghosh, S.; Khodadadian, M.; Rivera, B.; Farquhar, D.; Price, R.; Ravoori, M.; Kundra, V.; Freedman, R.; Klostergaard, J. Hyaluronic Acid-Paclitaxel: Antitumor Efficacy against CD44(+) Human Ovarian Carcinoma Xenografts. *Neoplasia (New York, N.Y.)* **2007**, *9*, 479–86.
60. Baker, S.; Zhao, M.; He, P.; Carducci, M.; Verweij, J.; Sparreboom, A. Simultaneous Analysis of Docetaxel and the Formulation Vehicle Polysorbate 80 in Human Plasma by Liquid Chromatography/tandem Mass Spectrometry. *Analytical Biochemistry* **2004**, *324*.
61. Gao, K.; Sun, J.; Liu, K.; Liu, X.; He, Z. Preparation and Characterization of a Submicron Lipid Emulsion of Docetaxel: Submicron Lipid Emulsion of Docetaxel. *Drug Dev Ind Pharm* **2008**, *34*, 1227–37.
62. Gralla, R.; Itri, L.; Pisko, S.; Squillante, A.; Kelsen, D.; Braun, D.; Bordin, L.; Braun, T.; Young, C. Antiemetic Efficacy of High-Dose Metoclopramide: Randomized Trials with Placebo and Prochlorperazine in Patients with Chemotherapy-Induced Nausea and Vomiting. *New England Journal of Medicine* **1981**, *305*, 905–909.
63. Decatris, M. P.; Sundar, S.; O'Byrne, K. J. Platinum-Based Chemotherapy in Metastatic Breast Cancer: Current Status. *Cancer Treat. Rev.* **2004**, *30*, 53–81.
64. Suzuki, A.; Tanaka, T. Phase Transition in Polymer Gels Induced by Visible Light. *Nature* **1990**, *346*.
65. Mamada, A.; Tanaka, T.; Kungwatchakun, D.; Irie, M. Photoinduced Phase Transition of Gels. *Macromolecules* **1990**, *23*.
66. Peng, J.; Qi, T.; Liao, J.; Chu, B.; Yang, Q.; Li, W.; Qu, Y.; Luo, F.; Qian, Z. Controlled Release of Cisplatin from pH-Thermal Dual Responsive Nanogels. *Biomaterials* **2013**, *34*, 8726–40.
67. Miyata, T.; Asami, N.; Uragami, T. A Reversibly Antigen-Responsive Hydrogel. *Nature* **1999**, *399*, 766–9.

68. Kataoka, K.; Miyazaki, H.; Bunya, M.; Okano, T.; Sakurai, Y. Totally Synthetic Polymer Gels Responding to External Glucose Concentration: Their Preparation and Application to On−Off Regulation of Insulin Release. *Journal of the American Chemical Society* **1998**, *120*.
69. Lin, C.; Zhong, Z.; Lok, M.; Jiang, X.; Hennink, W.; Feijen, J.; Engbersen, J. Novel Bioreducible Poly(amido Amine)s for Highly Efficient Gene Delivery. *Bioconjugate chemistry* **2006**, *18*, 138–45.
70. Go, R. S.; Adjei, A. A. Review of the Comparative Pharmacology and Clinical Activity of Cisplatin and Carboplatin. *Journal of Clinical Oncology* **1999**, *17*, 409–409.
71. Brigger, I.; Dubernet, C.; Couvreur, P. Nanoparticles in Cancer Therapy and Diagnosis. *Adv. Drug Deliv. Rev.* **2002**, *54*, 631–51.
72. Cuvier, C.; Roblot-Treupel, L.; Millot, J. M.; Lizard, G.; Chevillard, S.; Manfait, M.; Couvreur, P.; Poupon, M. F. Doxorubicin-Loaded Nanospheres Bypass Tumor Cell Multidrug Resistance. *Biochemical Pharmacology* **1992**, *44*, 509–517.
73. Larsen, A. K.; Escargueil, A. E.; Skladanowski, A. Resistance Mechanisms Associated with Altered Intracellular Distribution of Anticancer Agents. *Pharmacology & Therapeutics* **2000**, *85*, 217–229.
74. He, C.; Hu, Y.; Yin, L.; Tang, C.; Yin, C. Effects of Particle Size and Surface Charge on Cellular Uptake and Biodistribution of Polymeric Nanoparticles. *Biomaterials* **2010**, *31*, 3657–3666.
75. Fleischer, C.; Payne, C. Nanoparticle Surface Charge Mediates the Cellular Receptors Used by Protein-Nanoparticle Complexes. *The journal of physical chemistry. B* **2012**, *116*, 8901–7.
76. Qin, M.; Hah, H.; Kim, G.; Nie, G.; Lee, Y.-E.; Kopelman, R. Methylene Blue Covalently Loaded Polyacrylamide Nanoparticles for Enhanced Tumor-Targeted Photodynamic Therapy. *Photochemical & photobiological sciences : Official journal of the European Photochemistry Association and the European Society for Photobiology* **2011**, *10*, 832–41.
77. Goldburg, W. I. Dynamic Light Scattering. *American Journal of Physics* **1999**, *67*, 1152–1160.
78. Ware, B. R.; Flygare, W. H. The Simultaneous Measurement of the Electrophoretic Mobility and Diffusion Coefficient in Bovine Serum Albumin Solutions by Light Scattering. *Chemical Physics Letters* **1971**, *12*, 81–85.

–

Chapter 2.

Hydrogel Nanoparticle Matrix Density and Surface Charge Engineering: Tuning Chemodrug Loading, Release, and Cellular Uptake

The material in this chapter has been adapted with minor modifications from the following prospective publication.

Shirakura, T., Smith, C. Koo Lee, Y.-E., and Kopelman R. "Hydrogel Nanoparticle Matrix Density and Surface Charge Engineering: Tuning Chemodrug Loading, Release, and Cellular Uptake." **In preparation.**

Introduction

Cancer is the second highest cause of mortality in recent years in the US.[1] The main cancer treatments include surgery, radiation therapy, chemotherapy and their combinations. Chemotherapy of cancer is a non-invasive and powerful treatment, and cisplatin is one of the most widely used chemodrugs, which has been used to treat breast, ovarian, bladder, lung, and head and neck cancers.[2,3] On the other hand, it is also known that many types of cancer show resistance to cisplatin because of the cells' high expression of drug-efflux pumps, enhanced DNA repair mechanisms, avoidance of apoptosis, or high concentration of reducing agents or chloride ions, all together called multi-drug resistance (MDR).[4–7] An increase in the dose of cisplatin is helpful to override MDR. However, administering a globally high dose of cisplatin is likely to

cause serious side effects, due to its high reactivity to any types of rapidly dividing cells.[8] Therefore, a targeted delivery of cisplatin to cancer tumor is necessary so as to override MDR with an enhanced local dose, and, at the same time, to avoid an increased global dose that would results in side effects.

A *targeted* delivery of cisplatin to cancerous tumors via nanoparticles (NPs) can potentially achieve the required locally high dose of cisplatin in the tumors. The targeting ability of NPs to the tumor area depends on two different types of targeting mechanisms: active targeting and passive targeting. Active targeting utilizes antibody,[9] aptamer,[3] or peptide[10] conjugated NPs, so as to aim at receptors or biomarker that are highly expressed on the surface of cancer cells. On the other hand, passive targeting relies on the accumulation of macromolecules such as NPs in the tumors due to the so called "enhanced permeability and retention (EPR)" effect.[11,12]

Furthermore, the NP-based delivery can inherently avoid MDR, as NPs are taken up in the cells' endocytotic vesicles, and therefore, they and their contents are not immediately accessible to the efflux pumps located in the cellular membrane, unlike molecular drugs that diffuse in through the cell membrane.[13–16] Also, the large number of drug molecules released by one NP may overload the cell's efflux capacity.

Many groups have developed various types of nanoplatforms for cisplatin delivery, such as PLGA,[3] hyaluronic acid,[17] lipid[8,18,19] or block copolymer.[20,21] Our group has made various types of polyacrylamide-based NPs (PAA-NPs) for cancer diagnosis[13,22–24] and therapy,[10,25,26] due to its ideal characteristics as a platform drug delivery system. PAA-NPs have proven to be biocompatible both *in vitro* and *in vivo*.[10,27] In addition, the hydrophilicity and the surface charge of the NPs can be easy manipulated by changing the type and relative ratio of acrylamide

derivative monomers in the synthesis.[28] This high engineerability also allows for the conjugation of many different types of cancer-targeting moieties onto the surface of PAA-NPs for the active targeting.[10,29] We previously showed that cisplatin-loaded hydrogel NPs could target SKOV3 ovarian cancer and successfully shrink the tumor size, while free cisplatin had no effect at all on the tumor growth due to this tumors' known cisplatin resistance.[10]

Kinetically controlled release of the drugs is important for optimal drug delivery so that the NPs do not release drugs while still circulating in the blood-stream but release most of the drugs when reaching at the tumor area. Such temporally and spatially controlled release behavior can avoid, or at least reduce, the side effects that are associated with globally high doses of cisplatin.[29]

The drug release behavior of hydrogel can be tuned by changing its mesh size, porosity, tortuosity, and hydration rate.[30,31] In NP-based drug delivery systems, the mesh size plays an important role.[29,32,33] The mesh size is defined by the distance between two polymeric chain cross-linkers, which can be defined by equation 1.[32]

$$\xi = Q^{\frac{1}{3}}\left[C_n \frac{2\overline{M_C}}{M_r}\right]^{\frac{1}{2}} \qquad \text{Equation (1)}$$

Here, Q is the swell ratio of the matrix, C_n is the Flory characteristic ratio of the hydrogel, which describes the flexibility of the chain,[34] M_c is the average molecular weight of a chain between cross-linkers, and M_r is the molecular weight of a repeating unit. NPs with bigger mesh size release the drugs faster.[33]

The cross-linkers can be classified in two types: chemical and physical. In the typical hydrogel NPs, they coexist.[31] Chemical cross-linkers, such as tetraethylene glycol dimethacrylate,[32] or poly(ethylene glycol) dimethacrylate,[35] form rigid connections between polymer chains by forming covalent bonding. On the other hand, physical cross-linkers form

weak and reversible connections.[31] Some examples are hydrogen bonding, ionic bonding and crystallite formations. [31]

One approach to change the mesh size (i.e. tune the drug-release kinetics) is varying the relative ratio of chemical cross-linker in the hydrogel (i.e. change M_c in Equation 1).[32,35] This approach changes the distance between cross-linkers *permanently,* by varying the number of chemical cross-linkers.

Another approach is to make physical cross-linkers sensitive to the surrounding environment, such as pH and temperature.[36–38] By forming hydrogen bonding, by incorporating charged or polar components in the matrix, the hydrogen bonding can be broken upon change in environment.[38] This approach changes the distance between cross-linkers *temporarily* and *reversibly,* by varying the number of physical cross-linkers.

As an example of controlling drug release from NPs by environment-sensitive physical cross-linking, we previously reported poly(acrylamide-*co*-acrylic acid) hydrogels as carriers of cisplatin.[37] These NPs have a temperature-sensitive property, and swell as the temperature of the matrix increases, by cutting the physical cross-linking due to hydrogen bonding. This reduces the NPs' matrix density. The matrix density is directly related to the mesh size, because a denser matrix can form more physical cross-linking inside. Thus, the reduction of the matrix density increases the mesh size, and enhances the release of cisplatin from the NPs.[33]

However, these environment-responsive NPs turn on/off the drug release typically due to a combination of various factors. For example, in our system (will be further discussed in chapter 2), the enhancement of the release at higher temperature was a combination effect, including the expansion of the matrix volume (i.e. decline of the matrix density), faster diffusion of drugs and ions, and an enhanced kinetics of a chemical reaction of detaching cisplatin from the matrix.

Therefore, in order to further understand just the effect of the matrix density on the release profile, it is necessary to develop NPs where the release depends only on the NP matrix density.

Here, we synthesized distinct PAA-NPs that had a similar size, but different matrix density, and compared their release profile. The synthesis was done by using the property of the reverse micelle polymerization method, where the size of the synthesized NPs depends on the formed micelle size, but is little affected by the NP ingredients within the range of concentration of NPs forming ingredients we utilized.[10,39] This enables the synthesis of NPs that have similar degrees of chemical cross-linking, but different degrees of physical cross-linking, due to an increase of the empty space in the matrix. This can 1) mimic the situation of the swollen state of environment-responsive NPs, which would change the degree of physical cross-linking while maintaining the chemical cross-linking; 2) change the mesh size more drastically than the method of adjusting the ratio of the chemical cross-linkers.

Utilizing this system, we evaluated the effect of changing the matrix density of the NPs, so as to tune the release profile of cisplatin from two commonly used PAA NPs: amine-functionalized and carboxyl-functionalized.[10,28,37] Carboxyl-functionalized NPs loaded with more cisplatin and released more cisplatin, in a given time, than amine-functionalized NPs. More importantly, the synthesized NPs showed the similar cisplatin loading capacities regardless of the matrix density, but the kinetics of their cisplatin release showed an inverse relationship with their matrix density in both types of NPs. In other words, we successfully changed the release profile of cisplatin from the NPs while maintaining their drug-loading ability. Also, we evaluated the effect of the surface charge and chemistry of NPs on their cellular uptake, the latter being another important aspect of NPs' cytotoxicity, which we investigated on a *cisplatin-resistant cell line*, SKOV3.[10]

Materials and Methods.

Materials.

Cisplatin was purchased from Selleck Chemical LLC. RPMI media was purchased from Invitrogen. All other chemicals were purchased from Sigma-Aldrich. The de-ionized water used in this experiment was purified prior to the experiment, using a Milli-Q system from Millipore.

Preparation of Blank Poly(acrylamide-*co*-N-(3-aminopropyl)methacrylamide) NPs.

P(AAm-*co*-APMA) NPs were synthesized reverse micelle polymerization technique modifying the method described by Winer[10]. Briefly, 1.6 g of dioctyl sulfosuccinate (AOT) and 3.47 mL of Brij30 were added to 45 mL of argon-purged hexane, and continued to be stirred and purged with argon for 20 minutes in a round bottom flask. The mixture of acrylamide (AAm), N-(3-aminopropyl)methacrylamide hydrochloride (APMA), and 3-(acryloyoxy)-2-hydroxypropylmethacrylate (AHM) in 1.3 mL of water were added to the flask, and stirred and purged for additional 20 minutes. The polymerization was initiated by adding 100 μL of 10(w/v)% ammonium persulfate (APS) and N,N,N',N'-tetramethylethylenediamine (TEMED). After 2 hours, the polymerization was terminated by introducing the atmospheric oxygen. Hexane was removed by rotary evaporation. The remaining products were washed, in an Amicon stirred cell (Millipore), 5 times with 150 mL of ethanol and 5 times with 150 mL of water using 300 kDa MW cut-off membrane. The obtained solution was filtered through 0.2 μm pore size filter, and was lyophilized for 72 hours for the long term storage.

Preparation of Blank Poly(acrylamide-*co*-acrylic acid) NPs.

p(AAm-*co*-AA) NPs were synthesized in the same method as p(AAm-co-APMA) NPs with slight modifications. 4.8 g of dioctyl sulfosuccinate and 9.5 mL Brij30 were added to 120 mL of argon-purged hexane, and continued to be stirred and purged with argon for 40 minutes. The polymerization was initiated by adding 100 μL of 50(w/v)% APS and TEMED. After 4 hours, the polymerization was terminated by introducing the atmospheric oxygen. Hexane was removed by rotary evaporation. The remaining products were washed in an Amicon stirred cell (Millipore) 7 times with 150 mL of ethanol and 5 times with 150 mL of water using 300 kDa MW cut-off membrane. The obtained solution was filtered through 0.2 μm pore size filter, and was lyophilized for 72 hours for the long term storage.

Loading of Cisplatin into Blank NPs.

10 mg of NPs were mixed with 2 mg of cisplatin dissolved in 1 mL of water. For the loading to p(AAm-*co*-APMA) NPs, 25 mM NaOH was also added to enhance the reaction between the carboxyl group in the NPs and cisplatin. In case of the room temperature loading, the mixture was kept for 3 days at the room temperature. Then, unbound cisplatin was removed by washing the NPs 7 times with 7 mL of water using 100 kDa MW cut-off centrifugal membrane (Millipore). In case of the high temperature loading, the mixture was kept in 90 °C oil bath for 4 hours. Then, unbound cisplatin was removed in the same procedure as the NPs preparation in case of the room temperature loading. The amounts of cisplatin loaded onto NPs were quantified using inductively coupled plasma – optical emission spectroscopy (ICP-OES).

Size and Zeta-potential Measurement.

Dynamic light scattering was applied to measure the hydrodynamic size and the zeta-potential of NPs using a Delsa Nano C (Beckman Coulter). The size of NPs was measured in PBS (pH 7.4), while the zeta-potential of NPs was measured in water.

Cisplatin Release Study.

The amount of cisplatin released from the NPs over 72 h was evaluated in phosphate buffer saline (PBS) (pH 7.4). NPs suspensions in PBS were prepared in the way that the concentration of cisplatin was 25 μg/mL. 6 of 1.5 mL Ependorf tubes were prepared, and 1 mL of the NPs suspension was transferred to the tubes. The tubes were kept at 37 °C until a specific time points: 0 hours, 6 hours, 12 hours, 24 hours and 48 hours. At the specific time points, one tube was filtered using 100 kDa MW cut-off centrifugal membrane, and collected the filtrate. The cisplatin concentration in the filtrates were quantified using ICP-OES.

Cellular Cisplatin Uptake Assay.

SKOV3 cells were cultivated in a 100 x 20 mm Petri dish to over 80 % confluency. 700 μL of cisplatin-loaded NPs were prepared in PBS with a cisplatin concentration of 25 μg mL^{-1}, and mixed with cells in a Petri dish containing 5 mL of complete RPMI. The cells were incubated with NPs for 12 hours, and harvested after that. The populations on the Petri dishes were counted, and the Pt content in the cells was measured using ICP-OES. The Pt content per cell was calculated.

Results and Discussion.

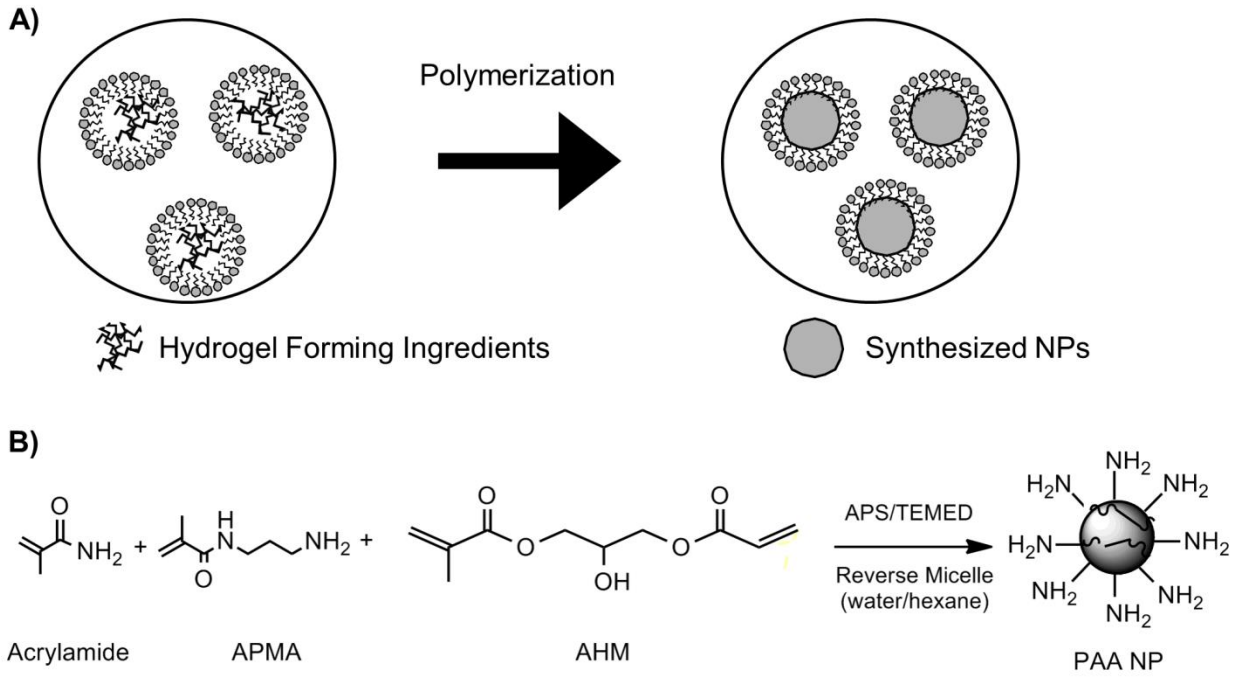

Scheme 2.1. Synthesis Scheme of p(AAm-co-APMA). A) Hydrogel forming ingredients are trapped inside the water droplets surrounded by micelles in the hexane bath. After the polymerization, NPs, with the size of the micelles are formed. B) Hydrogel forming ingredients are acrylamide (AAm), APMA, and AHM.

The cisplatin-loaded NPs were prepared in two steps: 1) synthesis of the blank NPs and 2) post-loading of cisplatin into the blank NPs. This method enabled high loading of cisplatin, because blank NPs can be mixed with high concentrations of cisplatin, which otherwise would disrupt the microemulsion system (used in our previous synthesis had cisplatin been pre-loaded [10]).

Temperature Dependency of Cisplatin Loading.

As a first step, in order to efficiently load cisplatin into the NPs, we investigated the relationship between the loading temperature and the wt% loading of cisplatin. We compared the loading of cisplatin at two different temperatures, utilizing the blank p(AAm-*co*-APMA) NPs.

High temperature is known to help improve the loading efficiency and also prevents the potential aggregation of NPs during the loading.[17] When cisplatin was loaded at room temperature (22 °C), the loading of cisplatin was 0.58%, while when cisplatin was loaded into NPs at high temperature (90 °C), the loading was 5.63%. Thus, almost 10 times higher loading of cisplatin was achieved at the elevated loading temperature. The higher the temperature, the more flexible the NPs matrix becomes, thus the cisplatin molecules can migrate further inside the hydrogel NPs.[37] Because of this high loading, we chose 90 °C as the loading temperature for the rest of the experiments.

Synthesis of PAA-NPs of Different Matrix Density.

In order to adjust the matrix density, NPs were synthesized with the so-called reverse micelle (w/o) emulsion method (Scheme 2.1A). In our system, the nano-sized water droplets, which contained monomers and cross-linkers, were coated by surfactants in the hexane. The free radical polymerization was performed, so as to form NPs inside the water droplets. The size of the water droplets is the critical factor for tuning the size of the synthesized NPs. One advantage of using this synthesis system was its ease in keeping the size of NPs constant, while changing the matrix density of the NPs. The matrix density was adjusted by changing the concentration of NP forming ingredients in the water phase, while keeping the solvent amount of the water phase fixed. We assume that the percent production yield of the NPs should be similar regardless of the concentration change. Using this method, we synthesized NPs that have different matrix densities as well as different compositions.

Table 2.1. Summary of NPs Formulations. A) NPs' composition in different categories of NPs; B) Varying densities for each distinct formulation of NPs. Abbreviations: AAm, acrylamide; AA, acrylic acid; APMA, N-(3-aminopropyl)methacrylamide; AHM, 3-(acryloyoxy)-2-hydroxypropylmethacrylate.

A. NPs Composition.

p(AAm-co-APMA)	mol %	p(AAm-co-AA) #1	mol %	p (AAm-co-AA) #2	mol %
AAm	81.3	AAm	81.3	AAm	71.5
APMA	2.5	AA	2.5	AA	15.2
AHM	16.2	AHM	16.2	AHM	13.3

B. NPs Matrix Density

p(AAm-co-APMA)	p(AAm-co-AA) #1	p(AAm-co-AA) # 2
8.4%	16%	4.9%
31%	25%	21 %
48%	40%	34%

The NPs formulations and their matrix densities are summarized in Table 2.1. The NP matrix density is estimated by the following equation (Equation 2).

$$\rho = \frac{A}{A+B} \times 100\ (\%), \qquad \text{Equation 2.}$$

Here, ρ is the matrix density, A is the weight of hydrogel forming ingredients, and B is the weight of aqueous solvent during the synthesis.

Loading of Cisplatin to AHM-APMA-AAm of Different Matrix Density.

First, p(AAm-co-APMA) NPs of different matrix density were synthesized (Scheme 2.1B) and were loaded with cisplatin. The result of the loading is summarized in Table 2.2. Interestingly, the wt% loading of cisplatin did not change with NPs of different polymer densities. The size of the NPs shrunk after the loading with cisplatin, possibly because cisplatin acts as a cross-linker, and also retracts polymer chains physically.[31] The sizes of the cisplatin-loaded NPs

of different matrix densities were similar, as is expected because the sizes of the micelles during the synthesis were similar. No change of ζ-potential was observed after the loading of cisplatin.

Table 2.2. Cisplatin loading to the p(AHM-APMA-AAm) NPs with different matrix density. The densities of NPs are defined by percentage, using equation 2.

	Blank			cisplatin-loaded			wt % loading
	size (nm)	PDI	ζ-potential (mV)	size (nm)	PDI	ζ-potential (mV)	
8.4 % NPs	40 (±0)	0.25 (±0.01)	10.3(± 1.6)	41 (±5)	0.27 (±0.02)	15.1(± 1)	4.7(± 0.5)
31 % NPs	47 (±3)	0.23 (±0.06)	18.1(± 0.9)	37 (±1)	0.19 (±0.03)	18.7(± 4.1)	5.9(± 0.8)
48 % NPs	63 (±1)	0.16 (±0.04)	30.5(± 1.9)	55 (±9)	0.17 (±0.07)	35.9(± 6.5)	5.2(± 0.7)

Release Profile of Cisplatin Loaded p(AAm-co-APMA) NPs.

The release profile of cisplatin from p(AAm-co-APMA) NPs of different matrix densities was investigated (Figure 2.1). The cisplatin-loaded 8.4 % NPs had significantly higher percent release of cisplatin than cisplatin-loaded 31 % and cisplatin-loaded 48 %, which should result from the looser matrix structure. However, we did not observe a significant difference in the % release of cisplatin between 48 % NPs and 31 % NPs. The change of the matrix density may not be significant enough to observe a notable change in the release profile.

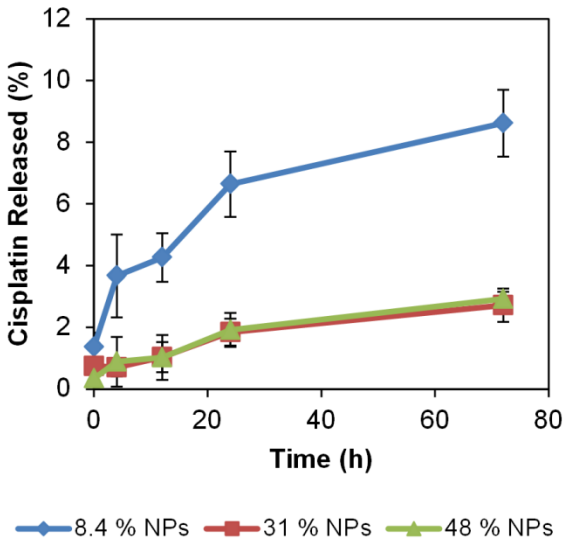

Figure 2.1. Cisplatin Release from cisplatin-loaded p(AAm-*co*-APMA) NPs over Time. The

release study was performed in PBS. The error bars represents the standard deviations of the measurement.

Also, Equation 3 was applied to fit each of the release curves, so as to calculate the effective diffusion coefficient (*D*). The fit data are shown in Figure 2.2. Note that before fitting the equation, each data set was normalized, by subtracting from the released cisplatin at different time points the release amount at time 0.

$$\frac{M_t}{M_\infty} = 1 - \frac{6}{\pi}\sum_{n=1}^{\infty}\frac{1}{n^2} exp\left[\frac{-Dn^2\pi^2 t}{a^2}\right] + C \qquad \text{Equation (3)}^{40}$$

Here, $\frac{M_t}{M_\infty}$ represents the release ratio at time *t*, *D* is the effective diffusion coefficient of the cisplatin, *a* is the radius of the NPs and *C* is the fraction of cisplatin that is released during the initial burst release.

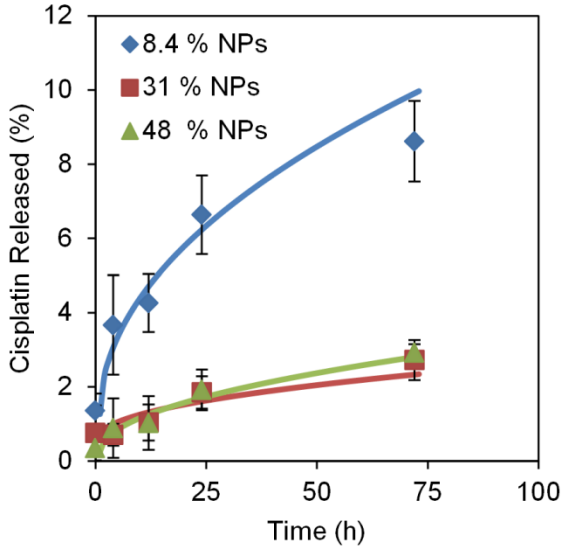

Figure 2.2. Fitted Data of Cisplatin Release from p(AAm-*co*-APMA). The dots represent the experimental data, while the lines represent the fitted curve using equation 3. Note that the absolute release pattern is similar to the % release pattern, within error, due to the similar loadings of the 3 NP categories, i.e., the 8.4% NPs give the highest release, by far.

The calculated *D*s are summarized in Table 2.3. The 8.4 % NPs had the highest *D*. This is attributed to the lowest density of 8.4 % NPs. On the other hand, 31 % NPs had lower diffusion

coefficient than 48 % NPs. This contradicts the design expectations. However, the difference could be within the error range (see the low R^2 value for the 24 % NPs).

Table 2.3. The effective diffusion coefficient of NPs of different densities.

NPs Density (%)	D (10^{-23} m^2 s^{-1})	R^2
8.4	0.11	0.96
31	$3.3x10^{-03}$	0.77
48	$1.7x10^{-02}$	0.91

We can conclude that the AHM-APMA-AAm NPs' cisplatin release could be tuned by changing the NP matrix density.

Construction of AHM-AA-AAm NPs.

As a next step, we evaluated the effect of the change of monomers mixed with acrylamide to further improve the loading and release of cisplatin (Scheme 2.2A). It has been reported that cisplatin chemically binds to the carboxyl groups in the absence of the Cl^{-1} ion (Scheme 2B).[41] In the presence of Cl^{-1}, such as in the body, or hydronium ions, such as inside cellular lysosomes, the carboxyl group binding to the platinum center of the cisplatin is substituted back by Cl^- or replaced with H^+, which results in the release of cisplatin from the NPs. Utilizing this chemical conjugation, the loading of cisplatin can be further increased.[37]

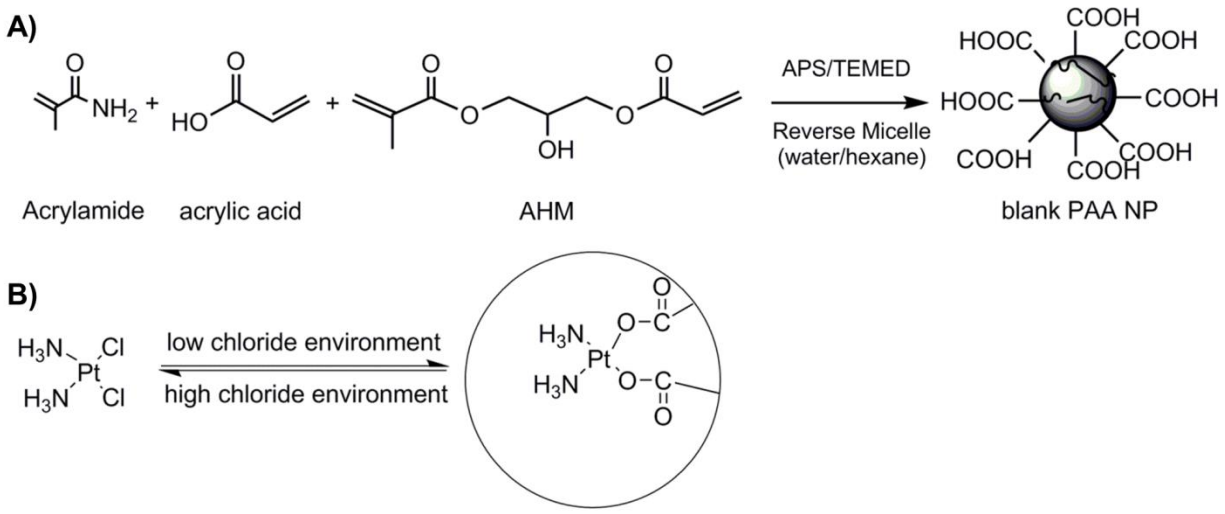

Scheme 2.2. Synthesis Scheme of p(AAm-co-AA). A) NPs forming ingredients are acrylamide, acrylic acid (AA), and AHM. B) Cisplatin chemically and reversibly binds to the NPs via the carboxyl groups on the NPs.

Table 2.4. Cisplatin loading into p(AHM-AA-AAm) NPs at different matrix densities. The densities of NPs are defined by percentage using equation 2.

	blank			cisplatin-loaded			wt % loading
	size (nm)	PDI	ζ-potential (mV)	size (nm)	PDI	ζ-potential (mV)	
4.9 % NPs	135 (± 5)	0.28 (± 0.03)	-39.9(± 2.7)	98 (±2)	0.26 (±0.08)	-44.8(± 2)	11.4(± 0.2)
21 % NPs	39 (± 1)	0.26 (± 0.03)	-35.8(± 1.9)	39 (±2)	0.39 (±0.14)	-51(± 5.3)	9.9(± 0.9)
34 % NPs	36 (± 1)	0.16 (± 0.01)	-45.6(± 5.7)	43 (±3)	0.24 (±0.06)	-46(± 1.6)	10.3(± 2.1)

First, we constructed NPs by substituting APMA with AA without changing the molar ratio of the composing ingredients (p(AAm-*co*-AA) #1 of Table 2.1B). Into these NPs, cisplatin could not be loaded either at room temperature or at high temperature. These NPs formed aggregates during the loading procedure, possibly due to the loss of surface charge, presumably because of too much consumption of carboxylic groups by cisplatin. Therefore, the molar percentage of acrylic acid was increased (2.5% to 15%) so as to increase the stability. Also, in this new category of NPs, we slightly reduced the amount of cross-linkers from 16 % to 13 % (p(AAm-*co*-AA) #2 of Table 2.1B). With this new ratio of the ingredients, we attempted to load cisplatin into these NPs.

When cisplatin was loaded to the above NPs at high temperature, no aggregation was

observed, whereas for the loading at room temperature, aggregation of the NPs was still observed. Also, it is reported that cisplatin can be more easily loaded into carboxyl group containing NPs under basic conditions; therefore, cisplatin was loaded into NPs in the presence of 25 mM NaOH.[36,42] The result of the loading is summarized in Table 2.4. The sizes of the NPs were measured after loading with cisplatin. The 21 % NPs and 34 % NPs showed relatively similar NP sizes (Table 2.4). On the other hand, the 4.9 % NPs had considerably larger sizes than the other two NPs categories. This could be because of the swelling of the NPs due to the low cross-linking of their matrix, as well as their high negative charge in the aqueous solvent, where there is no surfactant to restrict their size. Because the 4.9 % NPs were 4 times bigger size than the other NPs (Table 2.4), the density of 4.9 % is expected to be 8 times lower than the theoretical density.

As a next step, the cisplatin release profiles of the 21 % NPs and 34 % NPs were evaluated (Figure 2.3).

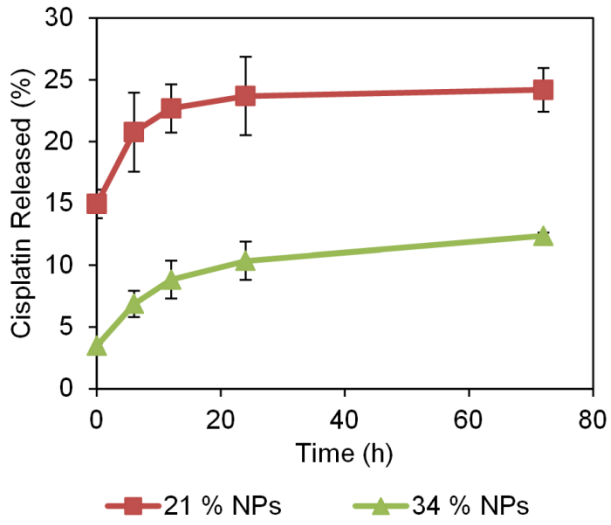

Figure 2.3. Cisplatin Release from cisplatin-loaded p(AAm-*co*-AA) NPs over Time. The error bars represent the standard deviation of the mean.

As we observed in the case of the AHM-APMA-AAm NPs, 21 % NPs released more

cisplatin than the 34%. However, the 21 % NPs had an initial burst release of cisplatin, possibly due to its loose matrix. This could be due to the much larger size of the NPs, which can significantly slow down the release kinetics of the NPs (Equation 3).

The effective diffusion coefficients (*D*) of the NPs were calculated, using Equation 3, so as to understand the relationship between the matrix density of the NPs and its effective diffusion coefficient. In order to calculate the effective diffusion coefficient, the released cisplatin at each time point was subtracted by the percent of cisplatin released during the initial burst.

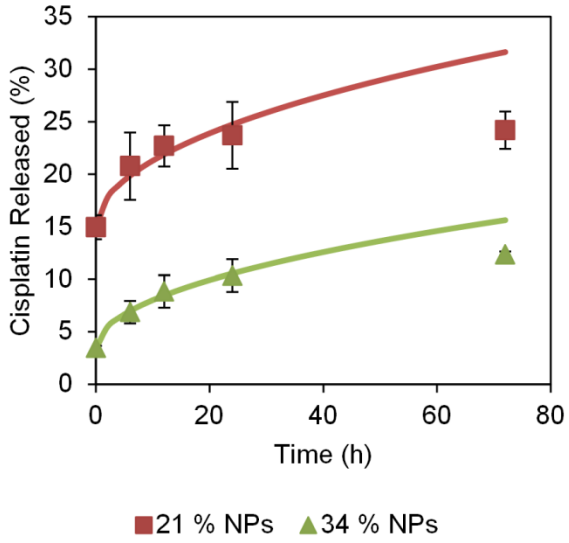

Figure 2.4. Fitted Data of Cisplatin Release from poly(AAm-co-AA). The dots represent the experimental data, while the lines represent the fitted curves, using equation 3. The experimental data up to 24 h was used to fit the data.

Table 2.5. The effective cisplatin diffusion coefficients for NPs of different densities.

NPs Density (%)	D (10^{-23} m^2 s^{-1})	R^2	Size (nm)
4.9	0.63	0.96	98 (±2)
21	0.39	0.94	39 (±2)
34	0.25	0.99	43 (±3)

The 34 % NPs had a smaller effective diffusion coefficient than the 34 % NPs, which is consistent with our intended design of the NPs and their release profile data (Figure 2.3). Also,

we calculated *D* for 4.9 % NPs as well. Even though the 21 % NPs showed the fastest release kinetics, the 4.9 % NPs had a higher effective diffusion coefficient. This is due to the size difference between 4.9 % NPs and 21 % NPs; the 4.9 % NPs are 2.5 times bigger than the 21 % NPs, on average (Table 2.5). The larger size of an NP slows down the release kinetics from the NP, because cisplatin molecules need to migrate over a longer distance inside the NP (Equation 3).

Comparison of Cellular Uptake between Amine-functionalized NPs and Carboxyl-functionalized NPs.

Cellular uptake is another important aspect of designing a highly effective drug delivery system, because releasing drugs inside the cells means that drugs are released closer to the site of action as well as that the NPs may overcome the MDR of cancer cells.[14,43] We evaluated how the difference in the surface of NPs affects the cellular uptake. The cellular uptake of cisplatin was compared between cisplatin-loaded 31 % p(AAm-*co*-APMA) NPs and cisplatin-loaded 21 % p(AAm-*co*-AA) NPs, where the percentages refer to the matrix density defined by Equation 2 (Figure 2.**5**).

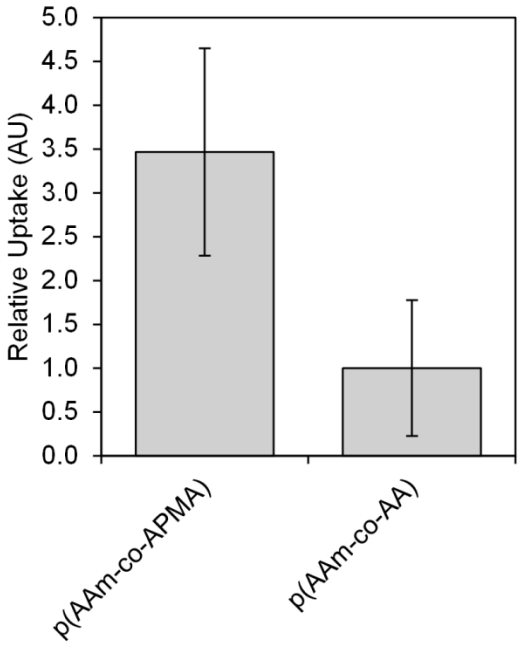

Figure 2.5. Cellular Uptake Study of Cisplatin from Positively Charged NPs and Negatively Charged NPs. The data is normalized to the cellular uptake of p(AAm-*co*-AA). The 31 % p(AAm-*co*-APMA) NPs and 21 % p(AAm-*co*-AA) NPs were picked for the experiment; the percentages refer to the matrix density.

There is an almost 3.5 times higher uptake of cisplatin when p(AAm-*co*-APMA) NPs were used as drug carriers than when p(AAm-*co*-AA) NPs were used. This higher cellular uptake of p(AAm-*co*-APMA) NPs is probably due to the preferable interaction of amine-functionalized NPs with cellular membranes, by electrostatic interactions, as well as by the enhancement by albumin.[44,45]

Summary and Conclusion.

Understanding the behavior of Drug-loaded NPs, such as drug release and cellular uptake, in tumor area is important for the development of highly potent NPs; especially, controlling the release profile of cisplatin from hydrogel NPs by tuning their matrix density was out interest. We used a simple method of changing the matrix density, utilizing the nature of the NPs synthesis by

employing reverse micelle polymerization. Two different formulations, p(AAm-*co*-APMA) NPs and p(AAm-*co*-AA) NPs, were tested for their release profile and cellular uptake, as function of their matrix density defined by equation 2. Both formulations showed an inverse relationship between their matrix density and their effective cisplatin diffusion coefficient, which has positive correlation with the mesh size of the NPs' matrix, which is one of the critical factors determining the release kinetics of the NPs. P(AAm-*co*-AA) NPs had a better loading of cisplatin, as well as a faster and higher release of cisplatin than p(AAm-*co*-APMA) NPs. The P(AAm-*co*-APMA) NPs showed higher cellular uptake than the p(AAm-*co*-APMA) NPs, presumably due to their amine-functionalization, which can facilitate the cellular uptake, via an electrostatic interaction with cell membranes, and assisted by albumin.[44,45] Precise control of drug release, which can be achieved by changing the NPs' matrix density, as well as the high cellular uptake, should enhance the efficacy of NP-assisted chemotherapy. We will evaluate the cytotoxicity of these formulations of NPs; such as study would be helpful to elucidate the balance among loading, release and cellular uptake.

Also, these observations give some insights into the swelling behavior of environment-responsive NPs. The matrix density had an inverse correlation with the release kinetics (or mesh size), and this confirms the potency of UCST-like NPs as drug carriers.[37] An initial burst release of cisplatin was observed for the 21 % NPs, but not for the 34 % NPs. This implies that the initial burst release is a phenomenon having an inverse correlation with the matrix density. It indicates that a similar burst release might occur in environment-responsive NPs, and environment-responsive NPs might release a significant amount of drugs rapidly, immediately after the surrounding environment changes.

Acknowledgements.

Financial Support was provided by a National Institutes of Health grant, R21NS084275 (RK). The authors thank James Windak in the Michigan Chemistry Instrument Shop for his instrumental support.

Appendix

Preliminary Cytotoxicity of Cisplatin-loaded NPs.

We evaluated the cytotoxicity of the synthesized NPs so as to evaluate the feasibility of our NP design.

Methods

Cytotoxicity Assay of Cisplatin-loaded NPs.

The human ovarian cancer cell line, SKOV3, was cultivated in RPMI with supplementation of 1 % of penicillin, streptomycin and glutamine and 10% of heat inactivated fetal bovine serum (HI-FBS). 2000 cells of SKOV3 cells were transferred to each well of 96-well plates. After 24 hours incubation, the cells settled down and NPs were added. 12 hours after the addition, the cell media containing the NPs were removed, rinsed twice with Dulbecco's Phosphate-Buffered Saline (DPBS), and added fresh 200 μL of complete RPMI. 48 hours later, the cell media were removed from the wells. Then 120 μL of 0.833 mg mL^{-1} MTT reagent in RPMI, without phenol red and HI-FBS, was added, and incubated for 4 hours. After the incubation, the media was removed from the wells, and 100 μL of dimethyl sulfoxide was added to the wells. 1 hour later, the absorbance at 550 nm from the wells was measured using 620 nm as a reference, utilizing a microplate reader (Anthos 2010, biochrom).

Results

Cytotoxicity Study of the NPs.

We evaluated the cytotoxicity of these cisplatin-loaded NPs using SKOV3, a cisplatin resistant ovarian cancer cell line (Appendix Figure 2.1)[10]. The 8.4 % NPs showed the highest

cytotoxicity, which is consistent with their highest cisplatin release (Figure 2.1). There was no significant difference in the cell viability between the 31 % NPs and 48 % NPs, which agrees with their similar cisplatin release. We note that no toxicity due to the blank NPs was observed, in this range of the concentration (Appendix Figure 2.2). Also, the IC_{50} values of these NPs was higher than that of free cisplatin (Appendix Figure 2.3), due to the low percent release of cisplatin from NPs. Note that this result did not take the targeting ability of NPs into consideration; therefore, these NPs may work significantly better *in vivo*, significantly increasing the local concentration at the tumor, compared to the global concentration, and thus also the therapeutic index.

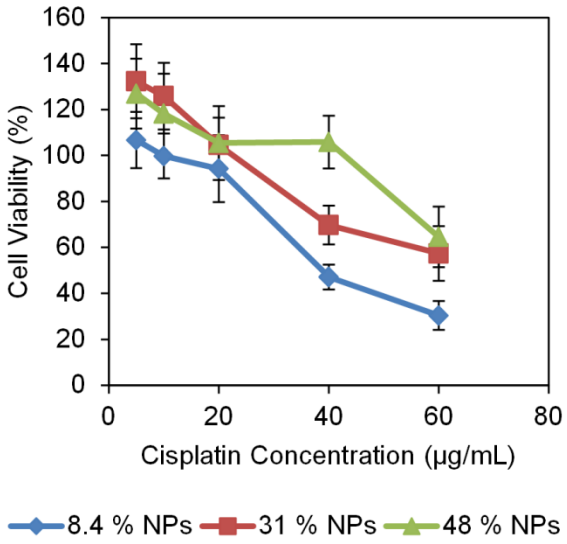

Appendix Figure 2.1. Cytotoxicity Study of Cisplatin-loaded p(AAm-co-APMA) NPs. SKOV3 cells were treated with cisplatin-loaded NPs for 12 hours followed by the extra 48 hours incubation after removing NPs from the cell media. The data is normalized to the viability of the cells that were treated with just PBS. The error bars represent the standard deviation of the mean.

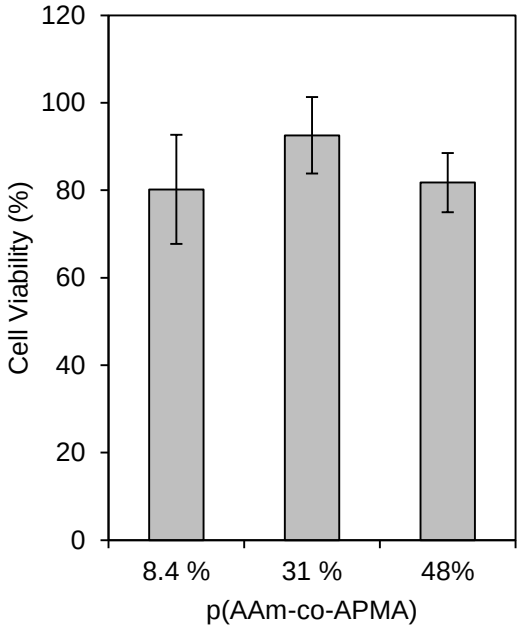

Appendix Figure 2.2. The Cytotoxicity of blank p(AAm-*co*-APMA) NPs. The NP concentration used in this experiment was 1.2 mg mL^{-1}, which is similar to the concentration of the NPs at the *highest* dose shown in Appendix Figure 2.1. The data is normalized to the population of the cells that were treated with PBS. The error bars represent the standard deviations of the mean.

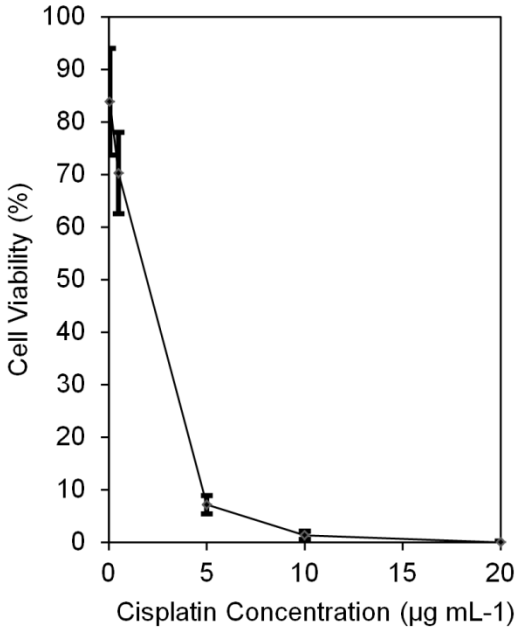

Appendix Figure 2.3. The Cytotoxicity of Free Cisplatin to SKOV3 ovarian cancer cell line. The data is normalized to the population of the cells that were treated with only PBS. The error bars represent the standard deviations from the mean.

Cytotoxicity Study of p(AAm-co-AA) NPs.

Based on the release study, the cytotoxicity assay was performed again using SKOV3 cells (Appendix Figure 2.4 and Appendix Figure 2.5). There was not a significant difference between the three types of NPs, which is against our expectation that 21 % NPs should have shown the highest cytotoxicity.

This could be because SKOV3 is a cisplatin resistant cell line, and cisplatin released prior to the cellular uptake did not significant cytotoxicity. The 21 % NPs had the biggest difference in the amount of released cisplatin at the initial/very early time point, which represents cisplatin released prior to the cellular uptake, compared to the other two NPs. On the other hand, there were milder differences in the amount of released cisplatin among the three NPs for the rest of the time, which presumably represents cisplatin released inside the cells (Figure 2.3) Thus, in the case of the 21 % NPs, a significant amount of cisplatin might be released even before entering the cells, and those drugs were not effective possibly due to SKOV3's cisplatin resistance while cisplatin in the NPs worked better by overcoming the resistance.[10,13–16]

Also, it should be noted that the range of cisplatin concentration we tested for p(AAm-*co*-AA) NPs was the same as that of the p(AAm-*co*-APMA) NPs, and no clear difference in the dose response is observed between these two types of NP formulations, even though p(AAm-*co*-AA) releases more cisplatin in 72 hours (about 5 times).

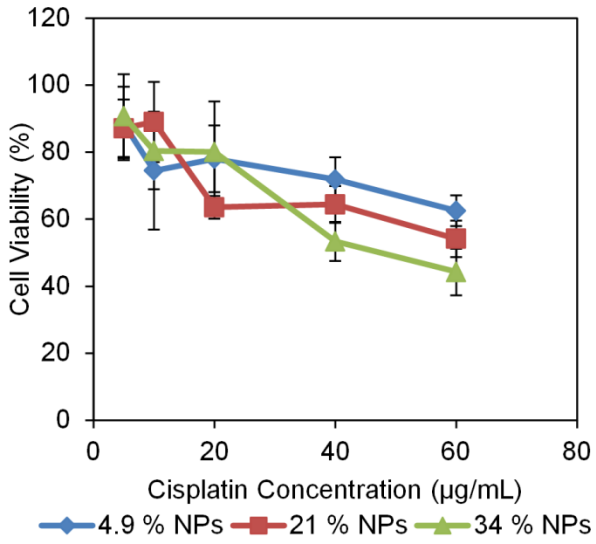

Appendix Figure 2.4. Cytotoxicity Study of Cisplatin-loaded p(AAm-*co*-AA) NPs. SKOV3 cells were treated with cisplatin-loaded NPs for 12 hours, followed by an extra 48 hours incubation period, after removing NPs from the cell media. The data is normalized to the viability of the cells that were treated with PBS. The error bars represent the standard deviation from the mean.

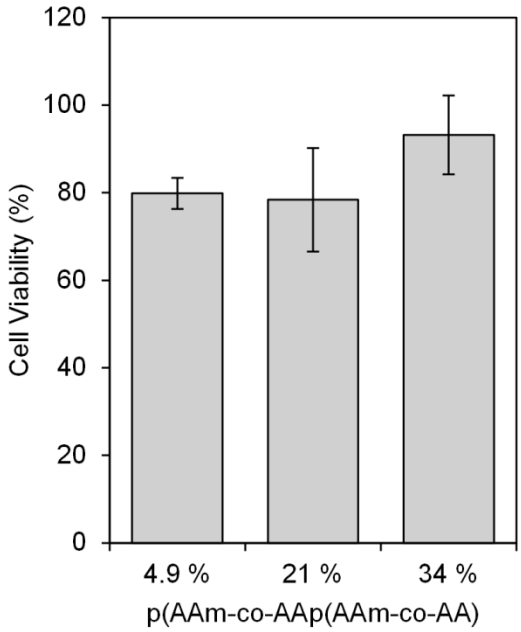

Appendix Figure 2.5. The Cytotoxicity of Blank p(AAm-*co*-AA) NPs. The NPs concentration used in this experiment was 0.7 mg mL^{-1}, which is similar to the concentration of NPs at the highest dose shown in Appendix Figure 2.4. The data is normalized to the population of the cells that were treated with only PBS. The error bars represent the standard deviations from the mean.

The cytotoxicity of cisplatin-loaded p(AAm-*co*-AA) NPs did not show a notable

correlation with their matrix density. This implies there are some factors that we might not take into consideration such as difference between cisplatin released outside SKOV3 cells and cisplatin released inside SKOV3 cells in terms of the interaction with cells, and the potential relationship between matrix density and cellular uptake.

Also, the IC_{50} of p(AAm-*co*-AA) NPs was similar to that of the p(AAm-*co*-APMA) NPs, regardless of the significant difference in release profiles. The difference in the cellular uptake seems to explain this apparent contradiction (Figure 2.**5**). There is an almost 3.5 times higher uptake of cisplatin when p(AAm-*co*-APMA) NPs were used as drug carriers than when p(AAm-*co*-AA) NPs were used. The significant difference in the NP cellular uptake between these two NP formulations could be the reason for their equal cytotoxic effect even though the p(AAm-*co*-AA) NPs can release 5 times more cisplatin in 72 hours than the p(AAm-*co*-APMA) NPs. The higher release per NP appears to be compensated by a higher NP uptake.

References

1. Siegel, R.; Ma, J.; Zou, Z.; Jemal, A. Cancer Statistics, 2014. *CA: A Cancer Journal for Clinicians* **2014**, *64*, 9–29.
2. Rosenberg, B.; VanCamp, L.; Trosko, J.; Mansour, V. Platinum Compounds: A New Class of Potent Antitumour Agents. *Nature* **1969**, *222*, 385–6.
3. Dhar, S.; Gu, F. X.; Langer, R.; Farokhzad, O. C.; Lippard, S. J. Targeted Delivery of Cisplatin to Prostate Cancer Cells by Aptamer Functionalized Pt(IV) Prodrug-PLGA-PEG Nanoparticles. *Proc. Natl. Acad. Sci. U.S.A.* **2008**, *105*, 17356–61.
4. Samimi, G.; Safaei, R.; Katano, K.; Holzer, A.; Rochdi, M.; Tomioka, M.; Goodman, M.; Howell, S. Increased Expression of the Copper Efflux Transporter ATP7A Mediates Resistance to Cisplatin, Carboplatin, and Oxaliplatin in Ovarian Cancer Cells. *Clinical cancer research : an official journal of the American Association for Cancer Research* **2004**, *10*, 4661–9.
5. Liu, F.-S. Mechanisms of Chemotherapeutic Drug Resistance in Cancer Therapy—a Quick Review. *Taiwanese Journal of Obstetrics and Gynecology* **2009**, *48*, 239–244.
6. Godwin, A.; Meister, A.; O'Dwyer, P.; Huang, C.; Hamilton, T.; Anderson, M. High Resistance to Cisplatin in Human Ovarian Cancer Cell Lines Is Associated with Marked Increase of Glutathione Synthesis. *Proceedings of the National Academy of Sciences of the United States of America* **1992**, *89*, 3070–4.
7. Salerno, M.; Yahia, D.; Dzamitika, S.; Vries, E. de; Pereira-Maia, E.; Garnier-Suillerot, A. Impact of Intracellular Chloride Concentration on Cisplatin Accumulation in Sensitive and Resistant GLC4 Cells. *J. Biol. Inorg. Chem.* **2009**, *14*, 123–32.
8. Kroon, A. I. de; Staffhorst, R. W.; Kruijff, B. d; Burger, K. N. Cisplatin Nanocapsules. *Meth. Enzymol.* **2005**, *391*, 118–25.
9. DeNardo, S. J.; DeNardo, G. L.; Miers, L. A.; Natarajan, A.; Foreman, A. R.; Gruettner, C.; Adamson, G. N.; Ivkov, R. Development of Tumor Targeting Bioprobes ((111)In-Chimeric L6 Monoclonal Antibody Nanoparticles) for Alternating Magnetic Field Cancer Therapy. *Clin. Cancer Res.* **2005**, *11*, 7087s–7092s.
10. Winer, I.; Wang, S.; Lee, Y.-E.; Lee, Y.-E.; Fan, W.; Gong, Y.; Burgos-Ojeda, D.; Spahlinger, G.; Kopelman, R.; Buckanovich, R. F3-Targeted Cisplatin-Hydrogel Nanoparticles as an Effective Therapeutic That Targets Both Murine and Human Ovarian Tumor Endothelial Cells in Vivo. *Cancer research* **2010**, *70*, 8674–83.
11. Maeda, H. Tumor-Selective Delivery of Macromolecular Drugs via the EPR Effect: Background and Future Prospects. *Bioconjugate chemistry* **2010**, *21*, 797–802.
12. Maeda, H. The Enhanced Permeability and Retention (EPR) Effect in Tumor Vasculature: The Key Role of Tumor-Selective Macromolecular Drug Targeting. *Advances in enzyme regulation* **2001**, *41*, 189–207.
13. Koo, Y.-E.; Reddy, G.; Bhojani, M.; Schneider, R.; Philbert, M.; Rehemtulla, A.; Ross, B.; Kopelman, R. Brain Cancer Diagnosis and Therapy with Nanoplatforms. *Advanced Drug Delivery Reviews* **2006**, *58*.
14. Brigger, I.; Dubernet, C.; Couvreur, P. Nanoparticles in Cancer Therapy and Diagnosis. *Adv. Drug Deliv. Rev.* **2002**, *54*, 631–51.
15. Cuvier, C.; Roblot-Treupel, L.; Millot, J. M.; Lizard, G.; Chevillard, S.; Manfait, M.; Couvreur, P.; Poupon, M. F. Doxorubicin-Loaded Nanospheres Bypass Tumor Cell Multidrug Resistance. *Biochemical Pharmacology* **1992**, *44*, 509–517.

16. Larsen, A. K.; Escargueil, A. E.; Skladanowski, A. Resistance Mechanisms Associated with Altered Intracellular Distribution of Anticancer Agents. *Pharmacology & Therapeutics* **2000**, *85*, 217–229.
17. Li, S.-D.; Howell, S. CD44-Targeted Microparticles for Delivery of Cisplatin to Peritoneal Metastases. *Molecular pharmaceutics* **2010**, *7*, 280–90.
18. Burger, K. N.; Staffhorst, R. W.; Vijlder, H. C. de; Velinova, M. J.; Bomans, P. H.; Frederik, P. M.; Kruijff, B. de Nanocapsules: Lipid-Coated Aggregates of Cisplatin with High Cytotoxicity. *Nat. Med.* **2002**, *8*, 81–4.
19. Terwogt, J.; Groenewegen, G.; Pluim, D.; Maliepaard, M.; Tibben, M.; Huisman, A.; Huinink, W.; Schot, M.; Welbank, H.; Voest, E.; *et al.* Phase I and Pharmacokinetic Study of SPI-77, a Liposomal Encapsulated Dosage Form of Cisplatin. *Cancer chemotherapy and pharmacology* **2002**, *49*, 201–10.
20. Nishiyama, N.; Koizumi, F.; Okazaki, S.; Matsumura, Y.; Nishio, K.; Kataoka, K. Differential Gene Expression Profile between PC-14 Cells Treated with Free Cisplatin and Cisplatin-Incorporated Polymeric Micelles. *Bioconjugate chemistry* **2002**, *14*, 449–57.
21. Nishiyama, N.; Yokoyama, M.; Aoyagi, T.; Okano, T.; Sakurai, Y.; Kataoka, K. Preparation and Characterization of Self-Assembled Polymer−Metal Complex Micelle from Cis -Dichlorodiammineplatinum(II) and Poly(ethylene glycol)−Poly(A ,β-Aspartic Acid) Block Copolymer in an Aqueous Medium. *Langmuir* **1999**, *15*.
22. Kopelman, R.; Koo, Y.-E.; Philbert, M.; Moffat, B.; Reddy, R.; McConville, P.; Hall, D.; Chenevert, T.; Bhojani, M.; Buck, S.; *et al.* Multifunctional Nanoparticle Platforms for in Vivo MRI Enhancement and Photodynamic Therapy of a Rat Brain Cancer. *Journal of Magnetism and Magnetic Materials* **2005**, *293*.
23. Koo Lee, Y. E.; Orringer, D. A.; Kopelman, R. Nanoparticles for Cancer Diagnosis and Therapy. Ch.11. *In Polymer based Nanostructures: Medical Applications*; ; Ed: Broz, P; pp. 333–353.
24. Orringer, D.; Koo, Y.-E.; Chen, T.; Kim, G.; Hah, H.; Xu, H.; Wang, S.; Keep, R.; Philbert, M.; Kopelman, R.; *et al.* In Vitro Characterization of a Targeted, Dye-Loaded Nanodevice for Intraoperative Tumor Delineation. *Neurosurgery* **2009**, *64*, 965–71; discussion 971–2.
25. Qin, M.; Hah, H.; Kim, G.; Nie, G.; Lee, Y.-E.; Kopelman, R. Methylene Blue Covalently Loaded Polyacrylamide Nanoparticles for Enhanced Tumor-Targeted Photodynamic Therapy. *Photochemical & photobiological sciences : Official journal of the European Photochemistry Association and the European Society for Photobiology* **2011**, *10*, 832–41.
26. Hah, H. J.; Kim, G.; Lee, Y.-E. K. E.; Orringer, D. A.; Sagher, O.; Philbert, M. A.; Kopelman, R. Methylene Blue-Conjugated Hydrogel Nanoparticles and Tumor-Cell Targeted Photodynamic Therapy. *Macromol Biosci* **2011**, *11*, 90–9.
27. Wenger, Y.; Schneider, R.; Reddy, G.; Kopelman, R.; Jolliet, O.; Philbert, M. Tissue Distribution and Pharmacokinetics of Stable Polyacrylamide Nanoparticles Following Intravenous Injection in the Rat. *Toxicology and applied pharmacology* **2011**, *251*, 181–90.
28. Qin, M.; Lee, Y.; Ray, A.; Kopelman, R. Overcoming Cancer Multidrug Resistance by Codelivery of Doxorubicin and Verapamil with Hydrogel Nanoparticles. *Macromolecular Bioscience* **2014**, *14*, 1106–1115.
29. Koo Lee, Y.; Kopelman, R. In *Multifunctional Nanoparticles for Drug Delivery Applications*; Svenson, S.; Prud'homme, R. K., Eds.; Nanostructure Science and Technology; Springer US: Boston, MA, 2012; pp. 225–255.

30. Washington, C Drug Release from Microdisperse Systems: A Critical Review. **1990**, *58*, 1–12.
31. Peppas, N. A.; Hilt, J. Z.; Khademhosseini, A.; Langer, R. Hydrogels in Biology and Medicine: From Molecular Principles to Bionanotechnology. *Advanced Materials* **2006**, *18*, 1345–1360.
32. Fisher, O.; Peppas, N. Polybasic Nanomatrices Prepared by UV-Initiated Photopolymerization. *Macromolecules* **2009**, *42*, 3391–3398.
33. Lin, C.-C.; Metters, A. Hydrogels in Controlled Release Formulations: Network Design and Mathematical Modeling. *Advanced Drug Delivery Reviews* **2006**, *58*, 13791408.
34. Echeverria, C.; Peppas, N.; Mijangos, C. Novel Strategy for the Determination of UCST-like Microgels Network Structure: Effect on Swelling Behavior and Rheology. *Soft Matter* **2011**, *8*, 337–346.
35. Satarkar, N.; Hilt, Z. Hydrogel Nanocomposites as Remote-Controlled Biomaterials. *Acta biomaterialia* **2008**, *4*, 11–16.
36. Peng, J.; Qi, T.; Liao, J.; Chu, B.; Yang, Q.; Li, W.; Qu, Y.; Luo, F.; Qian, Z. Controlled Release of Cisplatin from pH-Thermal Dual Responsive Nanogels. *Biomaterials* **2013**, *34*, 8726–40.
37. Shirakura, T.; Kelson, T.; Ray, A.; Malyarenko, A.; Kopelman, R. Hydrogel Nanoparticles with Thermally Controlled Drug Release. *ACS macro letters* **2014**, *3*, 602–606.
38. Owens, D.; Jian, Y.; Fang, J.; Slaughter, B.; Chen, Y.-H.; Peppas, N. Thermally Responsive Swelling Properties of Polyacrylamide/Poly(acrylic Acid) Interpenetrating Polymer Network Nanoparticles. *Macromolecules* **2007**, *40*.
39. Poulsen, A.; Arleth, L.; Almdal, K.; Scharff-Poulsen, A. Unusually Large Acrylamide Induced Effect on the Droplet Size in AOT/Brij30 Water-in-Oil Microemulsions. *Journal of colloid and interface science* **2007**, *306*, 143–53.
40. Ritger, P.; Peppas, N. A Simple Equation for Description of Solute Release I. Fickian and Non-Fickian Release from Non-Swellable Devices in the Form of Slabs, Spheres, Cylinders or Discs. *Journal of Controlled Release* **1987**, *5*.
41. Howe-Grant, M. E.; Lippard, S. J. Aqueous Platinum(II) Chemistry; Binding to Biological Molecules. In; Dekker: New York, 1980; Vol. 11, pp. 63–125.
42. Ohya, Y.; Oue, H.; Nagatomi, K.; Ouchi, T. Design of Macromolecular Prodrug of Cisplatin Using Dextran with Branched Galactose Units as Targeting Moieties toHepatomaCells. *Biomacromolecules* **2001**, *2*, 927–33.
43. Biswas, S.; Torchilin, V. Nanopreparations for Organelle-Specific Delivery in Cancer. *Advanced Drug Delivery Reviews* **2014**, *66*, 2641.
44. He, C.; Hu, Y.; Yin, L.; Tang, C.; Yin, C. Effects of Particle Size and Surface Charge on Cellular Uptake and Biodistribution of Polymeric Nanoparticles. *Biomaterials* **2010**.
45. Fleischer, C.; Payne, C. Secondary Structure of Corona Proteins Determines the Cell Surface Receptors Used by Nanoparticles. *J. Phys. Chem. B* **2014**, *118*, 14017 14026.

–

Chapter 3.

Hydrogel Nanoparticles with Thermally-controlled Drug Release.

The material in this chapter has been adapted with minor modifications from the following publication.

Shirakura, T.; Kelson, T.; Ray, A.; Malyarenko, A.; Kopelman, R. Hydrogel Nanoparticles with Thermally Controlled Drug Release. ACS Macro Letters 2014, 3, 602-606.

Introduction

The development of hydrogel nanoparticles (NPs) that transport and deliver chemodrugs selectively to the tumor area is a recent strategy for improving therapeutic efficacy and avoiding systemic side-effects, such as renal toxicity, phlebitis, bone marrow suppression, and nausea.[1,2] Such selective delivery may be achieved by active and/or passive targeting of such NPs.[3]

Two important aspects for consideration in the development of drug delivering NPs are the chemodrug loading capacity and the control over its release. An optimal design of the NPs would facilitate incorporation of a large amount of the drug, with efficient release to the tumor region, preferably in a controlled manner, while limiting release elsewhere.[4] The latter is one of the most challenging aspects. Designing the NP matrix to enhance and enable controlled release

of the drug is often based on environmental stimuli,[3] e.g. temperature, pH,[1] light,[5,6] glucose,[7] antigen,[8] and reducing agents, such as glutathione.[9]

Using temperature as a stimulus to control the drug release from NPs is particularly attractive, because it can exploit the variation in the local temperature, typical for tumor tissues.[10] Tumor tissues have been shown to have slightly elevated temperatures, compared to the host basal temperature, due to an increased metabolic rate.[11] Also, additional temperature differentials can be induced by external heating of the tumor region, e.g., by ultrasonic, magnetic field, or light mediated heating, targeted to the nanoparticles. [12–14]

The integration of temperature sensitive properties into the design of hydrogel nanoparticles has shown promise for enhancement of the drug release to the somewhat hotter tumor tissues, while limiting the release elsewhere.[10] Due to the flexible structures of these NPs, the polymer interactions inside the NPs can be made temperature sensitive, thereby altering the NP size and its polymer density; consequently the release efficiency of the loaded drugs changes.

Many different kinds of temperature-sensitive nanoparticle matrices have been formulated, such as poly(vinyl alcohol),[15,16] cellulose derivatives,[17] and complex core-shell polymer designs.[18] Among them, one of the most common matrix systems for hydrogel NPs is poly(N-isopropylacrylamide) (PNIPAM), which shows good biocompatibility, as well as temperature-sensitivity, a so- called Lower Critical Solution Temperature (LCST) behavior in aqueous solution, across a biologically relevant temperature and pressure range.[10,19,20] Hydrogen bonding is formed between the amide of PNIPAM and water, and a cage-like structure is formed around the isopropyl group below LCST; this solvates PNIPAM and expands the nanoparticles.[10,21,22] On the other hand, these structures are broken above LCST; the latter shrinks the NPs, thereby “squeezing out” chemodrugs from the NPs, or, alternatively, tightening

the pores of the hydrogel, so as to reduce the chemodrug's release.[1,20–22] This matrix is often combined with other components, such as SiO_2-coated, Fe_3O_4 nanoparticles, or butylmethacrylate, so as to enhance functionality and shift the LCST.[23,24]

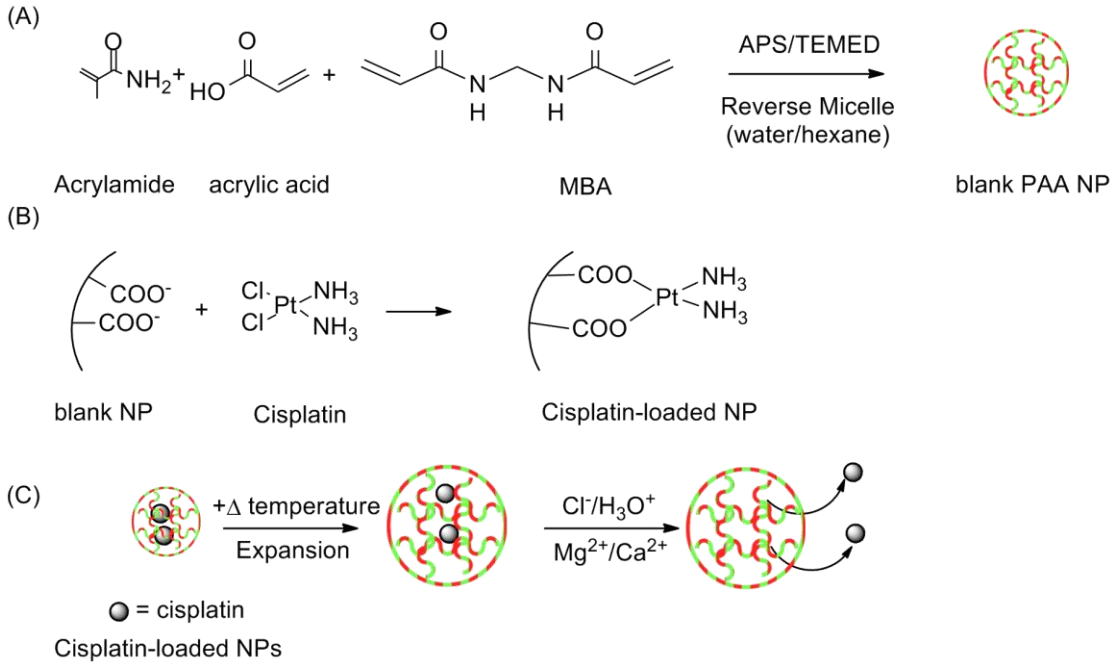

Figure 3.1. (A) CisPt-NPs Synthesis, (B) Post-loading Procedure, and (C) Release Mechanism.

We emphasize that an Upper Critical Solution Temperature (UCST)-like behavior, characterized by swelling rather than de-swelling at elevated temperature, potentially lends itself to being very valuable as well, because swollen hydrogels do enhance the release of chemodrugs due to their lower polymer density.[25,26] Some examples of UCST-based hydrogels are given in the review by Seuring and Agarwal.[27]

The combination matrix of acrylamide and acrylic acid is an example of a UCST-like hydrogel in the presence of a salt such as NaCl.[27] This combination has been studied for both bulk hydrogel and NPs, since acrylic acid forms hydrogen bonds with acrylamide, bonds that may break at elevated temperatures, causing the hydrogel matrix to swell.[25,28–30] Echeverria and

Mijangos have further demonstrated the ability to control the specific swelling properties of acrylamide-co-acrylic-acid particles by altering the crosslinker content and incorporating gold nanoparticles into the matrix.[31] Also, acrylic acid binds a certain type of drugs tightly, due to its carboxyl group.[1] Although these acrylamide-acrylic acid hydrogels show promising properties, as of yet no application of this matrix for temperature-responsive drug delivery systems has been reported, to the best of our knowledge, especially for cancer treatment, where the tumor is at a temperature slightly higher than that of the normal body temperature (37 °C).

Here we present NPs based on the combination of acrylic acid and acrylamide; they are specifically designed for temperature sensitive release of chemodrugs. We incorporated cisplatin into these copolymer NPs (CisPt-NPs). Cisplatin, which is a chemodrug commonly used for carcinoma and melanoma,[2,32] was chosen as a model drug. We present the temperature sensitive behavior of the cisplatin release, under physiological conditions, with and without some of the ions that are abundantly present *in vivo*. We also monitored the intracellular localization of the NPs in cancer cells, and observed them to accumulate primarily in the lysosomes. We thus also investigated the temperature-sensitive release of cisplatin in a lysosome-mimicking environment. CisPt-NPs showed increased cytotoxicity to tumor cells with increasing temperature. The results presented here show that acrylamide-co-acrylic acid hydrogel NPs may be a promising candidate for a stable and reliable temperature-sensitive drug delivery system.

Materials and Methods

Materials

Cisplatin was purchased from Selleck Chemical LLC. Dulbecco modified Eagle medium (DMEM) was purchased from Invitrogen. Fluorescein–5-thiosemicarbazide (5-FTSC) was

purchased from Marker Gene Technologies, Inc. All other chemicals were purchased from Sigma-Aldrich. The de-ionized water used in this experiment was purified using a Milli-Q system from Millipore prior to the experiment.

Preparation of blank p(AA-*co*-AAm) NPs.

P(AA-*co*-AAm) was synthesized, using the reverse micelle polymerization technique, modifying the method proposed by Owens[1]. 2.69 g dioctyl sulfosuccinate (AOT) and 1.34 g Brij 30 were added to 38 mL of argon-purged hexane, while continuing to purge with argon. To a scintillation vial, 0.12 g acrylamide monomer, 0.14 g acrylic acid monomer, 0.006 g Bis-acrylamide monomer, and 0.10 g ammonium persulfate was added. The components were dissolved in 1.5 mL of deionized water, and the mixture was sonicated until fully dissolved. While maintaining an inert atmosphere in the round bottom flask, the contents of the scintillation vial were added and the flask was stirred for another 20 minutes. The polymerization was initiated by adding 400 μL Tetramethylethylenediamine (TEMED) at room temperature. After 2 hours the reaction was quenched by opening the flask to the air for 10 minutes. Hexane was removed by rotary evaporation. Then, the product was washed in an Amicon stirred cell (Millipore) with ethanol (5x150 mL through a 300kDa MW cut-off membrane) and ddH2O (5 x 150 mL through a 300k MW cut-off membrane). The resultant solution was filtered through a 0.2 μm pore size filter, and was lyophilized for ~72 hours.

Preparation of 5-FTSC loaded NPs.

0.207 mg of Acrylic acid N-hydroxysuccinimide ester (NSA) was mixed with 3 mg of 5-FTSC in 50:50 mixture of 8 μL of DMF and DI water. After the overnight reaction, the mixture was mixed

with the monomer solution described in the section of the preparation of the blank p(AA-co-AAm) NPs.

Loading of cisplatin into blank p(AA-co-AAm) NPs.

Cisplatin was loaded into the blank p(AA-co-AAm) NPs in a weight ratio of 1 to 5. In a typical loading condition, 2 mg of cisplatin was dissolved in 1 mL of deionized water. Then, 10 mg of blank p(AA-co-AAm) NPs were added to the solution. The solution was covered to exclude light, and stirred for 3 days. After that, the CisPt-NPs were rinsed with at least 7 mL of water, 7 times, using a centrifugal filter (300 kDaMWCO) (Millipore). The concentration of the final solution was adjusted to be 10 mg mL^{-1} NP concentration in water. Inductively coupled plasma optical emission spectrometry (ICP-OES) (Optima 2000 DV, Perkin-Elmer) was used to determine the loading of cisplatin.

Size and Zeta-potential Measurement.

To measure the hydrodynamic diameter and the zeta-potential of the NPs, before and after the loading of cisplatin, dynamic light scattering was applied in PBS (pH 7.4) for the size analysis and in the deionized water for the zeta-potential measurement at room temperature using a Delsa Nano C (Beckman Coulter). Also, the temperature-sensitive swelling property of the CisPt-NPs in aqueous solution was measured using the Delsa Nano C with its temperature control function. In the typical experiment, 1 mL of 2 mg mL^{-1} NP solution was used for the measurement.

Transmission Electron Microscopy (TEM) of CisPt-NPs.

TEM image of CisPt-NPs was taken using Philips CM100. Carbon coated grid was utilized. NP concentration was adjusted to 0.01 mg mL^{-1}. No negative staining was performed.

Cisplatin Release Study.

The release of cisplatin from CisPt-NPs was evaluated either in pH 4 buffer (50 mM phthalate buffer with 150 mM NaCl), PBS (pH 7.4), PBS (pH 7.4) containing 1 mM MgCl2 and CaCl2, PBS (pH 7.4) with 10 % fetal bovine serum. A 1 mg mL^{-1} CisPt-NPs solution was prepared by suspending the CisPt-NPs in these solvents. Eighteen 1 mL aliquots of the CisPt-NPs solution were transferred to 1.5 mL Ependorf tubes. 6 tubes were placed into a 32 °C water bath, 6 of them were placed into a 37 °C water bath, and the remaining 6 were placed into a 42 °C water bath. At specific time points (0 hour, 6 hours, 12 hours, 24 hours, and 48 hours, for the test in PBS with fetal bovine serum, only 12 hours and 24 hours), one tube at each incubation temperature was removed and filtered, using a 100kDaMWCO centrifugal filter. Filtrates were collected for determination of the cisplatin released from the CisPt-NPs. ICP-OES was used to determine the concentration of cisplatin.

Evaluation of the intracellular Behavior of p(AA-co-AAm) NPs.

The internalization of the p(AA-co-AAm) NPs into MDA-MB-435 (MDA) cells was monitored by using fluorescence microscopy. The cells were incubated with the 5-FTSC labeled p(AA-co-AAm) NPs for six hours before washing away the non-internalized p(AA-co-AAm) NPs. A fluorescence confocal microscope (Leica SP-5X) was used for intracellular imaging. The p(AA-co-AAm) NPs and lysotracker were excited at 488 nm and 580 nm and the fluorescence was

collected between 500 nm to 550 nm and 590 nm to 620 nm, respectively. The images were acquired using a 60X objective in the confocal mode, with a slit width of 1 Airy unit.

Cytotoxicity Assay of CisPt-NPs.

The human melanoma cell line MDA cells were cultivated in DMEM containing 25 mM HEPES with addition of penicillin, streptomycin and glutamine (1%) and heat inactivated fetal bovine serum (10%).

MDA cells were transferred to two 96-well plates with a confluency of 2000 cells per well After 24 hour incubation the cells settled down and the drug was added. Following 12 hours incubation, the drugs were removed from the wells, and the cells were washed 2 times with DPBS before refilling them with 200 μL of complete DMEM. 48 hours later, the cell media was removed from the wells. Then, 120 μL of 0.833 mg mL^{-1} MTT reagent in DMEM, without phenol red, was added and further incubated for 4 hours. After four hours of incubation, the media with MTT reagent was removed and 100 μL of dimethyl sulfoxide was added to the wells, and the plate was shaken for 1 hour. The absorbances from the wells were measured using a microplate reader (Anthos 2010, biochrom).

Results and Discussion

The CisPt-NPs were synthesized in two steps (Figure 3.1). Similar NPs have shown temperature-dependent swelling property near the physiological temperature.[25] We have also confirmed that our CisPt-NPs have a temperature sensitivity by using dynamic light scattering (Figure 3.**2**), with emphasis on the lysosomal pH of 4.[33]

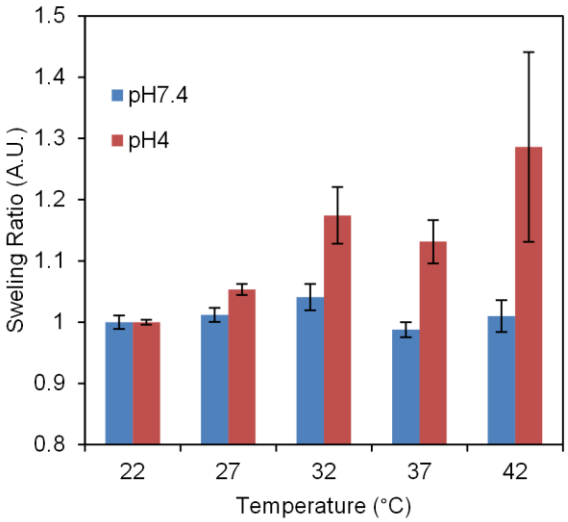

Figure 3.2. Swelling Study of NPs. The swelling ratio is calculated by (volume at the temperature)/(volume at 22 °C). The error bar represents the standard error. Temperature induced swelling is dramatic at pH=4. The temperature sensitivity of the size of the CisPt-NPs was examined in the range of 22 °C to 42 °C using dynamic light scattering. In a pH4 buffer (0.05 M phthalate buffer with 150 mM NaCl), Cis-NPs swelled with increasing temperature. In PBS (pH 7.4), Cis-NPs swell only slightly. In both cases, we observed the distribution of the size becoming broader as the sample is heated up, which is another sign of swelling, as reported previously.

The feeding ratio of acrylamide to acrylic acid was chosen to have equal Moles of the monomers after the polymerization.[25] When the NPs are synthesized only from acrylamide or only from acrylic acid, the temperature sensitivity decreases.[25] The emulsifier concentration and solvent were chosen based on Owens and our standard protocol.[34,35] The combination produces

NPs whose size distribution is narrow, and with a size that is ideal for drug delivery application (i.e. avoiding rapid clearance from the body, and targeting the tumor passively *in vivo*).[3]

Before cisplatin loading, the size of the p(AA-co-AAm) NPs, at room temperature, was found to be 90 (±2) nm with polydispersity index (PDI) of 0.30 (±0.01), while after the loading the size was 132 (± 3) nm with PDI of 0.30 (±0.01), using dynamic light scattering (Figure 3.3A). The images from transmission electron microscopy showed a uniform NP size distribution (Figure 3.3B). Both methods showed a narrow size distribution. As expected, swelling drastically increases size. The zeta-potential of the p(AA-co-AAm) NPs was -57 (± 5) mV before the cisplatin loading, while it was -56 (±5) mV after the loading. Thus, there was significant size expansion with cisplatin postloading. However, there was little change in surface potential, indicating that the cisplatin was not just adsorbing to the surface. The loading of cisplatin was 11 (±3) (cisplatin/CisPt-NPs) wt% of the unloaded particles.

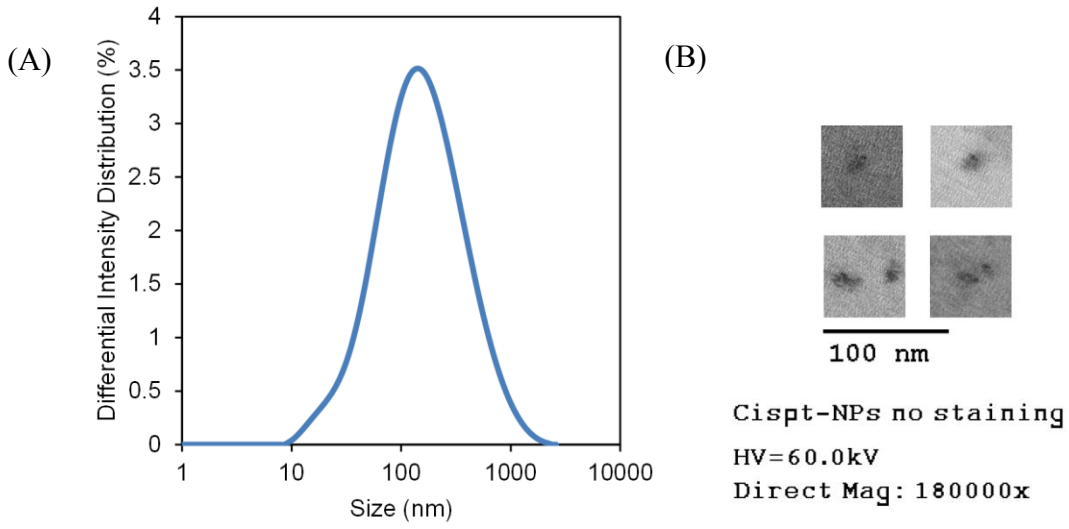

Figure 3.3(A) Typical intensity distribution of CisPt-NPs at 22 °C in PBS. The mean size (wet) is 132 (± 3) nm. (B). Typical TEM Image of CisPt-NPs. TEM image of CisPt-NPs was taken to evaluate the size distribution of the NPs. The average size (dry) was 20.9 (± 2.5) nm.

Acrylic acid enhances the incorporation of cisplatin by the substitution of its chlorides with carboxyl groups of the NPs (Figure 3.1B),[1,36] What is more, the bonding of the carboxyl group and the platinum of cisplatin is reversible, under physiological conditions.[1,36,37] In the presence of a high concentration of Cl^-, hydronium ions, or metallic cations, the carboxyl group interaction with the platinum center of cisplatin gets looser (Figure 3.1C).[1,29] This may also explain the pH enhanced release of cisplatin from the CisPt-NPs, discussed below.

The temperature dependent release of cisplatin was assessed in phosphate buffered saline (PBS) (pH 7.4), which mimics serum conditions, at three different temperatures: 32 °C, 37 °C, and 42 °C (Figure 3.4). The percent release of the cisplatin (η) was calculated according to the following equation (Eq.1).

$$\eta(t,T) = C(t,T)/C_0(T) \times 100 \qquad (1),$$

where t is the time point of the drug release study, T is the temperature of the drug release study, $C(t,T)$ is the concentration of cisplatin released at that time point, and $C_0(T)$ is the initial (t=0) concentration of cisplatin in the CisPt-NPs. Also, the percent enhancement of the cisplatin release in PBS (Figure 3.4 inset) was calculated by the following equation (Eq.2).

$$\kappa(t,T) = \left(\eta(t,T) - \eta_0(t)\right)/\eta_0(t) \times 100 \qquad (2),$$

where $\eta_0(t)$ is the percent release of the cisplatin at 32 °C, at a given time point, t.

We monitored the cisplatin release over a period of 48 hours, starting at six hours. Over the time scale we monitored, cisplatin always showed the highest release percentage at 42° C, compared to 37°C and 32°C. After 48 hours, 25 % of cisplatin got released from the CisPt-NPs at

42 °C, while only 19 % and 17 % of the cisplatin got released at 37 °C and 32 °C, respectively. Although the average cisplatin release is slightly higher at 37 °C, compared to 32 °C, this is not statistically significant.

The above temperature sensitivity of the drug release is attributable to three different factors. First, the swelling property of the CisPt-NPs decreases the density of the matrix at higher temperature, which could facilitate the escape of cisplatin from the matrix. Second, the reverse substitution reaction rate of the carboxyl group, attached to the platinum center of the cisplatin with chloride, is enhanced at higher temperature, because of the higher accessibility of the Cl^- ions.[1,26] Third, the rate of diffusion of the cisplatin molecules increases with temperature.

As described above, another major factor that governs the release of the drug is the presence of divalent ions.[29] Therefore, we evaluated the effects of such ions on the drug release profile, particularly those of Mg^{2+} and Ca^{2+}, which are abundantly present in the blood stream, as shown in Figure 3.5. The concentration of each ion used is 1 mM, similar to their blood levels.[38]

The difference in the release of cisplatin becomes more evident after 6 hours. We observe that, over 48 hrs, 32.0 % of the cisplatin got released when the solution was at 42 °C, while only 22.0 % and 17.8 % of cisplatin got released at 37 °C and 32 °C, respectively.

The increase in drug release observed in the presence of divalent ions over longer incubation times may be attributed to the disruption by the divalent cations of the loose interaction between the carboxyl groups of the NP matrix and the cisplatin molecule's center.[29]

We evaluated the release profile of CisPt-NPs in PBS with 10% fetal bovine serum, and confirmed the temperature-sensitivity (Figure 3.6).

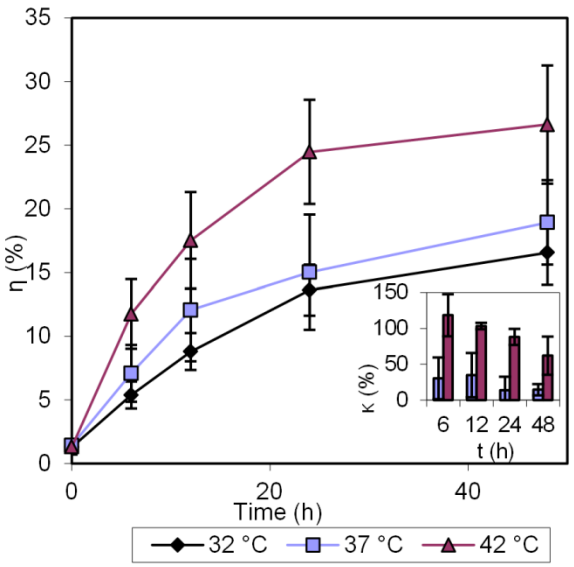

Figure 3.4. Cisplatin Release in PBS at three different temperatures: 32 °C, 37 °C, and 42 °C. Error bars show the standard deviation. Inset: % Enhancement of Cisplatin Release at 37 °C and 42 °C, compared to 32 °C.

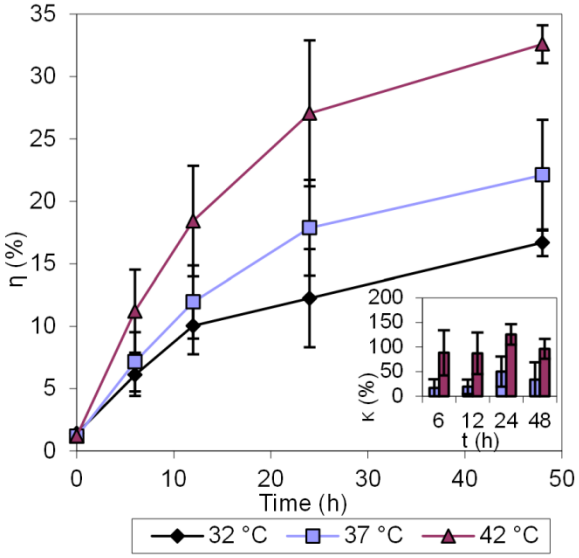

Figure 3.5. Cisplatin Release in PBS, containing 1 mM each of Ca2+ and Mg2+, at three different temperatures: 32 °C, 37 °C and 42 °C. Error bars show the standard deviation. Inset: % Enhancement of Cisplatin Release at 37 °C and 42 °C, compared to 32 °C.

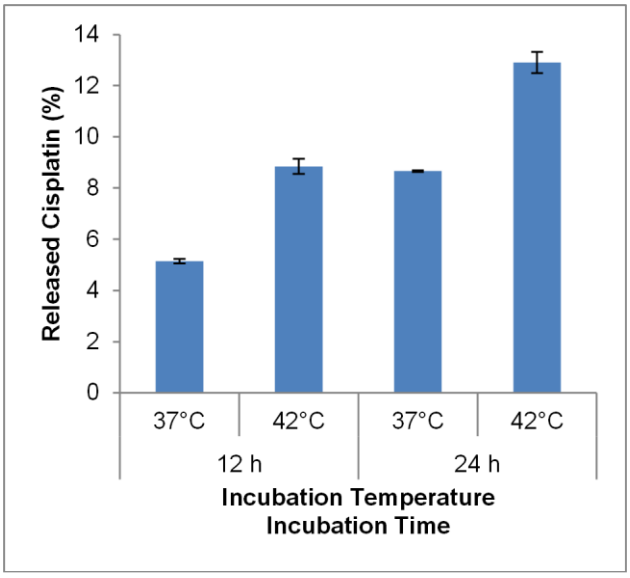

Figure 3.6. Cisplatin Release study in PBS with 10% FBS at 37 °C and 42 °C. Error bar represent standard deviations. Release rises with temperature. Effect of FBS on temperature-sensitivity was evaluated in PBS with 10% FBS. Both at 12 hour and 24 hour time points, we observed statistically more significant cisplatin being released at the higher temperature. Interestingly, the overall release was slightly lower from the test only in PBS.

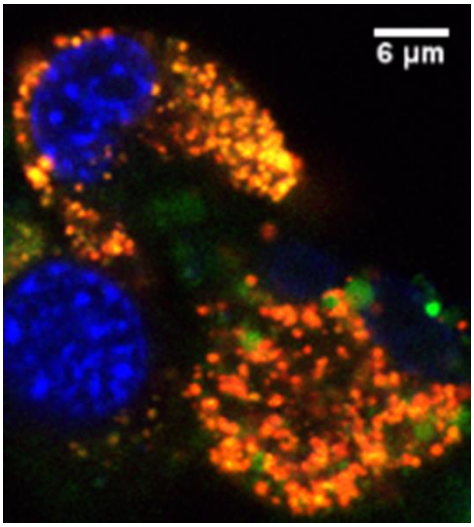

Figure 3.7. Cellular Uptake Study of 5-FTSC-loaded p(AA-co-AAm) NPs using MDA-MB-435. Blue indicates the nucleus, stained with Hoechst Blue. Green indicates the 5-FTSC-loaded p(AA-co-AAm) NPs. Red indicates the lysotracker. A significant amount of co-localization of red and green is observed (shown in yellow/orange).

Determining the intracellular fate of the p(AA-co-AAm) NPs is essential to designing a drug release process, due to the importance of the local chemical environment inside the cells. The p(AA-co-AAm) NPs can be taken up by the cells via various intracellular pathways that dictate the intracellular fate of the p(AA-co-AAm) NPs. The intracellular co-localization of the p(AA-co-AAm) NPs was monitored using fluorescence confocal microscopy. We observe that these p(AA-co-AAm) NPs mostly co-localize with lysosomes, as shown in Figure 3.7. The overlapping of the fluorescence (seen as Yellow/Orange) from the 5-FTSC labeled NPs (green) with the lysotracker labeled acidic vesicles (Red) shows the co-localization. We have previously observed similar phenomena for the amine-functionalized hydrogel nanoparticles.[35] Late endosomes and lysosomes are acidic in nature and have a pH value in the range of 4-5.[33] Since we observe that most of the p(AA-co-AAm) NPs are trapped into low pH environments, we next studied the temperature sensitive release of drugs at acidic conditions (Figure 3.8).

The release studies were performed by suspending the CisPt-NPs in a pH 4 buffer (50 mM phthalate buffer containing 150 mM NaCl), which mimics the lowest pH level in the intact lysosome.[33]

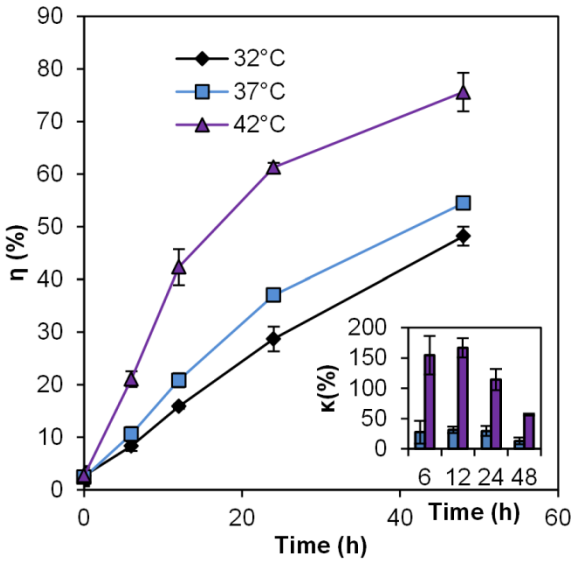

Figure 3.8.Cisplatin Release study in pH4 buffer at three different temperatures: 32 °C, 37 °C, and 42 °C. Error bars represent standard deviations. Inset: % Cisplatin Release Enhancements, relative to Release at 32 °C.

The release of cisplatin in 48 hours at 42 °C was 75.6 %, while the release at 37 °C and 32 °C was 54.5 % and 48.2 %, respectively. The difference in the drug release became evident within the first 6 hours, and remained so over the rest of the observed time period. Increasing amount of cisplatin was released at this low pH than in PBS and in PBS with metallic ions, which is consistent with what is reported previously with rhodamine 6G.[39] The higher release, under acidic conditions, such as inside the tumor tissue as well as the lysosomes, will further increase the tumor selectivity of the delivered cisplatin.[33,40]

Acrylamide-co-acrylic acid hydrogel shrinks at low pH because of the protonation of the carboxyl groups and formation of more hydrogen bonds. [29,41] However, when the system was heated, these hydrogen bonds were broken, which resulted in the decrease of the matrix density (Figure 3.**2**).[25] In addition, the carboxyl groups on the conjugated cisplatin were substituted by the hydronium ions, and cisplatin was released from the CisPt-NPs.[1]

Also, we compared the total cisplatin release from CisPt-NPs to that from cisplatin-loaded nanoparticles made of poly(acrylic acid-co-methyl methacrylate), which reported about 80 % of cisplatin released in PBS at 37 °C. [42] This is a 4 times higher release of cisplatin than from our CisPt-NPs. However, as is shown above, more cisplatin was released from the CisPt-NPs at the elevated temperature, at the pH of lysosomes, where we showed that CisPt-NPs were trapped. This selective and controlled release can further increase the therapeutic index.

As a proof of principle, to demonstrate the effectiveness of this technique towards *in vivo* applications, we monitored the cytotoxicity of the CisPt-NPs at two different temperatures: 37 °C (body temperature) and 40 °C using MDA-MB-435 (Figure 3.9). Although the cells can survive at temperatures greater than 40 °C, this temperature range was considered safe, avoiding protein denaturation. The cell viability was calculated by normalizing the signal of each condition to the signal from the cells treated only with PBS, at each of the two temperatures.

At both temperatures, a dose-dependent decline of the cell viability was observed. The cell viabilities, under doses of 10 μg mL^{-1} and 40 μg mL^{-1} cisplatin, were significantly lower at 40 °C than at 37 °C, based on the unpaired two-tailed Student's *t* test. Also, in general, at all concentrations tested, the cells treated at 40 °C showed lower cellular viability than cells treated at 37 °C. On the other hand, treatment with free cisplatin did not show any significant difference in cell viability between tests conducted at the two different temperatures (Figure 3.10).

Also, the cytotoxicity of free cisplatin was evaluated at two different temperatures: 37 °C and 40 °C. Based on the unpaired two-tailed Student's t test, no significant difference in cell viability was observed. The results confirmed that the difference in the cell viability at the two temperatures we observed with CisPt-NPs (Figure 3.9) was due to the temperature sensitivity of the CisPt-NPs, and not because of the cisplatin itself.

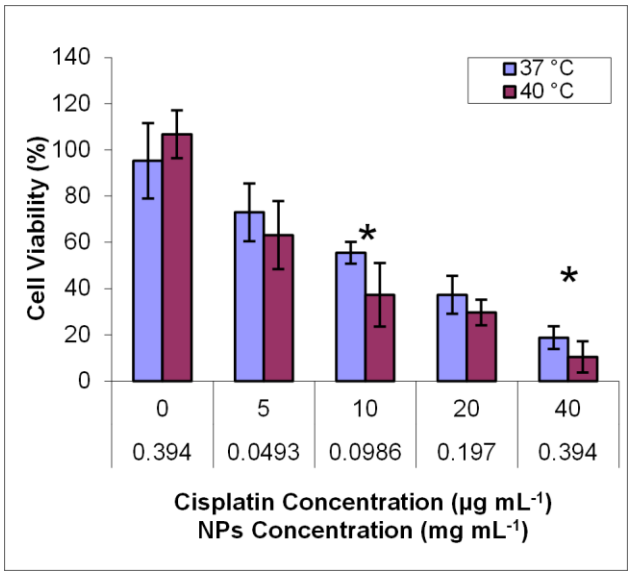

Figure 3.9. Cell viability study of CisPt-NPs at two different temperatures: 37 °C and 40 °C. * is $p < 0.05$ on the two-tailed Student's t-test. Nanoparticle containing drug shows higher cytotoxicity at higher temperature.

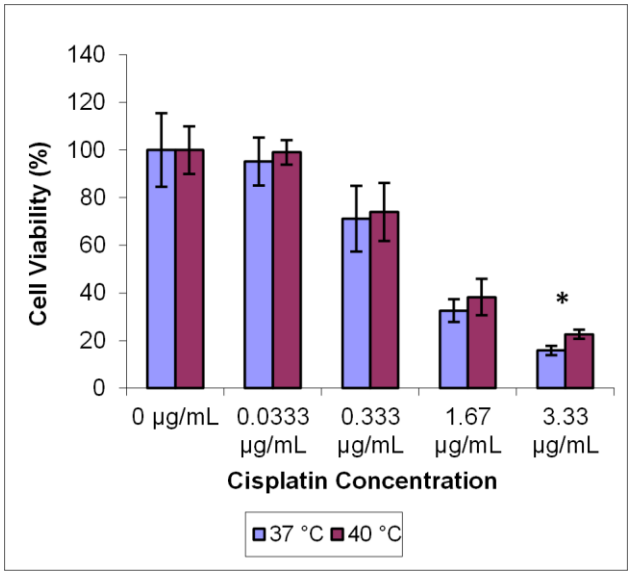

Figure 3.10. Free drug temperature sensitivity. The star (*) sign represents the cisplatin concentrations for which $p<0.05$ in the unpaired two-tailed Student's t test. Cisplatin (free drug) shows unchanged or lower cytotoxicity at higher temperatures.

Conclusion

In summary, temperature-sensitive NPs (CisPt-NPs), with a matrix of p(AA-*co*-AAm), were synthesized as a carrier for the chemotherapeutic drug, cisplatin, with the aim of reducing side effects; the latter is expected from the lowering of the release of free cisplatin in the blood stream and by selectively increasing its release in the tumor region, due to the temperature difference. We evaluated the temperature dependent release profiles of the drug from the matrix, as well as its *in vitro* cytotoxicity. With increasing temperature, these NPs showed a very significant increase in the release of cisplatin, in PBS, even in the absence of divalent metallic ions. Furthermore, adding divalent ions, which are physiologically present in the body, further accelerated the drug release with increasing temperature. Intracellular fluorescence imaging showed that most of the nanoparticles co-localize with lysosomes. The release of cisplatin showed an even stronger correlation with the temperature at the low lysosomal pH. Furthermore, we have shown that the *in vitro* cytotoxicity of the CisPt-NPs also increases with higher temperature, correlating well with the temperature enhanced drug release. We believe that the above results demonstrate both the feasibility and the potential utility of such temperature sensitive NPs as drug carriers with a high therapeutic index.

Acknowledgements

Financial support was provided by a National Institutes of Health grant, R21 NS084275 (RK). The authors thank Yue Hou for help with the drug release study. They also thank the Microscopy and Image Analysis Laboratory of the University of Michigan and the Chemistry Instrument Shop for their support.

References

(1) Peng, J.; Qi, T.; Liao, J.; Chu, B.; Yang, Q.; Li, W.; Qu, Y.; Luo, F.; Qian, Z. *Biomaterials* **2013**, *34*, 8726–8740.

(2) Decatris, M. P.; Sundar, S.; O'Byrne, K. J. *Cancer Treat. Rev.* **2004**, *30*, 53–81.

(3) Koo Lee, Y.; Kopelman, R. In *Multifunctional Nanoparticles for Drug Delivery Applications*; Svenson, S.; Prud'homme, R. K., Eds.; Nanostructure Science and Technology; Springer US: Boston, MA, 2012; pp. 225–255.

(4) Koo Lee, Y.-E.; Orringer, D. A.; Kopelman, R. In *Polymer-based Nanostructures*; Broz, P., Ed.; RSC Publishing: Cambridge, UK, 2010; pp. 333–353.

(5) Suzuki, A.; Tanaka, T. *Nature* **1990**, *346*, 345–347.

(6) Mamada, A.; Tanaka, T.; Kungwatchakun, D.; Irie, M. *Macromolecules* **1990**, *23*, 1517–1519.

(7) Kataoka, K.; Miyazaki, H.; Bunya, M.; Okano, T.; Sakurai, Y. *J. Am. Chem. Soc.* **1998**, *120*, 12694–12695.

(8) Miyata, T.; Asami, N.; Uragami, T. *Nature* **1999**, *399*, 766–769.

(9) Lin, C.; Zhong, Z.; Lok, M. C.; Jiang, X.; Hennink, W. E.; Feijen, J.; Engbersen, J. F. J. *Bioconjug. Chem.* **2007**, *18*, 138–145.

(10) Schmaljohann, D. *Adv. Drug Deliv. Rev.* **2006**, *58*, 1655–1670.

(11) Stefanadis, C.; Chrysochoou, C.; Markou, D.; Petraki, K.; Panagiotakos, D. B.; Fasoulakis, C.; Kyriakidis, A.; Papadimitriou, C.; Toutouzas, P. K. *J. Clin. Oncol.* **2001**, *19*, 676–681.

(12) Lammers, T.; Kiessling, F.; Hennink, W. E.; Storm, G. *Mol. Pharm.* **2010**, *7*, 1899–1912.

(13) Alvarez-Berríos, M. P.; Castillo, A.; Mendéz, J.; Soto, O.; Rinaldi, C.; Torres-Lugo, M. *Int. J. Nanomedicine* **2013**, *8*, 1003–1013.

(14) Curry, T.; Epstein, T.; Smith, R.; Kopelman, R. *Nanomedicine (Lond).* **2013**, *8*, 1577–1586.

(15) Li, J. K.; Wang, N.; Wu, X. S. *J. Control. Release* **1998**, *56*, 117–126.

(16) Ghugare, S. V; Mozetic, P.; Paradossi, G. *Biomacromolecules* **2009**, *10*, 1589–1596.

(17) Lu, X.; Hu, Z.; Gao, J. *Macromolecules* **2000**, *33*, 8698–8702.

(18) Wu, W.; Aiello, M.; Zhou, T.; Berliner, A.; Banerjee, P.; Zhou, S. *Biomaterials* **2010**, *31*, 3023–3031.

(19) Ebeling, B.; Eggers, S.; Hendrich, M.; Nitschke, A.; Vana, P. *Macromolecules* **2014**, *47*, 1462–1469.

(20) Fan, T.; Li, M.; Wu, X.; Li, M.; Wu, Y. *Colloids Surf. B. Biointerfaces* **2011**, *88*, 593–600.

(21) Cho, E. C.; Lee, J.; Cho, K. *Macromolecules* **2003**, *36*, 9929–9934.

(22) Deshmukh, S. a; Sankaranarayanan, S. K. R. S.; Suthar, K.; Mancini, D. C. *J. Phys. Chem. B* **2012**, *116*, 2651–2663.

(23) Lien, Y.-H.; Wu, J.-H.; Liao, J.-W.; Wu, T.-M. *Macromol. Res.* **2013**, *21*, 511–518.

(24) Jeong, B.; Gutowska, A. *Trends Biotechnol.* **2002**, *20*, 305–311.

(25) Owens, D. E.; Jian, Y.; Fang, J. E.; Slaughter, B. V.; Chen, Y.-H.; Peppas, N. A. *Macromolecules* **2007**, *40*, 7306–7310.

(26) Amsden, B. *Macromolecules* **1998**, *31*, 8382–8395.

(27) Seuring, J.; Agarwal, S. *Macromol. Rapid Commun.* **2012**, *33*, 1898–1920.

(28) Okano, T. *Adv. Polym. Sci.* **1993**, *110*, 179–197.

(29) Tang, Q.; Wu, J.; Lin, J.; Li, Q.; Fan, S. *J. Mater. Sci.* **2008**, *43*, 5884–5890.

(30) Echeverria, C.; López, D.; Mijangos, C. *Macromolecules* **2009**, *42*, 9118–9123.

(31) Echeverria, C.; Mijangos, C. *Macromol. Rapid Commun.* **2010**, *31*, 54–58.
(32) Rosenberg, B.; Vancamp, L.; Trosko, J. E.; Mansour, V. H. *Nature* **1969**, *222*, 385–386.
(33) Poole, B. *J. Cell Biol.* **1981**, *90*, 665–669.
(34) Poulsen, A. K.; Arleth, L.; Almdal, K.; Scharff-Poulsen, A. M. *J. Colloid Interface Sci.* **2007**, *306*, 143–153.
(35) Ray, A.; Lee, Y. K.; Kim, G.; Kopelman, R. *Small* **2012**, *8*, 2213–2221.
(36) Nishiyama, N.; Yokoyama, M.; Aoyagi, T.; Okano, T.; Sakurai, Y.; Kataoka, K. *Langmuir* **1999**, *15*, 377–383.
(37) Howe-Grant, M. E.; Lippard, S. J. In *Metal Ions in Biological Systems*; Sigel, H.; Sigel, A., Eds.; Dekker: New York, 1980; pp. 63–125.
(38) Walser, M. *J. Clin. Invest.* **1961**, *40*, 723–730.
(39) Zhao, C.; Chen, Q.; Patel, K.; Li, L.; Li, X.; Wang, Q.; Zhang, G.; Zheng, J. *Soft Matter* **2012**, *8*, 7848.
(40) Vaupel, P.; Kallinowski, F.; Okunieff, P. *Cancer Res.* **1989**, *49*, 6449–6465.
(41) Thakur, A.; Wanchoo, R. K.; Singh, P. *Chem. Biochem. Eng. Q.* **2011**, *25*, 181–194.
(42) Lee, K. D.; Jeong, Y.; Kim, D. H.; Lim, G.; Choi, K.-C. *Int. J. Nanomedicine* **2013**, *8*, 2835–2845.

Chapter 4

Polyethylenimine-Incorporation into Hydrogel Nanoparticles for Enhanced Chemotherapy.

The material in this chapter has been adapted with minor modifications from the following prospective publication.

Shirakura, T. Ray, A. Kopelman R. "Incorporating-Polyethylenimine into Hydrogel Nanoparticles for Enhanced Chemotherapy." **In preparation**.

Introduction

Chemotherapy is one of the most widely used forms of cancer treatment. [1] It is noninvasive, and can be used for various types of tumors, especially those that are difficult to treat with surgery. However, it is also known that chemotherapy causes side effects, especially damaging those healthy cells that are growing rapidly, due to high systemic doses of the drug and its nonspecificity. [1,2] In order to reduce side effects, it is necessary to deliver the chemotherapeutic agents selectively to the tumor areas i.e., achieve a high local dose, at the tumor, with a low global dose. Additionally this will also reduce the systemic drug dose. Achieving a low therapeutic index is one of the key challenges in chemotherapy. [3]

Nanoparticle (NP)-based chemotherapy has been a recently used strategy to achieve selective delivery of these antitumor drugs. The NPs target the tumor tissue, due to their "active

targeting", with surface moieties, such as antibodies, peptides and aptamers, targeting cancer cells, [4–6] and due to their intrinsic "passive targeting" property, the so-called enhanced retention and permeability effect. [7] Thus, by containing the antitumor drugs inside the biocompatible NPs, the selectivity of the drug delivery to the tumor is enhanced. Additionally, drugs inside the NPs cannot interact with other cells in the body until they are released. [2] By loading them inside the NP's, the drugs themselves can be protected from degradation by the enzymes in the plasma. [2,8]

The cellular uptake is an important property of the NPs' design. The higher the amount of NPs that are taken up by the cells, the more drug molecules that can be delivered, leading to higher cytotoxicity. [9] Also, a high cellular uptake is a requirement for other important properties of NPs, such as controlled release of drugs, and organelle-specific delivery of NPs. Controlling the drug release so that they can be released after the NPs are internalized is another key aspect of the NPs' design. [10] Drug molecules that are released outside cells have a low probability of entering the cells. [11] Additionally, these drug molecules are subject to being pumped out from the cells, through the drug efflux transporters on the cellular membrane, leading to the multidrug resistant (MDR) effect. [12] However, this phenomenon can be overcome to some extent by using NPs as drug carriers that release drugs deep inside the cells. [8,13] Several strategies have been utilized for controlled release, such as thermally, [10] pH [14] and photochemically [15,16] controlled release systems. Also, delivery of the drug to the specific subcellular location may enhance its efficacy. [17] Drugs are mostly designed to work on a particular sub-cellular component, such as nucleus, mitochondria, etc., and, thus the degree of delivery to the particular organelle governs its efficacy. NP's are often localized within the vesicles, such as endosomes and lysosomes, and various techniques have been proposed to transfer the NPs into the cytosol for even more precise targeting (so-called endosomal escape).[177] In other situations, it is advantageous for the NPs to

avoid certain organelles, e.g., avoid the lysosomes and get to the perinuclear environment. [18] In any case, to deliver high concentrations of NPs into the cells and even closer to the site of action without being affected by these efflux transporters, it is important to develop nanoparticles with high efficiency of cellular uptake.

One of the common strategies researchers have taken to increase the cellular uptake was to make the surface of these NPs positive. [9] Because the cellular membrane is negatively charged, coating with positive charged chemical groups, e.g. amines, helps NPs in binding to the surface of the cells; thus more positively charged NPs can be uptaken better by cells. [19] Also, the amine-functionalization on the surface is important not only because of the electrostatic interactions between the NPs and cells, but also because the interaction with serum proteins plays an important role. It is reported that the cellular uptake is significantly higher in the presence of albumin, in case of amine-functionalized NPs, while the cellular uptake was significantly suppressed in case of carboxyl-functionalized NPs. [20]

Previously, we had developed amine-functionalized polyacrylamide based NPs for diagnostics and therapeutic applications, both at the *in vivo* and *in vitro* level. [21,22] The amine-functionalized PAA NPs show good cellular uptake as well as delivery of contrast agents and drugs. However, while the primary amine-containing acrylate monomer, N-(3-aminopropyl)methacrylamide, which was used in those applications, increases the cellular uptake, its fraction in the NP formulation is limited, due to the problematic solubility of the primary amine-containing acrylate monomer.

In this work, we explore a hypothesized method for improving the efficacy of the drug-loaded hydrogel NPs by making a hybrid matrix of polyacrylamide and polyethylenimine (PEI). PEI is a commonly used cationic polymer that has been widely used as a DNA and RNA carrier

for gene therapy, especially the branched polymer with molecular weight of 25 kDa. [23,24] However, the 25 kDa branched PEI itself is known to be toxic, due to its high positive charge on its surface, which leads to a cell-specific cause of apoptosis, such as mitochondrial damage. [24,25] By incorporating PEI into PAA NPs, we expect our formulation to have 1) an increase in cellular uptake, due to the PEI in the NPs; 2) Increase in the therapeutic efficacy, due to the higher uptake; 3) a reduction in the toxicity effects of PEI in the NPs, using full/partial coverage by the polyacrylamide matrix.

We additionally explore the endosomal escape ability of the synthesized PEI-incorporated PAA NPs (PEI-PAA NPs). We hypothesize that the endosomal escape of PEI-PAA NPs can further enhance the efficacy of NPs, i.e., increasing the time NPs stay inside cancer cells, thereby overcoming NP exocytosis, while the higher cellular uptake increases the drug concentration in the cells. Thus, NPs' having both higher cellular uptake and higher endosomal escape synergistically increases the drug efficacy.

Our observation confirmed the above hypothesizes; we observe up-to three-times higher cytotoxicity from cisplatin-loaded PEI-PAA NPs, compared to cisplatin-loaded PAA NPs without PEI. Also, cisplatin quantification experiments on the cells confirmed the hypothesis of a significantly higher cellular uptake of PEI-PAA NPs, compared to PAA NPs. However, the zeta-potentials of the PEI-PAA NPs were lower than those of PAA NPs, against our expectation. Having PEI on the surface of the PEI-PAA NPs might contribute to the enhancement of the cellular uptake, but not just by increasing the average overall charge of the NPs. Also, the PEI-PAA NPs did have a slight effect, of membrane disruption, on the endosomal escape, and this effect might contribute to the significant efficacy increase of the cisplatin-loaded PEI-PAA NPs.

Materials and Methods

Materials

Cisplatin was purchased from Selleck Chemical LLC. RPMI media was purchased from Invitrogen. Calcein was purchased from ICN Biomedicals Inc.All other chemicals were purchased from Sigma-Aldrich. The de-ionized water used in this experiment was purified prior to the experiment, using a Milli-Q system from Millipore.

NPs Synthesis

NPs were synthesized utilizing the standard protocol of polyacrylamide-based nanoparticles in Kopelman group.[6] In brief, NPs were synthesized utilizing the reverse micelle microemulsion polymerization.[5] Acrylamide, N-(3-aminopropyl)methacrylamide hydrochloride, 3-(acryloyloxy)-2-hydroxypropyl methacrylate, and PEI were dissolved in 1.3 mL water. Then, the solution was mixed with 45 mL of argon-purged hexane containing 1.6 g of sodium dioctylsulfosuccinate, as well as Brij30. The amount of Brij30 was varied, depending on the formulation of NPs, so as to increase the stability of NPs: In case of PAA, 3.47 mL of Brij30 was added; in case of L-PEI PAA, 4.47 mL of Brij30 was added; in case of H-PEI PAA, 5.27 mL of Brij30 was added; and in case of 90 PEI, 5.47 mL of Brij30 was added. After 20 minutes of further argon-purging, 100 μL of 10 w/v% of ammonium persulfate and N,N,N′,N′-tetramethylethylenediamine were added to the mixture, so as to initiate the polymerization. The reaction was complete in 2 hours. Hexane was removed by a rotary evaporator, and the remaining product was washed 5 times with 175 mL of ethanol and 150 mL of water, using an Amicon filtration system (Millipore). The NPs suspension was lyophilized, and stored at – 20 °C, for further investigation.

Loading of Alexa 647

0.1 mg of Alexa 647 was mixed with 40 mg of PAA in 4 mL of PBS (pH 7.4) and left overnight. Then, the free Alexa 647 was removed from the solution by washing the NPs, using a centrifugal filter (100kDaMWCO,from Millipore), 7 times. For the PEI-NPs, Alexa 647-labeled PEI was used during the synthesis of the NPs.

Conjugation of Triphenylphosphonium (TPP)

TPP was conjugated to the surface of the NPs in the following method. For each 10 mg of NPs, 21.4 mg of EDC, and 48.0 mg of (3-carboxypropyl)triphenylphosphonium bromide (CTPB) were mixed in 1.5 mL PBS and 0.5 mL DMSO. The reaction mixture was stirred overnight, and washed with the centrifugal filter (100kDaMWCO). The final product was concentrated to 20 mg mL^{-1} for further investigation.

Loading of Cisplatin

Cisplatin was loaded in the same method as previously described. [10] Briefly, cisplatin was loaded into the NPs in the weight ratio of 1 to 5, in deionized water. Then, the NPs were washed with 7 mL of water 7 times, using a centrifugal filter (100 kDaMWCO). Cisplatin content was measured using Inductively coupled plasma optimal emission spectroscopy (ICP-OES).

Cytotoxicity Assay

A rat glioma cell line, 9L was cultivated in RPMI, with addition of certified heat inactivated fetal bovine serum (10%) and penicillin, streptomycin and glutamine (1%). The 9L cells were transferred to a 96-well plate with a cell population of 2000 cells per well. 100 μL of complete RPMI was added to each well. After 24 hour incubation, 20 μL of NP suspension in PBS was added to the wells, to evaluate the cytotoxicity. After 12 hours incubation, NPs in the

cell media were removed, and the cells were rinsed twice with 100 μL per well of Dulbecco's Phosphate Buffered saline (DPBS). Then, 200 μL of complete RPMI was added, and incubated for another 48 hours. After the incubation, the cell media was removed from the wells, and 120 μL of 0.833 mg mL^{-1} of MTT reagent in RPMI, without phenol red, was added. After 4 hours incubation, the media was removed and 100 μL of dimethylsulfoxide was added. 1 hour later, the absorbances from the wells were measured, using a microplate reader (Anthos 2010, biochrom).

Pt Uptake Assay

The 9L cells were cultivated in a 100 x 20 mm Petri dish. When the confluency reached 80%, the cell media was removed, and 5 mL of fresh complete RPMI, and 700 μL of 25 μg mL^{-1} cisplatin-loaded NPs were added. After 12 hours incubation, NPs that were not uptaken by the cells were removed, and the cells were rinsed twice with 5 mL of DPBS. The cells were trypsinized, and the population counted. After that, the cells were digested by soaking cells in 70% nitric acid, for 2 days. The cisplatin contents of the cells were measured, using ICP-OES.

F3-PEG Conjugation

The F3 peptide and polyethylene glycol (PEG) were conjugated onto the surface of the NPs, following a procedure previously described. [26] Briefly, 10 mg of NPs were conjugated with 2.2 mg of F3 peptide, using 0.8 mg of Mal-PEG(2 k)-NHS as a crosslinker. All the reactions were performed in PBS.

Fluorescence microscopy

The fluorescence microscopy was performed using a Leica confocal microscope (SP-5X), located at the Microscopy image analysis Lab, University of Michigan. This microscope has a wide range of excitation source including 405nm, 455nm, and 480-600nm. The fluorescence

emission was detected using a CCD camera ranging and the appropriate wavelength range can be selected using an acousto-optic tunable filter. The pH measurements were taken with the diode laser at 405 nm and the white light laser at 450 nm, and the fluorescence emission was detected at 510nm. The lysotracker and mitotracker were irradiated at 577nm and 579nm, respectively, whereas the fluorescence emission was detected at 590nm and 599nm, respectively.

Lysotracker

The 9L cells were plated on an glass bottom Petri dish (Mat Tek) and grown for a few days before incubation with NPs. The nanoparticles were incubated with the cells at 0.5 mg/mL final concentration for 2 hour and then washed with fresh buffer, three times, to remove any unbound NP. The cells with NP were further allowed to grow for 48 hours before being used for imaging. Then the cells were treated with a lysosomal staining probe, lysotracker red DNB-99 for 10 minutes. The excess lysotrakcer probe was removed by washing with colorless RPMI media one more time.

Results and Discussion

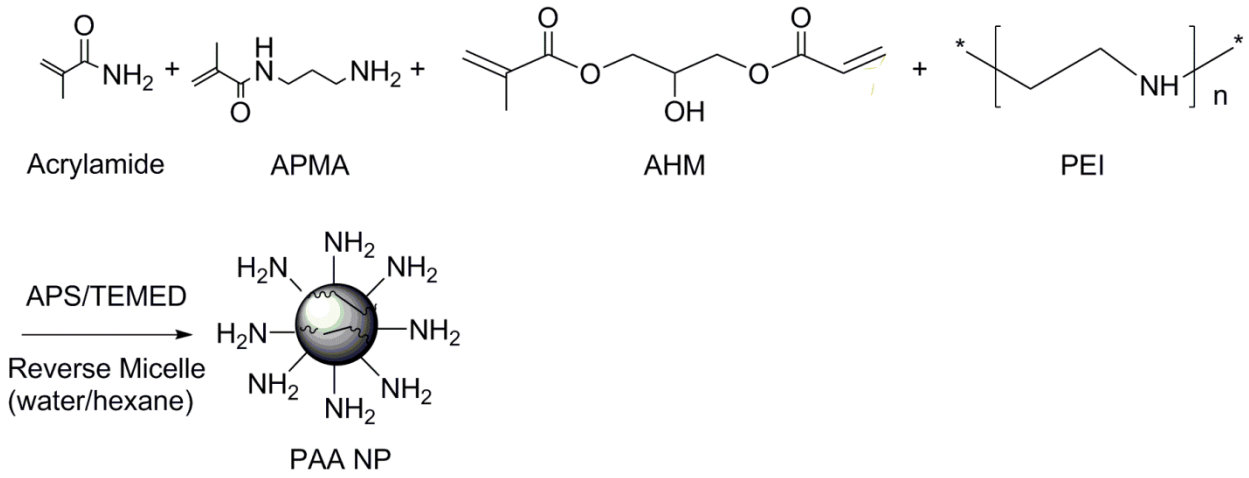

Scheme 4.1.Synthesis Scheme of PEI NPs.

PEI-PAA NPs and PAA NPs were synthesized modifying a method reported previously. [6] PEI was mixed with the monomers and cross-linkers prior to the polymerization. Extra volume of Brij30 was added during the polymerization of PEI-PAA NPs because PEI de-stabilized the microemulsion. The size and the zeta-potential of synthesized NPs are summarized in Table 4.1.

Table 4.1.PEI amount, size and ζ-potential of the synthesized NPs. PEI content describes the initial amount of PEI added per batch of NPs, as described in the Materials and Methods section.

		Blank		with Cisplatin		Blank	with Cisplatin
	PEI (mg)	size (nm)	PDI	size (nm)	PDI	ζ-potential (mV)	
PAA	0	63 (±1)	0.16 (± 0.04)	69 (±1)	0.25(±0.01)	16.3 (± 1.1)	18.9(±1.0)
L-PEI PAA	35.9	53(± 1)	0.25(± 0.01)	87 (±1)	0.28(±0.01)	12.3 (± 1.0)	8.0(±0.3)
H-PEI PAA	54	93(± 1)	0.28(± 0.01)	91 (±2)	0.25(±0.01)	15.9 (± 1.3)	8.3(±0.5)

Two types of PEI-PAA NPs were synthesized, with higher and lower PEI concentration. H-PEI PAA contains more PEI in the NPs than L-PEI PAA. The blank L-PEI PAA sample shows a similar size as the blank PAA sample. The blank H-PEI PAA samples showed significantly larger sizes of NPs, compared to the blank PAA and blank L-PEI PAA samples. On the other hand, the ζ-potential of both blank L-PEI PAA and blank H-PEI PAA samples was slightly lower than that of the PAA NPs, regardless of adding PEI, which was expected to make the NPs' ζ-potential more positive. The lower charge could be attributed to the bigger size of the PEI-PAA NPs. After loading cisplatin, the size of the NPs did not change significantly except L-PEI PAA.

Into these NPs, cisplatin was post-loaded by the method previously described. [10] The weight % drug loadings of the NPs were calculated, using the following equation (Equation 1).

$$wt\%loading = \frac{m_{cisplatin}}{m_{cisplatin} + m_{NPs}} \times 100(\%) \qquad \text{Equation 1}$$

Here, $m_{cisplatin}$ is the mass of cisplatin in the NPs after the loading, m_{NPs} is the mass of NPs used in the synthesis. The cisplatin loading percentage is summarized in Table 4.2. There was no significant difference in the loading between PEI-PAA NPs and PAA NPs. Also, the amount of PEI in the matrix did not affect the cisplatin amount in the NPs.

Table 4.2. wt % Loading of Cisplatin.

	Cisplatin wt % loading
PAA	0.58 (±0.30)
L-PEI PAA	1.2 (±0.76)
H-PEI PAA	0.85 (±0.37)

The H-PEI PAA NPs were synthesized utilizing Alexa 647-conjugated PEI, so as to confirm the loading of PEI into NPs. The calculated loading of PEI was 53.9 (±7.9) μg per 1 mg of NPs. This confirms that almost all the PEI was successfully loaded into the NPs.

The cytotoxicity of the NPs was evaluated without loading cisplatin (Figure 4.1).

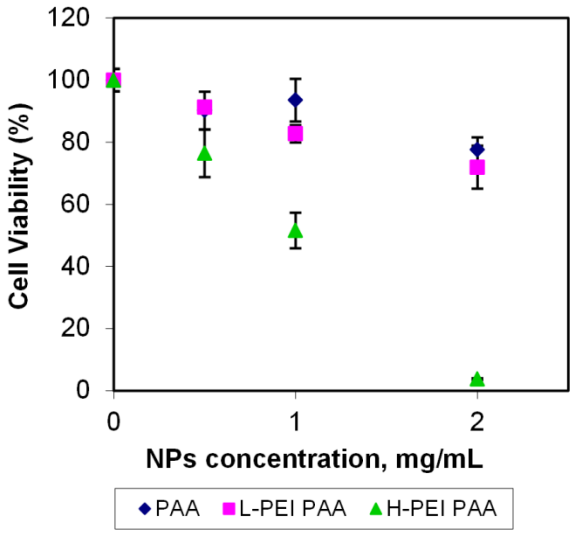

Figure 4.1.Cytotoxicity of Blank NPs in 9L cells (rat glioma cell line). The error bars represent the standard deviations.

The L-PEI PAA and PAANPs showed a similar degree of toxicity, while the H-PEI PAA showed a significantly higher cytotoxicity, especially for the NP concentrations at and above 1 mg mL^{-1}. The cytotoxicity of the H-PEI PAA indicates a possible interaction of cells with PEI, leading to cell death due to the cytotoxicity of PEI itself. [24] However, it is noted that these PEI-loaded NPs are approximately two times less cytotoxic than free PEI (Figure 4.2). The lesser toxicity of PEI-PAA NPs implies coverage of PEI by PAA matrix, i.e. shielding from its potential toxicity.

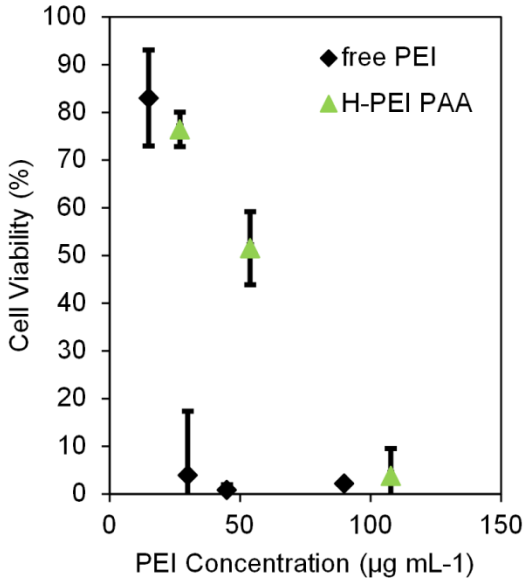

Figure 4.2. MTT Cell Assay for free PEI in 9L cells (rat glioma cell line). The error bars represent the standard deviations. As a comparison, H-PEI in Figure 4.1 is plotted. The data is normalized to the viability of cells treated with PBS.

To understand the relationship between the amount of PEI and the properties of NPs, we synthesized another batch of PEI-NPs with double the amount of PEI, compared to the previous H-PEI PAA NPs batch. The size of the NPs increased to 112 (± 1) nm, and the zeta-potential dropped 12.4 (± 0.5) mV. The NPs were equally toxic to H-PEI NPs. This confirms that

incorporation of PEI enlarges the size of the NPs, reduces the zeta-potential, and increases the cytotoxicity.

Then, we evaluated the cytotoxicity of the cisplatin-loaded NPs (Figure 4.3).

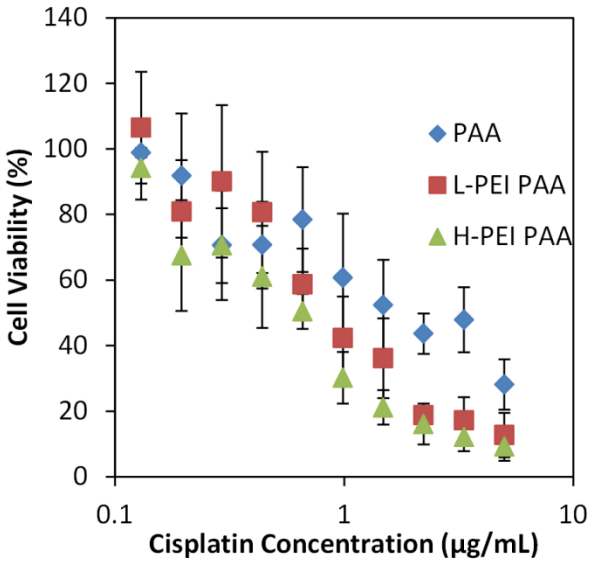

Figure 4.3. MTT Assay of Cisplatin-loaded NPs in 9L cells (rat glioma cell line). Cisplatin concentration is shown on a logarithmic scale. The error bars represent the standard deviations. The data is normalized to the viability of cells treated with PBS.

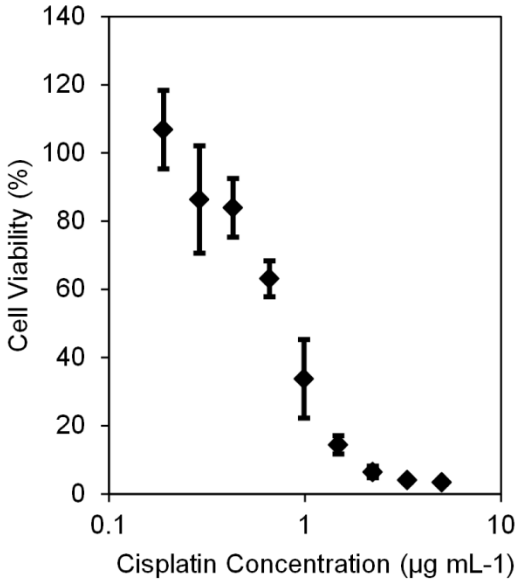

Figure 4.4. MTT Assay of Free Cisplatin in 9L cells (rat glioma cell line). Cisplatin concentration is shown on a logarithmic scale. The error bars represent the standard deviations. The data is normalized to the viability of cells treated with PBS.

IC_{50} values of PAA, L-PEI PAA, and H-PEI PAA were 1.85 μg mL^{-1}, 0.950 μg mL^{-1}, and 0.60 μg mL^{-1}, respectively. Based on Table 4.2, we need 0.86 mg/mL of PAA, 0.42 mg/mL of L-PEI PAA, and 0.59 mg/mL of H-PEI PAA in order to achieve a 5 μg/mL cisplatin concentration, which is the highest concentration we tested in Figure 4.3. Blank NPs in those concentrations (Figure 4.1) were much less toxic (~90 % for PAA NPs and L-PEI PAA NPs and ~80 % for H-PEI PAA NPs) than cisplatin-loaded NPs at 5 μg/mL cisplatin concentration (~ 30 % for PAA NPs and ~ 10% for L-PEI PAA and H-PEI PAA NPs) (Figure 4.3). In other words, the toxicity observed in Figure 4.3 is attributed to cisplatin. Also, when the cytotoxicity of these cisplatin-loaded PEI-PAA NPs was compared to the cytotoxicity of free cisplatin, cisplatin-loaded PEI-PAA NPs showed similar levels of cytotoxicity (See Figure 4.4).

In order to elucidate the mechanism of having different levels of cytotoxicity among three different NPs, we evaluated the release profile of these NPs in PBS (pH 7.4) (Figure 4.5).

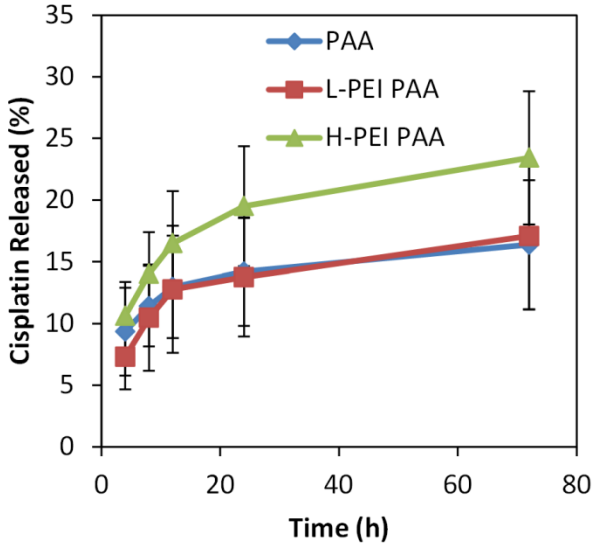

Figure 4.5. Cisplatin Release Profile from NPs in PBS. Error bars represent the standard deviations from 4 trials of release study.

There was almost no difference in the release profile between the PAA and L-PEI PAA NPs. The H-PEI PAA sample released 1.4 times higher amounts of cisplatin, in 72 hours, than the PAA sample, but the difference is not statistically significant. Accordingly, the cisplatin release profile of these NPs cannot account for the difference in the cytotoxicity since they have similar amounts of cisplatin encapsulated.

As Figure 4.5 shows, there is no significant difference in the release profile observed between three different formulations, so, in order to further analyze the cause for the high cytotoxicity of the L-PEI PAA and H-PEI PAA NPs, the cellular uptake of cisplatin was measured (Figure 4.6).

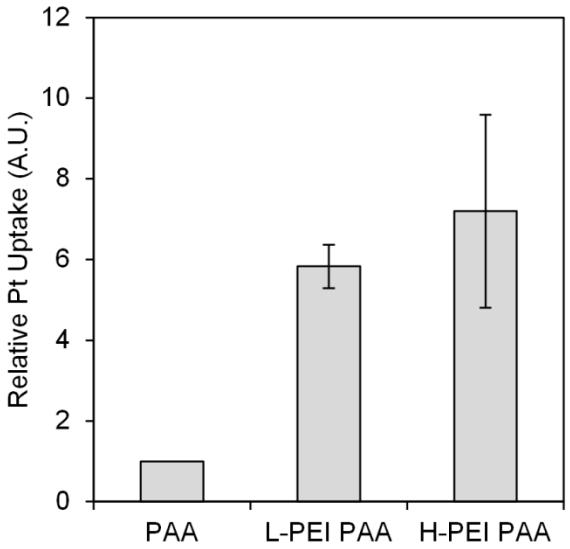

Figure 4.6. Cellular Uptake of Cisplatin from Various NP Formulations in 9L cells (rat glioma cell line). The uptake signal is normalized to the cisplatin uptake when PAA NPs were utilized. The error bars represent the standard deviations of 3 repeating experiments.

The data is normalized to the cellular uptake of PAA NPs. We observe a 6 times higher uptake of cisplatin when cisplatin was loaded into L-PEI PAA NPs, and a 7 times higher uptake of cisplatin from the H-PEI PAA. In general, more positive NPs are better uptaken by cancer cells. [19] However, our data showed that the PEI-PAA NPs can be better uptaken by cells

regardless of their lower zeta-potential. This implies that incorporation of PEI into the NP-matrix enhances the cellular uptake, not by simply changing the zeta-potential, i.e. average overall surface charge.

Based on the above data, the higher cellular cisplatin concentration inside the cells with L-PEI PAA and H-PEI PAA NPs most probably plays a significant role in increasing the cytotoxicity of the cisplatin loaded L-PEI PAA and H-PEI PAA, compared to PAA NPs.

In order to determine the distribution of the PEI encapsulated inside the NP, the release profile of PEI was evaluated using the H-PEI PAA NPs whose PEI were fluorescently-labeled. We observe that 19 % of PEI was released in 1 day, and 35 % of PEI was released in 3 days. This indicates that a significant fraction of the PEI was on or close to the surface. Thus, most probably, the free amine groups from the PEI have led to the increase in cellular uptake of the PEI encapsulated NP's. Also, this would be consistent with the higher cytotoxicity observed in blank H-PEI PAA (Figure 4.1) being due to the high release of PEI.

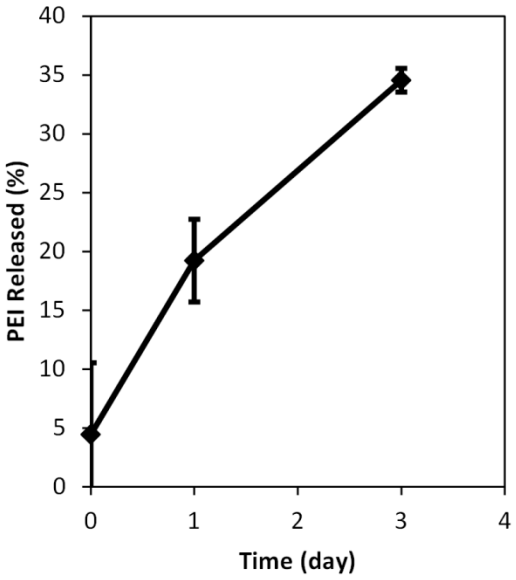

Figure 4.7.Release of PEI from PEI-NPs in PBS at 37°C. Error bars represent the standard deviations

In order to confirm that the much higher cell uptake is because of the PEI on the surface of the NPs, the surfaces of PEI containing NPs were coated with PEG (polyethylene glycol), and with the nucleolin-targeting peptide, F3 (attached to the PEG). Cellular uptakes of F3-PEG coated, PEI containing, NPs were evaluated using these cisplatin-loaded NPs (Figure 4.8).

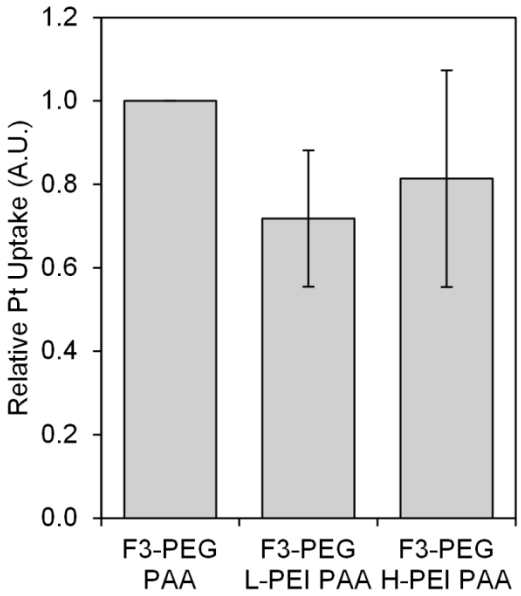

Figure 4.8. Pt uptake experiment with F3-PEG coated PEI-NPs in 9L cells (rat glioma cell line). The signals are normalized to the cisplatin uptake when F3-PEG coated PAA NPs were used. Error bars represent the standard deviations.

After coating of the NP surface with F3-PEG, no significant difference in the uptake between PEI-PAA NPs and PAA NPs was observed (Figure 4.8). Apparently, PEI on the surface was successfully covered by the F3-PEG, and the coverage diminished the difference in cellular uptake.

In addition to PEI enhancing the uptake of the NP's, it can facilitate the improving of the efficacy of the chemo-drugs in several other ways. It is widely known that PEI has an ability to induce endosomal escape of nanoparticles, and this extends the time NPs stay inside the cells; otherwise, half of the NPs may be removed by exocytosis within 0.5 hour. [27] In order to test if the higher cytotoxicity of cisplatin-loaded L-PEI PAA and cisplatin-loaded H-PEI PAA can also be attributed to this ability, the NP endosomal escaping ability was evaluated.

We compared the transfection efficiency of L-PEI PAA and H-PEI PAA NPs with that of a widely accepted transfection agent, lipofectamine, using the green fluorescence protein (GFP) plasmid (Figure 4.9).

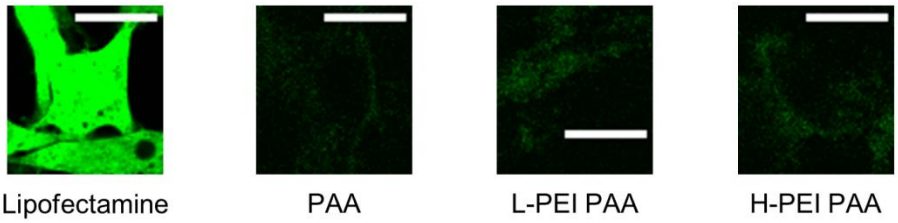

Figure 4.9. GFP Transfection Experiment in 9L cells (rat glioma cell line). The scale bars represent 20 μm. The 9L cells were transfected with GFP plasmid, using different plasmid carriers. The green color on the images shows the expression level of GFP. Lipofectamine is a commercially available transfection agent.

We could observe a strong GFP fluorescence from the transfected cells when lipofectamine was used as a transfection agent. However, the level of the fluorescence was much weaker when L-PEI PAA and H-PEI PAA NPs were used. However, the intracellular fluorescence was slightly (~20%) higher than the control, i.e. the cell incubated with the plasmid and PAA NP as the transfection agent. This indicates that the PEI-NP's may not be very efficient in escaping the endosomes. But the slight increase does indicate that some transfection, which could potentially indicate that a larger percent of drugs delivered using the PEI-NPs could reach the cytosol, compared to the NPs without PEI. This can also potentially play a significant part in increasing the drug efficacy.

We next measured the pH of the microenvironment of the NPs so as to monitor any change due to the presence of PEI. The NPs are generally taken up by the cells via the process of endocytosis, and they are then located inside the endosomes and lysosomes. [18] As a result the average pH from of the NP microenvironment is generally observed to be slightly acidic (6.2

±0.2). [28] It has been previously shown that causing significant damage to the endosomal compartment can avoid staying inside the lysosome, and leads to a slight increase in the pH value. [29] However, in our case we do not observe any significant changes in the pH value of the NP microenvironment. This indicates that the PEI inside the NP does not cause much damage to the lysosomal membrane. However the membrane rupture often caused due to the proton sponge effect in the presence of the transfection agents does not necessarily perturb the pH. [30] We next tested the ability of the NP's to escape the endosomes and lysosomes. This was tested in two different ways. We first monitor the co-localization of the nanoparticles with the acidic vesicles, as shown in Figure 4.10.

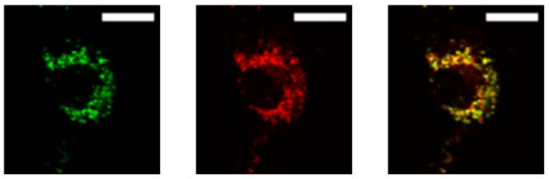

Figure 4.10. Co-localization experiment of H-PEI PAA with lysotracker in 9L cells (rat glioma cell line). NPs and lysotracker are shown in green and red, respectively. A high degree of co-localization is observed here (yellow/orange). The scale bars represent 20 μm.

The cells were incubated with NPs both with and without PEI for two hours and then washed. Two days following internalization of the NP's, the cells were prepared for the co-localization experiment by staining the acidic vesicles with lysotracker. The co-localization between the PEI-PAA NPs and the PAA-NPs were then compared. We do not observe any significant difference between the levels of co-localization of these NPs with the acidic vesicles. The Pearson's coefficients quantify the degree of co-localization. [31] When the value is 1, -1, or 0, the green and red channels are perfectly correlated, perfectly but inversely correlated, and not correlated, respectively. The Pearson's coefficients were found to be 0.88 (± 0.02) and 0.68 (± 0.02) for PEI-PAA NPs and PAA NPs, respectively. This shows that the PEI-NP's are not very

efficient in escaping the endosomes. In addition we also use PEI-NPs with TPP, which targets the mitochondria. This was done to deliver any NP that escapes out of the endosome to the mitochondria.

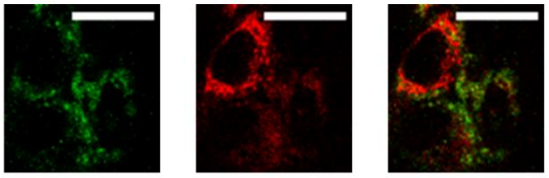

Figure 4.11. Mitotracker co-localization experiment using TPP-conjugated NPs in 9L cells (rat glioma cell line). NPs and mitotracker are shown in green and red, respectively. Absence of yellow/orange color in the image shows negative co-localization of green and red. The scale bars represent 20 μm.

Figure 4.11 shows the degree of co-localization of the PEI-NP with the mitochondria. We do observe some co-localization but at an extremely low level, a Pearson's coefficient of 0.46 (± 0.03). This observation confirms that most of the PEI-PAA are trapped inside the endosomal/lysosomal vesicles and only a tiny fraction are able to escape from the endosome.

As a final experiment we prepared calcein loaded PEI-NPs, to check if these PEI-NPs cause small changes in the membrane permeability. Calcein is known to be a membrane-impermeable dye.

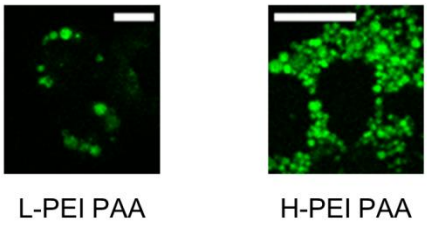

Figure 4.12. The fluorescence distribution of the calcein-loaded NPs in 9L cells (rat glioma cell line). Green color represents the signal from calcein. The scale bars represents 10 μm.

Calcein was loaded into the PEI-incorporated NPs by mixing calcein with NPs in water, and incubated with cells for 48 hours before imaging. The fluorescence images of the calcein loaded NPs are shown in Figure 4.12. Calcein leaches out of the NPs and is entrapped inside the vesicles as it is membrane impermeable. We observe most of the fluorescence from the confinements of the vesicles of endosomes/lysosomes. The fluorescence from the cytosol was not significantly different from the background. This shows that only a small fraction of the dye was able to leach out of the vesicles. These experiments on NP co-localization and calcein leaching demonstrate that the damage to the membrane due to the PEI is present but not very significant. However, it has been shown before that transfection agents in some cases do not change the pH of the endosomes, or enable NP's endosomal escape, but still do efficiently transfect luciferase.[30] The exact mechanism of transfection is still unclear and hotly debated. [30] Additionally, cisplatin molecules are extremely small and thus even minute damage to the endosomal membrane will be sufficient to increase its cytosolic concentration, while not affecting the NPs or calcein, which is a relatively larger molecule (M.W. = 666.51 Da).

It has been reported that the PEI-cisplatin complex is more toxic than cisplatin alone, because of PEI's ability of endosomal escaping.[9] Our results seem to support this claim.

Conclusions

(1)We successfully incorporated PEI into hydrogel PAA-NPs. (2) The PEI-incorporated NPs are much more cytocompatible than free PEI. (3) These PEI-PAA NPs still retain the pure PEI's property of highly enhanced cellular uptake, i.e. resulting in *enhancing the hydrogel NPs' cellular uptake by 600% to 700%*. (4) The H-PEI PAA NPs result in a higher amount of drugs inside the cells (5) The cisplatin loaded PEI-incorporated NPs show a much enhanced

cytotoxicity. (6) The enhanced uptake of the NPs by the incorporation of PEI cannot be simply explained by their average surface properties (i.e., zeta-potential), and the exact mechanism of the phenomenon. Is it due to the surface heterogeneity? This needs further investigation. (7) PEI PAA NPs showed a marginal endosomal escaping ability for prolonged localization of cisplatin inside the cells.

The embedding of PEI into the hydrogel matrix highly improves on the NPs' cellular uptake. There may be also a marginal enhancement on the release of the cisplatin they carry, and the endosomal escaping ability. Overall, these factors results in an improvement on the cytotoxicity.

Acknowledgements

Financial Support was provided by a National Institutes of Health grant, R21NS084275 (RK). The author thanks Antonina E. Malyarenko for help with the drug release study. The author thanks Ming Qin and the Brent R. Martin group (Department of Chemistry, University of Michigan) for the use of their fluorescence microplate reader, and the Chemistry Instrument Shop in University of Michigan.

References

1. Chabner, B.; Roberts, T. Chemotherapy and the War on Cancer. *Nature Reviews Cancer* **2005**, *5*, 65–72.
2. Koo Lee, Y.; Kopelman, R. In *Multifunctional Nanoparticles for Drug Delivery Applications*; Svenson, S.; Prud'homme, R. K., Eds.; Nanostructure Science and Technology; Springer US: Boston, MA, 2012; pp. 225–255.
3. Koo Lee, Y.-E.; Reddy, G.; Bhojani, M.; Schneider, R.; Philbert, M.; Rehemtulla, A.; Ross, B.; Kopelman, R. Brain Cancer Diagnosis and Therapy with Nanoplatforms. *Advanced Drug Delivery Reviews* **2006**, *58*.
4. DeNardo, S. J.; DeNardo, G. L.; Miers, L. A.; Natarajan, A.; Foreman, A. R.; Gruettner, C.; Adamson, G. N.; Ivkov, R. Development of Tumor Targeting Bioprobes ((111)In-Chimeric L6 Monoclonal Antibody Nanoparticles) for Alternating Magnetic Field Cancer Therapy. *Clin. Cancer Res.* **2005**, *11*, 7087s–7092s.
5. Dhar, S.; Gu, F. X.; Langer, R.; Farokhzad, O. C.; Lippard, S. J. Targeted Delivery of Cisplatin to Prostate Cancer Cells by Aptamer Functionalized Pt(IV) Prodrug-PLGA-PEG Nanoparticles. *Proc. Natl. Acad. Sci. U.S.A.* **2008**, *105*, 17356–61.
6. Winer, I.; Wang, S.; Lee, Y.-E.; Lee, Y.-E.; Fan, W.; Gong, Y.; Burgos-Ojeda, D.; Spahlinger, G.; Kopelman, R.; Buckanovich, R. F3-Targeted Cisplatin-Hydrogel Nanoparticles as an Effective Therapeutic That Targets Both Murine and Human Ovarian Tumor Endothelial Cells In Vivo. *Cancer Research* **2010**, *70*, 8674–83.
7. Maeda, H. The Enhanced Permeability and Retention (EPR) Effect in Tumor Vasculature: The Key Role of Tumor-Selective Macromolecular Drug Targeting. *Advances in enzyme regulation* **2001**, *41*, 189–207.
8. Qin, M.; Lee, Y.; Ray, A.; Kopelman, R. Overcoming Cancer Multidrug Resistance by Codelivery of Doxorubicin and Verapamil with Hydrogel Nanoparticles. *Macromolecular Bioscience* **2014**, *14*, 1106–1115.
9. Sun, X.; Chen, J.; Chen, H.; Liang, W. Polyethylenimine Modified Liposomes as Potential Carriers for Antitumor Drug Delivery in Vitro. *Die Pharmazie* **2012**, *67*, 426–31.
10. Shirakura, T.; Kelson, T.; Ray, A.; Malyarenko, A.; Kopelman, R. Hydrogel Nanoparticles with Thermally Controlled Drug Release. *ACS macro letters* **2014**, *3*, 602–606.
11. Ganta, S.; Devalapally, H.; Shahiwala, A.; Amiji, M. A Review of Stimuli-Responsive Nanocarriers for Drug and Gene Delivery. *Journal of controlled release : official journal of the Controlled Release Society* **2008**, *126*, 187–204.
12. Mimeault, M.; Batra, S. New Promising Drug Targets in Cancer- and Metastasis-Initiating Cells. *Drug discovery today* **2010**, *15*, 354–64.
13. Cuvier, C.; Roblot-Treupel, L.; Millot, J. M.; Lizard, G.; Chevillard, S.; Manfait, M.; Couvreur, P.; Poupon, M. F. Doxorubicin-Loaded Nanospheres Bypass Tumor Cell Multidrug Resistance. *Biochemical Pharmacology* **1992**, *44*, 509–517.
14. Peng, J.; Qi, T.; Liao, J.; Chu, B.; Yang, Q.; Li, W.; Qu, Y.; Luo, F.; Qian, Z. Controlled Release of Cisplatin from pH-Thermal Dual Responsive Nanogels. *Biomaterials* **2013**, *34*, 8726–40.
15. Suzuki, A.; Tanaka, T. Phase Transition in Polymer Gels Induced by Visible Light. *Nature* **1990**, *346*.
16. Mamada, A.; Tanaka, T.; Kungwatchakun, D.; Irie, M. Photoinduced Phase Transition of Gels. *Macromolecules* **1990**, *23*.

17. Biswas, S.; Torchilin, V. Nanopreparations for Organelle-Specific Delivery in Cancer. *Advanced Drug Delivery Reviews* **2013**, *66*, 26–41.
18. Karamchand, L.; Kim, G.; Wang, S.; Hah, H.; Ray, A.; Jiddou, R.; Lee, Y.-E.; Philbert, M.; Kopelman, R. Modulation of Hydrogel Nanoparticle Intracellular Trafficking by Multivalent Surface Engineering with Tumor Targeting Peptide. *Nanoscale* **2013**, *5*, 10327–44.
19. He, C.; Hu, Y.; Yin, L.; Tang, C.; Yin, C. Effects of Particle Size and Surface Charge on Cellular Uptake and Biodistribution of Polymeric Nanoparticles. *Biomaterials* **2010**, *31*, 3657–3666.
20. Fleischer, C.; Payne, C. Secondary Structure of Corona Proteins Determines the Cell Surface Receptors Used by Nanoparticles. *J. Phys. Chem. B* **2014**, *118*, 14017 14026.
21. Ray, A.; Yoon, H.; Lee, Y.; Kopelman, R.; Wang, X. Sonophoric Nanoprobe Aided pH Measurement in Vivo Using Photoacoustic Spectroscopy. *Analyst* **2013**, *138*, 3126–30.
22. Wang, S.; Fan, W.; Kim, G.; Hah, H.; Lee, Y.; Kopelman, R.; Ethirajan, M.; Gupta, A.; Goswami, L.; Pera, P.; *et al.* Novel Methods to Incorporate Photosensitizers into Nanocarriers for Cancer Treatment by Photodynamic Therapy. *Lasers in Surgery and Medicine* **2011**, *43*, 686–695.
23. Intra, J.; Salem, A. Characterization of the Transgene Expression Generated by Branched and Linear Polyethylenimine-Plasmid DNA Nanoparticles in Vitro and after Intraperitoneal Injection in Vivo. *J Control Release* **2008**, *130*.
24. Cheng, H.; Zhu, J.-L.; Zeng, X.; Jing, Y.; Zhang, X.-Z.; Zhuo, R.-X. Targeted Gene Delivery Mediated by Folate-Polyethylenimine-Block-Poly(ethylene Glycol) with Receptor Selectivity. *Bioconjugate Chemistry* **2009**, *20*, 481–487.
25. Xia, T.; Kovochich, M.; Liong, M.; Zink, J. I.; Nel, A. E. Cationic Polystyrene Nanosphere Toxicity Depends on Cell-Specific Endocytic and Mitochondrial Injury Pathways. *ACS nano* **2008**, *2*, 85–96.
26. Nie, G.; Hah, H.; Kim, G.; Lee, Y.-E.; Qin, M.; Ratani, T.; Fotiadis, P.; Miller, A.; Kochi, A.; Gao, D.; *et al.* Hydrogel Nanoparticles with Covalently Linked Coomassie Blue for Brain Tumor Delineation Visible to the Surgeon. *Small (Weinheim an der Bergstrasse, Germany)* **2012**, *8*, 884–91.
27. Panyam, J.; Labhasetwar, V. Dynamics of Endocytosis and Exocytosis of poly(D,L-Lactide-Co-Glycolide) Nanoparticles in Vascular Smooth Muscle Cells. *Pharm. Res.* **2003**, *20*, 212–20.
28. Ray, A.; Lee, Y.-E. K. E.; Kim, G.; Kopelman, R. Two-Photon Fluorescence Imaging Super-Enhanced by Multishell Nanophotonic Particles, with Application to Subcellular pH. *Small (Weinheim an der Bergstrasse, Germany)* **2012**, *8*, 2213–21.
29. Akinc, A.; Thomas, M.; Klibanov, A.; Langer, R. Exploring Polyethylenimine-Mediated DNA Transfection and the Proton Sponge Hypothesis. *The journal of gene medicine* **2005**, *7*, 657–63.
30. Benjaminsen, R.; Mattebjerg, M.; Henriksen, J.; Moghimi, S.; Andresen, T. The Possible "Proton Sponge " Effect of Polyethylenimine (PEI) Does Not Include Change in Lysosomal pH. *Molecular therapy : the journal of the American Society of Gene Therapy* **2012**, *21*, 149–57.
31. Dunn, K.; Kamocka, M.; McDonald, J. A Practical Guide to Evaluating Colocalization in Biological Microscopy. *Am. J. Physiol., Cell Physiol.* **2011**, *300*, C723–42.

–

Chapter 5

Summary and Future Directions

5.1 Summary

5.1.1. Chapter 1.

Chemotherapy is one of the most common cancer treatments. However, current chemotherapy has problems. One of the problems is its severe side effects that are associated with the non-targeted distribution in the body.[1,2] Another problem is that some of the cancer cells have a resistance against chemotherapy, the so-called multidrug resistance (MDR).[3] This MDR ability of the cancer cells plays an important role in cancer recurrence because the origin of the recurrence, so-called cancer stem cells, is known to have MDR.[3]

Nanoparticle (NP)-assisted chemotherapy may solve both problems due to their advantages discussed in chapter 1. NPs serve as carriers of chemotherapeutic agents, and release the agents in the tumor. The NPs' targeting ability can reduce the systemic side effects.[1] NPs have an intrinsic property to selectively accumulate in the tumor areas, by enhanced permeability and retention (EPR).[4] EPR can reduce the side effects. Also, the conjugation of targeting moieties on the surface of NPs can further increase the targeting ability, so the side effects can be further reduced.[1,5]

The NPs' targeting ability, their longer blood circulation time, and their intrinsic MDR avoidance can overcome cancer MDR. Targeting ability of NPs can increase the concentration of

drugs in the tumor area.[1,5] The conjugation of polyethylene glycol on the surface of NPs can increase the blood circulation time, and can further increase the chance of the delivery of NPs to the tumor areas (i.e. increase the local dose of the drugs).[6] Due to this targeting ability and enhanced blood circulation time, NPs-assisted chemotherapy can deliver more drugs to the tumor areas than the treatment with free drugs, which can help override the cancer MDR ability. Also, NPs are reported to have an intrinsic ability to overcome the MDR ability as discussed in chapter 1.[7,8]

In addition to solving many of the current problems of chemotherapy, NPs can help in protecting the drugs from degradation by enzymes in the blood.[9]

In my research, I utilized highly engineerable polyacrylamide (PAA) -based NPs. PAA NPs have shown their high biocompatibility both *in vitro* and *in vivo*.[5,10] Also, various properties of the NPs, such as their surface charge and hydrophilicity, can be tuned by varying the type and the ratio of acrylamide, acrylamide-derivatives, and cross-linkers.

I utilized cisplatin as a model drug.[11] It is widely used for chemotherapy, but known to have severe side effects.[2] In addition, the platinum atom at the center of the cisplatin molecule makes it easy to be quantified inside NPs as well as inside the cells.

Utilizing this system, I assessed three critical factors of NP-assisted chemotherapy: the % loading of cisplatin, the release of cisplatin, and the cellular uptake of the NPs. The loading efficiency was discussed in chapter 2. The release efficiency was discussed in chapters 2 and 3. Finally cellular uptake was discussed in chapters 2 and 4.

5.1.2. Chapter 2

The effect of the NPs' matrix structure on cisplatin loading and release is evaluated in chapter 2. I proposed a simple method of changing the matrix density, utilizing a characteristic of

reverse micelle polymerization. Two different formulations, p(AAm-*co*-APMA) NPs and p(AAm-*co*-AA) NPs, were evaluated for the effect of the matrix density upon their cisplatin-loading ability, release profile, and cytotoxicity . No significant change in weight percent loading of cisplatin was observed for the NPs of different matrix density. The matrix density of both formulations showed an inverse relationship between the matrix density and the effective cisplatin diffusion coefficient (i.e. release profile), which is positively correlated with the mesh size of the NPs' matrix. Also, we evaluated the cellular uptake of the amine-functionalized NPs, p(AAm-*co*-APMA) NPs, and the carboxyl-functionalized NPs, p(AAm-*co*-AA) NPs because this is another important factor to determine the therapeutic efficacy of the NPs. Amine-functionalized NPs had significantly higher cellular uptake than carboxyl-functionalized NPs due to their higher interaction with cellular membrane and enhanced uptake facilitated by albumin.[12,13] The release of cisplatin showed a slight correlation with its cytotoxicity. Cisplatin-loaded p(AAm-*co*-APMA) NPs and cisplatin-loaded p(AAm-*co*-AA) NPs have similar IC_{50} values, even though the p(AAm-*co*-AA) NPs release more cisplatin more rapidly. The similarity of the IC_{50} values can be explained by the lower cellular uptake of p(AAm-*co*-AA) NPs, compared to p(AAm-*co*-APMA) NPs. In principle, the tuning of the matrix density can be easily performed utilizing a property of the reverse micelle polymerization, and this tuning helps in controlling the release profile of drugs, towards optimal release. The tuned release enhances the delivery of drugs *specifically* to the targeted area, and minimizes systemic side effects.

5.1.3. Chapter3

Cisplatin-loaded, temperature-responsive NPs (CisPt-NPs), with a matrix consisting of acrylamide and acrylic acid, were synthesized so as to incorporate a trigger of cisplatin release and reduce its side effects. The NPs were designed to swell at the higher temperature (typical to a

tumor area) due to the internal temperature difference of the tumor areas and the rest of the body. This could also be useful for therapy with the aid of or an external heat source. The synthesized NPs are expected to have a reduced release of free cisplatin in the bloodstream while increasing the release in the tumor areas. The temperature dependence of the cisplatin release was evaluated in PBS, with and without divalent metallic ions. Enhancement of the release at higher temperature was indeed observed, and the metallic ions further accelerated the release. Fluorescence imaging analysis showed a high co-localization of CisPt-NPs with lysosomes, indicating that the NPs were at a low pH environment inside the cells. The release study at pH 4, mimicking the lysosomal pH, showed a further enhancement of the temperature-responsiveness, as well as a boost in overall release of cisplatin. Furthermore, the *in vitro* cytotoxicity of the CisPt-NPs was shown to get accelerated at higher temperature. These results prove the feasibility of my temperature-responsive formulation for drug delivery applications.

5.1.4. Chapter 4.

Polyethylenimine (PEI) was incorporated into cisplatin-loaded PAA-NPs, and then we evaluated its changes with respect to cellular uptake and cytotoxicity. The PEI-PAA NPs were significantly more cytocompatible, compared with free PEI (25 kDa branched), but still retained a higher cellular uptake than the PAA-NPs, due to the presence of PEI. The PEI-PAA NPs showed higher cytotoxicity and higher cellular uptake, compared to PAA NPs. Coating the surface of the NPs with F3-PEG diminished the difference in their cellular uptake, between PEI-PAA NPs and PAA-NPs, indicating PEI as a key factor for the enhancement of the cellular uptake. The enhanced uptake of NPs by the incorporation of PEI is not a simple phenomenon, attributable to their surface (i.e. ζ-potential) because the ξ-potential of PEI-PAA NPs were similar to that of the PAA NPs; further investigation is needed to understand the exact

mechanism. Also, marginal effect of endosomal escape of the PEI-PAA was observed. Thus, the higher cytotoxicity of PEI-incorporated PAA NPs than PAA NPs was the combination effect of significantly higher cellular uptake, enhanced release and loading, and endosomal escape.

5.1.5. Overall Conclusions

Throughout the research conducted, the following conclusions were arrived at:

(a). Loading

- Carboxyl-functionalized NPs can load more cisplatin than amine-functionalized NPs.
- Loading after the synthesis of the NPs (post-loading) can achieve a higher loading than loading before the synthesis of the NPs (encapsulation)
- High temperature helps in loading more cisplatin
- The loading of cisplatin is independent of the matrix density

(b). Release

- While loading at high temperature can load more drugs, the percent release is lower, because cisplatin is trapped deeper inside the NP's matrix.
- The looser the matrix density, the more cisplatin is released, and the faster the release.
- P(AAm-co-AA) can form both temperature and pH sensitive matrixes.

  Carboxyl-functionalized NPs can release more cisplatin and can do it faster than amine-functionalized NPs

(c). Cellular Uptake

- Amine-functionalized NPs are uptaken more by the cells than carboxy-functionalized NPs.

- Overall surface charge (ζ-potential) is not the only factor that controls the NPs' cellular uptake. Partial charge or charge distribution on the surface may play an important role as well.

Through these studies, new methods for controlling drug release from polyacrylamide-based NPs were established: (1) tuning the matrix density (chapter 2) and (2) upper critical solution temperature-like behavior (chapte3). These methods enrich the options of controlling the drug release from hydrogel nanoparticles. Also, the enhanced cellular uptake of polyethylenimine-incorporated NPs, regardless of their lower ζ-potential, implies that PEI is enhancing the cellular uptake, not only by increasing the overall surface positivity of NPs, which is widely accepted, [12] but also by using other mechanisms such as the introduction of surface heterogeneity.

5.2. Future Directions

5.2.1. In vivo Analysis.

The analysis of NPs-assisted chemotherapy *in vitro* has many limitations because there is no blood circulation in the *in vitro* system. First, the passive targeting (i.e. EPR), cannot be evaluated using *in vitro* systems. Therefore, it is difficult to evaluate how effectively NPs can target the tumor areas. Second, the biodistribution of the NPs cannot be evaluated. Thus, no evaluation of systemic side effects could be made. Also, no information on the pharmacokinetics can be obtained. Therefore, the information on the blood circulation time of the synthesized NPs could not be obtained. In order to answer these questions, it is necessary to test these synthesized NPs *in vivo*.

5.2.2. Change drugs.

The knowledge acquired through my projects should be applicable to other types of antitumor drugs as well. As a next step, different drugs should be loaded into the NPs. Some possible drug candidates are paclitaxel, docetaxel, disulfiram and CPA-7. Paclitaxel and docetaxel are drugs that are currently widely used in cancer treatment.[14,15] As mentioned in chapter 1, abraxane is made of paclitaxel-loaded albumin nanoparticles, and is commercially available.[16,17] However, it is difficult to chemically modify the abraxane further, because abraxane is composed of a protein-based carrier.[17] Using PAA instead of albumin gives NPs more flexible functionalities. Disulfiram is a sulfhydryl-reacting agent, and can potentially act in various locations inside the cell, including the drug efflux pumps.[18] However, disulfiram is very hydrophobic, and requires, for intravenous administration, an assist from a delivery system such as the above PAA-NPs. CPA-7 is the inhibitor of Stat3, which is also known to be highly expressed in cancer cells. In the appendix, it is discussed in more detail.[19]

5.2.3. Incorporation of the Redox Sensitivity into the Nanoparticle Matrix.

The extracellular region is known to be an oxidizing environment while the intracellular region is known to be a reducing environment, because of molecules such as glutathione.[20] Taking advantage of this environmental difference, NPs that are responsive to the redox environment can be synthesized. N,N'-cystamine bisacrylamide (CBA) is a cross-linker that has a disulfide bond in its structure. [20,21] Using CBA as a cross-linker of the NPs, the NPs can selectively degrade inside the cells. The molecular weight of the degraded polymer chain should be as small as possible for effective degradation.[22] Chain transfer polymerization may be performed instead of our current method of free radical polymerization, due to the ability of chain transfer polymerization to reduce the molecular weight of polymer chains. [22] This type of NPs could be utilized for delivery of macromolecules such as proteins, DNA and RNA. [20]

5.2.3. Endosomal escape and organelle targeting.

One of the current problems of the hydrogel NPs discussed as a drug delivery system is the destination of the NPs inside the cells. They are trapped in the endosome/lysosomes. However, as mentioned in chapter 1, the closer drugs are released from the NPs to the site of action, the better the efficacy is. Therefore, it will be helpful if the NPs can escape from the endosomes, enter the cytosol, and eventually reaches the targeted organelle.[23]

There are some mechanisms proposed for endosomal escape: the proton sponge effect and the cell membrane-fusion by liposomes.[23] For PAA-NPs, where membrane fusion is not possible, the proton sponge effect is an ideal mechanism for the endosomal escape, due to its easiness of incorporation into PAA. The proton sponge effect is the rapture of the endosomal membranes by osmotic pressure. Basic functional groups, typically amines, function as a buffer inside the endosomes. The buffering effect results in the recruitment of protons and Cl^-, which increases the ionic strength inside the endosomes.[24] Due to the imbalance between the inside and outside of the endosome, the membranes of the endosomes rapture. Typically, high amine containing molecules such as polyethylenimine, polylysine or endosome disrupting peptides containing a high amount of histidine[23] are incorporated into the NPs.

Combining the endosomal escape ability with organelle targeting moieties, NPs can be selectively delivered to the targeted organelles. Some possible organelles worth targeting are the mitochondria and nucleus.[23]

References

1. Koo Lee, Y.; Kopelman, R. In *Multifunctional Nanoparticles for Drug Delivery Applications*; Svenson, S.; Prud'homme, R. K., Eds.; Nanostructure Science and Technology; Springer US: Boston, MA, 2012; pp. 225–255.
2. Decatris, M. P.; Sundar, S.; O'Byrne, K. J. Platinum-Based Chemotherapy in Metastatic Breast Cancer: Current Status. *Cancer Treat. Rev.* **2004**, *30*, 53–81.
3. Dean, M.; Fojo, T.; Bates, S. Tumour Stem Cells and Drug Resistance. *Nat. Rev. Cancer* **2005**, *5*, 275–84.
4. Maeda, H. The Enhanced Permeability and Retention (EPR) Effect in Tumor Vasculature: The Key Role of Tumor-Selective Macromolecular Drug Targeting. *Advances in enzyme regulation* **2001**, *41*, 189–207.
5. Winer, I.; Wang, S.; Lee, Y.-E.; Lee, Y.-E.; Fan, W.; Gong, Y.; Burgos-Ojeda, D.; Spahlinger, G.; Kopelman, R.; Buckanovich, R. F3-Targeted Cisplatin-Hydrogel Nanoparticles as an Effective Therapeutic That Targets Both Murine and Human Ovarian Tumor Endothelial Cells In Vivo. *Cancer Research* **2010**, *70*, 8674–83.
6. Wenger, Y.; Schneider, R.; Reddy, G.; Kopelman, R.; Jolliet, O.; Philbert, M. Tissue Distribution and Pharmacokinetics of Stable Polyacrylamide Nanoparticles Following Intravenous Injection in the Rat. *Toxicology and applied pharmacology* **2011**, *251*, 181–90.
7. Brigger, I.; Dubernet, C.; Couvreur, P. Nanoparticles in Cancer Therapy and Diagnosis. *Adv. Drug Deliv. Rev.* **2002**, *54*, 631–51.
8. Cuvier, C.; Roblot-Treupel, L.; Millot, J. M.; Lizard, G.; Chevillard, S.; Manfait, M.; Couvreur, P.; Poupon, M. F. Doxorubicin-Loaded Nanospheres Bypass Tumor Cell Multidrug Resistance. *Biochemical Pharmacology* **1992**, *44*, 509–517.
9. Yoon, H.; Lou, X.; Chen, Y.-C.; Lee, Y.-E.; Yoon, E.; Kopelman, R. Nanophotosensitizers Engineered to Generate a Tunable Mix of Reactive Oxygen Species, for Optimizing Photodynamic Therapy, Using a Microfluidic Device. *Chem. Mater.* **2014**, *26*, 1592–1600.
10. Shirakura, T.; Kelson, T.; Ray, A.; Malyarenko, A.; Kopelman, R. Hydrogel Nanoparticles with Thermally Controlled Drug Release. *ACS macro letters* **2014**, *3*, 602–606.
11. ROSENBERG, E.; VANCAMP, L.; TROSKO, J.; MANSOUR, V. Platinum Compounds: A New Class of Potent Antitumour Agents. *Nature* **1969**, *222*, 385–386.
12. He, C.; Hu, Y.; Yin, L.; Tang, C.; Yin, C. Effects of Particle Size and Surface Charge on Cellular Uptake and Biodistribution of Polymeric Nanoparticles. *Biomaterials* **2010**, *31*, 3657–3666.
13. Fleischer, C.; Payne, C. Secondary Structure of Corona Proteins Determines the Cell Surface Receptors Used by Nanoparticles. *J. Phys. Chem. B* **2014**, *118*, 14017 14026.
14. Blagosklonny, M.; Fojo, T. Molecular Effects of Paclitaxel: Myths and Reality (a Critical Review). *Int. J. Cancer* **1999**, *83*, 151–156.
15. Crown, J.; O'Leary, M.; Ooi, W.-S.; Crown, J.; O'Leary, M.; Ooi, W.-S. Docetaxel and Paclitaxel in the Treatment of Breast Cancer: A Review of Clinical Experience. *The Oncologist* **2004**, *89*, 328–331.
16. US Food and Drug Administration FDA Approves Abraxane for Late-Stage Pancreatic Cancer.
17. Green, M.; Manikhas, G.; Orlov, S.; Afanasyev, B.; Makhson, A.; Bhar, P.; Hawkins, M. Abraxane®, a Novel Cremophor®-Free, Albumin-Bound Particle Form of Paclitaxel for the Treatment of Advanced Non-Small-Cell Lung Cancer. *Annals of Oncology* **2006**, *17*, 1263–1268.

18. Sauna, Z.; Shukla, S.; Ambudkar, S. Disulfiram, an Old Drug with New Potential Therapeutic Uses for Human Cancers and Fungal Infections. *Molecular bioSystems* **2005**, *1*, 127–34.
19. Assi, H.; Paran, C.; VanderVeen, N.; Savakus, J.; Doherty, R.; Petruzzella, E.; Hoeschele, J.; Appelman, H.; Raptis, L.; Mikkelsen, T.; *et al.* Preclinical Characterization of Signal Transducer and Activator of Transcription 3 Small Molecule Inhibitors for Primary and Metastatic Brain Cancer Therapy. *The Journal of pharmacology and experimental therapeutics* **2014**, *349*, 458–469.
20. Lin, C.; Zhong, Z.; Lok, M.; Jiang, X.; Hennink, W.; Feijen, J.; Engbersen, J. Novel Bioreducible Poly(amido Amine)s for Highly Efficient Gene Delivery. *Bioconjugate chemistry* **2006**, *18*, 138–45.
21. Park, K.; Lee, M.-Y.; Kim, K.; Hahn, S. Target Specific Tumor Treatment by VEGF siRNA Complexed with Reducible Polyethyleneimine-Hyaluronic Acid Conjugate. *Biomaterials* **2010**, *31*, 5258–65.
22. Gao, D.; Xu, H.; Philbert, M.; Kopelman, R. Bioeliminable Nanohydrogels for Drug Delivery. *Nano Lett.* **2008**, *8*, 3320–4.
23. Biswas, S.; Torchilin, V. Nanopreparations for Organelle-Specific Delivery in Cancer. *Advanced Drug Delivery Reviews* **2013**, *66*, 26–41.
24. Akinc, A.; Thomas, M.; Klibanov, A.; Langer, R. Exploring Polyethylenimine-Mediated DNA Transfection and the Proton Sponge Hypothesis. *The journal of gene medicine* **2005**, *7*, 657–63.

–

Thesis Appendix

CPA-7-loaded Hydrogel Nanoparticles for the Treatment of Glioma

Introduction

STAT3 is highly expressed in various types of cancer cells, such as glioma, melanoma, and breast cancer, and reported to play an important role for the tumor growth. [1,2] Inhibition of the STAT3 activity can reduce the cell proliferation, and cause the death of cancer cells. [1,3]

CPA-7, trichloronitritodiammineplatinum (IV), is a promising inhibitor of STAT3. [1] Despite success *in vitro* and peripheral tumor models, it could not treat tumors in the brain because of its poor blood-brain barrier (BBB) penetration ability. [1] Therefore, it is necessary for CPA-7 to be loaded onto a carrier that can pass through the BBB.

Our polyacrylamide (PAA)-based NPs can pass through the BBB. We delivered Coomassie blue-loaded NPs for glioma intraoperative delineation and photoacoustic imaging, MRI contrast agent-loaded NPs for magnetic resonance imaging (MRI) of brain tumors, and PHOTOFRIN-loaded NPs for the treatment of glioma. [4–6] Thus, CPA-7 can potentially reach glioma by utilizing PAA-NPs as carriers. What is more, CPA-7 has a chemical structure similar to cisplatin; [1] therefore, the knowledge and the techniques for the synthesis of cisplatin NPs can be applied for the CPA-7 NP formulation development.

Materials and Methods

Materials.

CPA-7 was provided from our collaborator in Eastern Michigan University. RPMI media was purchased from Invitrogen. All other chemicals were purchased from Sigma-Aldrich. The de-ionized water used in this experiment was purified prior to the experiment, using a Milli-Q system from Millipore.

Synthesis of blank NPs.

NPs were synthesized using our standard protocol. 31 % and 48% p(AAm-*co*-APMA), and 21 % and 34 % p(AAm-*co*-AA) from chapter 2 were synthesized for this experiment. Briefly, AOT and Brij30 were mixed with hexane (oil phase). There, a water phase, containing monomers and cross-linkers, was mixed with hexane, to form reverse micelles. Polymerization was initiated using APS and TEMED. After the polymerization, the hexane was removed from the mixture using rotor evaporation, and the surfactants and unreacted monomers were removed using an Amicon Stir Cell (Millipore) with 300 kDaMWCO membrane.

Loading of CPA-7 onto NPs.

10 mg of NPs were mixed with 0.5 mg/mL of CPA-7 in water. The mixture was kept overnight for the loading at room temperature, and 4 hours for the loading at 90 °C. Then, the solution was centrifuged at 5000 g over 5 minutes, for the removal of any insoluble materials. The supernatants were transferred to a 100 kDaMWCO centrifugal filter, and washed 7 times with 7 mL of DI water. The CPA-7 amount in the NPs was quantified using inductively coupled plasma optical emission spectroscopy (ICP-OES).

Synthesis of NPs without Acrylamide-Derived Cross-Linkers.

The NPs were synthesized adopting the method reported in chapter 3. 2 mg of CPA-7 was mixed with 133.2 μL of acrylic acid and 1.3 mL of water, and incubated at 90 °C for 1 hour. Then, 0.12 g of acrylamide and 100 mg of APS were added. This mixture was used as a water phase. The rest of the synthesis was the same as the synthesis of NPs in chapter 3. Briefly, the mixture was mixed with surfactant-containing hexane, and polymerization was initiated by TEMED. The product was removed from hexane by rotor evaporation, and the unreacted monomers and free CPA-7 were removed by 7 times washing with 175 mL ethanol, followed by 5 times washing with 150 mL waterm, using an Amicon Stir Cell with a 100 kDaMWCO membrane.

Results and Discussion

Comparison of the loading at room temperature and high temperature.

48 % poly(AAm-*co*-APMA) and 34 % poly(AAm-*co*-AA), which were synthesized in chapter 2, were compared for their CPA-7 loading efficiency at two different temperatures: room temperature and a higher temperature of 90 °C. The NPs were mixed with free CPA-7 for 4 hours in the case of the high temperature loading, while the NPs were mixed overnight in the case of the room temperature loading. The result of the loading is summarized in Table A.1.

The loading is calculated by equation 1.

$$\text{Wt \% loading} = \frac{A}{A+B} \times 100\ (\%) \qquad \text{Equation 1}$$

Here, A is the weight of CPA-7 in the NPs, and B is the weight of the blank NPs.

More CPA-7 was loaded onto both types of NPs at the higher temperature than at room temperature. The loading at room temperature was too low for drug delivery applications. No

clear difference in loading was observed between p(AAm-*co*-APMA) and p(AAm-*co*-AA). Based on these results, the loading temperature was set to 90 °C.

The Comparison of the CPA-7 Release from amine-functionalized NPs to that of carboxyl-functionalized NPs.

As a next step, the release profile was compared between p(AAm-*co*-APMA) and p(AAm-*co*-AA). Here, because of the expectation that a lower matrix density helps in increasing the release of CPA-7 (chapter 2), the matrix densities of both p(AAm-*co*-APMA) and p(AAm-*co*-AA) were reduced (Figure A.1). More CPA-7 was released from p(AAm-*co*-AA) than from the p(AAm-*co*-APMA) over 7 days. Based on this result, we decided to use p(AAm-*co*-AA) as a matrix for CPA-7 delivery.

We tested the formulations in cell lines that had a high expression of Stat3, but no notable effect was observed (data not shown). The result of no notable cytotoxicity might be due to the NPs' low overall release of drug (Figure A.1).

The Effect of Cross-Linkers.

Since the formulations did not have notable cytotoxicity, the NP-matrix was further optimized. In order to maximize the effective diffusion of CPA-7 inside the NPs, NPs without acrylamide-derived cross-linker were synthesized. Instead of acrylamide-derived cross-linker, CPA-7 itself was utilized as a cross-linker, as cisplatin was utilized in the previous work.[7] Cisplatin can reversibly substitute its two chloride atoms with carboxyl groups, depending on the concentration of chloride ions in the environment.[8] How CPA-7 changes its structure under physiological conditions is not known yet, but the chlorides in CPA-7 might behave in a similar way to that in cisplatin. To make CPA-7 a cross-linker, CPA-7 was mixed with acrylic acid, so as to facilitate the substitution of the chlorides in the CPA-7 with carboxyl groups in the acrylic

acid, prior to the polymerization reaction. The NPs were made from acrylamide and acrylic acid, roughly in a 1:1 ratio, as reported in chapter 3. The weight percent loading of CPA-7 was 0.41 %. The hydrodynamic light scattering based size of the NPs was 90 (±1) nm, with the polydispersity index of 0.25 (±0.03). The loading of CPA-7 was significantly lower than the formulations in which we tested the cytotoxicity, because this synthesis method reduced the ratio of CPA-7 to the matrix of the NPs.

The synthesized NPs had a significantly higher overall percent release of CPA-7 (Figure A.2), and showed a statistically significant cytotoxicity (Figure A.3).

In order to increase the CPA-7 loading, additional CPA-7 was loaded onto these no cross-linker NPs at 90 °C, using the same protocol as for the loading at high temperature. This formulation had the highest loading of CPA-7, among all the synthesized formulations. However, as shown in Figure A.2, the overall release of CPA-7 (labeled as "extra loading") was lower than for the no cross-linker NPs. Also, the release kinetics of these extra-good loading NPs was similar to that of the original no-cross-linker NPs. Thus, the extra-loading at the higher temperature. did not help in increasing the efficacy of the NPs.

Future Directions

The current problem of the formulation is its initial rapid release of CPA-7 from the NPs, as well as the low wt % loading of the NPs. Here are the possible solutions to these problems.

Initial Rapid Release of CPA-7

(1) The matrix needs to be tighter by adding a small amount of acrylamide-derived cross-linkers. This should reduce the burst release. (2) No optimization of the ratio of acrylic acid and acrylamide has been performed. There may be a ratio -dependent difference in the release

behavior. Therefore, finding the optimal ratio of acrylic acid and acrylamide may solve the problem. (3) Albumin-PAA NPs have shown a slightly different behavior from PAA-NPs in the loading and release of antitumor drugs. [9] The investigation of the loading and release profile of CPA-7-loaded albumin-PAA NPs should be performed. (4) The NPs can be washed with Phosphate Buffer Saline (PBS) (pH 7.4) or saline solution right before the incubation with cells. The washing should remove CPA-7 released from the NPs due to the burst release.

Low Loading of CPA-7

(1) The low loading of CPA-7 is attributed to the low CPA-7 feeding during the synthesis. Increasing the feeding amount of CPA-7 should increase the wt % loading of CPA-7 in the NPs.

Table A.1. Comparison of Loading of Two Formulations at Two Different Temperatures.

	Loading Temperature	Wt% loading
p(AAm-*co*-APMA)	Room Temperature	0.27 %
	90 °C	1.3 %
p(AAm-*co*-AA)	Room Temperature	0.17%
	90 °C	1.4 %

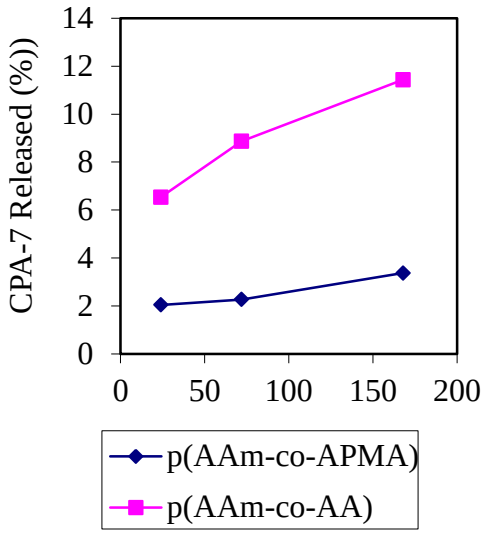

Figure A.1. Comparison of CPA-7 Release from Two Different Formulations.

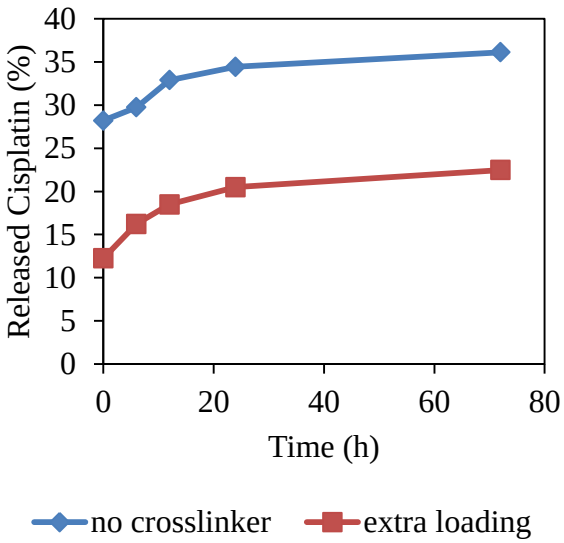

Figure A.2. Comparison of CPA-7 Release from no cross-linker NPs and Extra loading NPs.

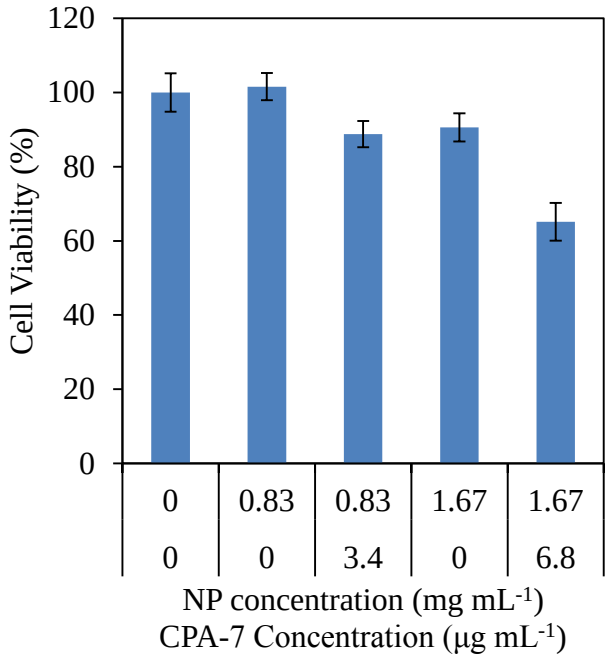

Figure A.3. MTT Assay of no cross-linker NPs using GL26 cells. 2.5 days Incubation with cells.

Acknowledgements.

Financial support was provided by a National Institutes of Health grant, R21 NS084275 (RK), and a University of Michigan MCubed grant. We thank Professors Maria Castro and Pedro Lowenstein for their valuable advice and for allowed me to use their facilities. The author also thanks Robert Doherty and Hikmat Assi for their support in cell-based assays. He also thanks the Chemistry Instrument Shop for their support.

References

1. Assi, H.; Paran, C.; VanderVeen, N.; Savakus, J.; Doherty, R.; Petruzzella, E.; Hoeschele, J.; Appelman, H.; Raptis, L.; Mikkelsen, T.; *et al.* Preclinical Characterization of Signal Transducer and Activator of Transcription 3 Small Molecule Inhibitors for Primary and Metastatic Brain Cancer Therapy. *The Journal of pharmacology and experimental therapeutics* **2014**, *349*, 458–469.
2. Weinberg, R. A. *The Biology of Cancer*; 1st ed.; Garland Science: New York, NY, 2006.
3. Stechishin, O.; Luchman, H.; Ruan, Y.; Blough, M.; Nguyen, S.; Kelly, J.; Cairncross, J.; Weiss, S. On-Target JAK2/STAT3 Inhibition Slows Disease Progression in Orthotopic Xenografts of Human Glioblastoma Brain Tumor Stem Cells. *Neuro-oncology* **2013**, nos302.
4. Nie, G.; Hah, H.; Kim, G.; Lee, Y.-E.; Qin, M.; Ratani, T.; Fotiadis, P.; Miller, A.; Kochi, A.; Gao, D.; *et al.* Hydrogel Nanoparticles with Covalently Linked Coomassie Blue for Brain Tumor Delineation Visible to the Surgeon. *Small (Weinheim an der Bergstrasse, Germany)* **2012**, *8*, 884–91.
5. Ray, A.; Wang, X.; Lee, Y.-E.; Hah, H.; Kim, G.; Chen, T.; Orringer, D.; Sagher, O.; Liu, X.; Kopelman, R. Targeted Blue Nanoparticles as Photoacoustic Contrast Agent for Brain Tumor Delineation. *Nano Res.* **2011**.
6. Kopelman, R.; Koo, Y.-E.; Philbert, M.; Moffat, B.; Reddy, R.; McConville, P.; Hall, D.; Chenevert, T.; Bhojani, M.; Buck, S. Multifunctional Nanoparticle Platforms for in Vivo MRI Enhancement and Photodynamic Therapy of a Rat Brain Cancer. *Journal of Magnetism and Magnetic Materials* **2005**, *293*, 404–410.
7. Li, S.-D.; Howell, S. CD44-Targeted Microparticles for Delivery of Cisplatin to Peritoneal Metastases. *Molecular pharmaceutics* **2010**, *7*, 280–90.
8. Peng, J.; Qi, T.; Liao, J.; Chu, B.; Yang, Q.; Li, W.; Qu, Y.; Luo, F.; Qian, Z. Controlled Release of Cisplatin from pH-Thermal Dual Responsive Nanogels. *Biomaterials* **2013**, *34*, 8726–40.
9. Yoon, H.; Ray, A.; Lee, Y.-E.; Kim, G.; Wang, X.; Kopelman, R. Polymer-Protein Hydrogel Nanomatrix for Stabilization of Indocyanine Green towards Targeted Fluorescence and Photoacoustic Bio-Imaging. *Journal of Materials Chemistry B* **2013**, *1*, 5611–5619.

–